

CHAPTER 6

SCENARIOS AND INFORMATION FOR POLICYMAKERS

Lead Authors

L.J. Carpenter
J.S. Daniel

Coauthors

E.L. Fleming
T. Hanaoka
J. Hu
A.R. Ravishankara
M.N. Ross
S. Tilmes
T.J. Wallington
D.J. Wuebbles

Contributors

J.B. Burkholder
A. Engel
Ø. Hodnebrog
R. Hossaini
L.J.M. Kuijpers
S.A. Montzka
R.J. Salawitch
W.R. Tribett
G. Velders
H. Walter-Terrinoni

Review Editors

N.R.P. Harris
M.J. Prather

Cover photo: The development of future scenarios of ODSs and HFCs are key products of the Montreal Protocol Scientific Assessment Panel. These products are developed using computer models that incorporate observed concentrations, production and consumption estimates, and the amounts of manufactured chemicals in existing equipment and application banks. These scenarios are an important part of the Executive Summary, which conveys policy relevant information to the Parties of the Montreal Protocol. Photo: Lynn Daniel and Konner Syed.

CHAPTER 6

SCENARIOS AND INFORMATION FOR POLICYMAKERS

CONTENTS

| | |
|---|----|
| SCIENTIFIC SUMMARY..... | 1 |
| 6.1 INTRODUCTION..... | 7 |
| 6.1.1 Summary of Findings from the Previous Ozone Assessment | 7 |
| 6.1.2 Key Issues to Be Addressed in This Assessment | 8 |
| 6.2 ISSUES OF POTENTIAL IMPORTANCE TO STRATOSPHERIC OZONE AND CLIMATE | 9 |
| 6.2.1 Halocarbons Controlled Under the Montreal Protocol | 9 |
| 6.2.1.1 Replacement Compounds | 10 |
| 6.2.1.2 Kigali Amendment | 11 |
| 6.2.1.3 HFC-23 | 12 |
| 6.2.2 Breakdown Products | 12 |
| 6.2.3 Very Short-Lived Substances (VSLs; Biogenic and Anthropogenic) | 14 |
| 6.2.4 The Key Climate Gases: Carbon Dioxide, Methane, and Nitrous Oxide | 15 |
| 6.2.5 Deliberate Climate Intervention..... | 16 |
| 6.2.5.1 Geoengineering via Stratospheric Sulfate Aerosol Modifications..... | 16 |
| 6.2.5.2 Geoengineering via Solar Irradiance Reduction | 17 |
| Box 6-1. Stratospheric Aerosol Geoengineering | 17 |
| 6.2.6 Other Potential Influences on Stratospheric Ozone | 18 |
| 6.3 METRICS FOR CHANGES IN OZONE AND CLIMATE | 21 |
| 6.3.1 Metrics for Changes in Ozone | 21 |
| 6.3.2 Metrics for Changes in Climate | 22 |
| 6.4 SCENARIOS AND SENSITIVITY ANALYSES | 25 |
| 6.4.1 Tools Used in Analyses of Ozone and Climate Effects | 25 |
| 6.4.2 Baseline Scenario for Ozone and Climate | 27 |
| 6.4.3 Alternative Future Scenarios | 34 |
| 6.4.3.1 Stratospheric Ozone Implications | 38 |
| 6.4.3.2 Climate Implications | 42 |
| REFERENCES | 46 |
| APPENDIX 6A: CURRENT STATE OF KNOWLEDGE ON STRATOSPHERIC SULFATE GEOENGINEERING | 57 |
| 6A.1 Impact of Stratospheric Sulfate Geoengineering on Net Chemical Ozone Production | 57 |



| | | |
|--|--|----|
| 6A.2 | Impact of Stratospheric Sulfate Geoengineering on Dynamics | 59 |
| 6A.3 | Impact of Sulfate Aerosol Geoengineering on Column Ozone | 59 |
| APPENDIX 6B: COMPARISON OF PAST AND FUTURE OZONE PROJECTIONS OF THE GSFC 2-D MODEL WITH GEOSCCM 3-D SIMULATIONS | | 61 |
| APPENDIX 6C: EVALUATION OF ALTERNATIVE SCENARIOS USING NEW EESC FORMALISM | | 69 |



CHAPTER 6

SCENARIOS AND INFORMATION FOR POLICYMAKERS

SCIENTIFIC SUMMARY

In the sections below, we note the significance of various improvements in our understanding concerning actions related to the Montreal Protocol and its Amendments that could alter the recovery of the ozone layer and/or impact Earth's climate. As in previous Assessments, we use equivalent effective stratospheric chlorine (EESC) as a proxy for the amount of stratospheric ozone depletion caused by ozone-depleting substances (ODSs) that contain chlorine and/or bromine and reside in the atmosphere for more than a few months. The return of EESC to 1980 values is used as a metric to compare the effects of different future scenarios of production and emission of ozone-depleting gases on ozone layer recovery. In this chapter, we also use 2-D model simulations to estimate changes in future ozone depletion for these different scenarios. (Note that 3-D model projections of global and polar ozone and analyses of expected recovery dates are presented in Chapters 3 and 4. These calculations include changes in greenhouse gas levels and in atmospheric transport and are not expected to be equivalent to the EESC recovery dates). Our ability to predict future changes in the ozone layer is limited more by uncertainties in future levels of CO₂, CH₄, and N₂O than by uncertainties in the levels of ODSs, especially as we approach the 1980 values of EESC. Indeed, ozone levels in some regions of the atmosphere could exceed natural levels, due to climate change, with possible consequences to humans and natural ecosystems, assuming natural levels represent a harmonious balance. The influence of CO₂ occurs through its role in the climate system as a driver of change in temperature and atmospheric circulation. The influences of CH₄ and N₂O occur primarily through their roles as chemical reagents in the atmosphere. ODSs themselves are greenhouse gases, and their influence on climate and ozone layer depletion are intricately intertwined, even though we note them separately for clarity of presentation. Lastly, note that the various additional actions discussed below impact future ozone to a much smaller degree than what has already been accomplished by the Montreal Protocol.

Post-Kigali information of interest and concern

- **The Kigali Amendment to the Montreal Protocol, along with regional and national regulatory and voluntary actions taken before Kigali entered into force, is expected to substantially limit future climate forcing by HFCs.** Projections of HFC emissions that include compliance with Kigali Amendment control measures suggest that the radiative forcing (a metric for global warming) from HFCs, currently 0.025 W m⁻² (not including HFC-23), will reach 0.13 W m⁻² by 2050, about half as high as that projected without the Kigali Amendment and prior national and regional regulation. The estimated benefit of these actions is 2.8–4.1 Gt CO₂-eq. yr⁻¹ of avoided Global Warming Potential (GWP)-weighted emissions by 2050. The projected surface temperature contribution from HFCs (excluding HFC-23) reduces from 0.3–0.5 °C to less than 0.1 °C in 2100 due to entry into force of the Kigali Amendment.
- **Options are available to further decrease the climate impact of HFCs.** Use of commercially available low-GWP alternatives in place of high-GWP HFCs in refrigeration and air-conditioning equipment, thermal insulating foam, metered-dose inhalers, fire protection, and miscellaneous HFC applications during the phasedown would further reduce climate change. Additional benefits would be gained by such actions via development of more energy-efficient equipment and thermal insulating foam that use these low-GWP replacements.
- **Sustained increases in anthropogenic chlorinated very short-lived substances (VSLs Cl) emissions, as seen for CH₂Cl₂ in the 2000s, would decrease stratospheric ozone levels in the coming decades. However, observed growth rates of CH₂Cl₂ continue to be highly variable, and there is insufficient information to**

confidently predict future concentrations. If the growth in emission rates seen during the first decade of this century continues, CH_2Cl_2 is projected to deplete as much column ozone between 2020 and 2060 as that by the controlled ODSs emitted during that period. However, such large growth projections do not account for a more recent reduction in the CH_2Cl_2 growth rate, nor have they been shown to be consistent with expectations for global demand over the coming decades. Any control of CH_2Cl_2 production and consumption under the Montreal Protocol would be rapidly effective, since this VSLs will be cleansed out of the stratosphere within a few years.

Ozone-depleting substances (ODSs) and equivalent effective stratospheric chlorine (EESC)

Below, we discuss potential changes in the projected trajectory of ozone depletion and EESC that result from improvements in our understanding of the emissions or other characteristics of individual gases or groups of gases. We reference these potential changes to the so-called baseline scenario—which should be considered a plausible future pathway for these gases. The baseline scenario for ODSs is developed from atmospheric concentration observations, combined with estimates of the amounts of ODSs in existing equipment or other products containing ODSs, referred to as banks. The 2018 baseline scenario for HFCs takes into account global control measures introduced by the Kigali Amendment and other regional and national actions. For all baseline scenarios, we assume that the long-lived greenhouse gases N_2O , CH_4 , and CO_2 follow the Representative Concentration Pathway (RCP) 6.0 scenario. Note that for some of the metrics the combined consequence of these gases is generally not simply the addition of each of the changes. It is also important to recognize that the return date of EESC to 1980 levels is quite sensitive to any change in EESC concentration because of the relatively small rate at which EESC is projected to decline in the middle of this century.

- **Global emissions of CFC-11 derived from atmospheric observations show an increase in recent years that is not consistent with our understanding of release from its banks and suggests new global production that is not reported to the United Nations Environment Programme (UN Environment).** If total emissions of CFC-11 were to continue at levels experienced from 2002–2016 (67 Gg yr^{-1}), the return of mid-latitude and polar EESC to the 1980 value would be delayed by about seven years and 20 years, respectively. Such an assumption of continuing emissions implicitly assumes that the unidentified emissions will grow to counteract the expected decline in bank emissions.
- **Emissions from current ODS banks continue to be a slightly larger future contribution than ODS production to ozone layer depletion over the next four decades, assuming maximum production levels allowed by the Montreal Protocol.** Future business-as-usual emissions from HCFCs and from banks of CFCs and banks of halons are each projected to contribute roughly comparable amounts to EESC in the next few decades.
- **Elimination of future production of methyl bromide (CH_3Br) for quarantine and pre-shipment (QPS) applications, not controlled by the Montreal Protocol, would accelerate the return of mid-latitude EESC to 1980 levels by about a year.** Production for QPS use has remained relatively stable over the last two decades and now constitutes almost 90% of the reported production of CH_3Br since emissions from other uses have declined dramatically. Non-QPS applications of CH_3Br were completely phased out in 2015, except for approved critical use exemptions, which have declined by a factor of ~ 30 since 2005.
- **If CCl_4 emissions continue to decline at the rate observed over the last two decades of $2.5\% \text{ yr}^{-1}$, future concentrations will be about 14 ppt higher in 2050 than projected in the previous Assessment.** CCl_4 emissions inferred from atmospheric observations continue to be much greater than those assumed from feed-stock uses as reported to UN Environment; by-product emissions from chloromethane and perchloroethylene plants and fugitive emissions from the chlor-alkali process have been quantified as significant contributors to these additional emissions. Elimination of all CCl_4 emissions in 2020 would accelerate the return of mid-latitude EESC to 1980 levels by almost three years compared to the baseline scenario

of a continued emissions decrease of 2.5% yr⁻¹. Alternatively, if future emissions do not decline but remain at the current level, the return of mid-latitude EESC to 1980 levels would be delayed almost two years.

- **The return of mid-latitude EESC to 1980 levels is estimated to be delayed by almost two years compared to the previous Assessment, due primarily to the higher projected future concentrations of CCl₄.** The mid-latitude EESC change from CCl₄ alone leads to a delay larger than two years, but future CH₃Br baseline projections are now lower than in the previous Assessment and offset some of the effect from CCl₄. The delay in polar EESC returning to 1980 levels is slightly more than two years when compared with the previous Assessment. A new EESC formalism alters the time evolution of EESC and dates when EESC returns to 1980 levels, but it has little effect on the relative impacts of the various alternative future scenarios. When compared with the previous Assessment's EESC formalism, the new EESC formalism leads to a projected EESC return to the 1980 level 11 years later at mid-latitudes and by less than two years later at polar latitudes.
- **Reducing anthropogenic emissions of N₂O from those in RCP-6.0 to the Concerted Mitigation scenario¹ would have a similar positive impact on stratospheric ozone over the next four decades as eliminating production of HCFCs from 2020. This N₂O emissions reduction would have a larger benefit to climate over 2020–2060 than the sum of all the options for controlled ODSs considered (based on GWP-weighted emissions).**

Updates on the climate impact of gases controlled by the Montreal Protocol

- **Future emissions of HFC-23, a potent greenhouse gas and a by-product of HCFC-22 production, are expected to be limited by the Kigali Amendment,** which mandates the destruction of HFC-23 to the extent practicable. Globally, HCFC-22 is currently produced in roughly equal quantities for controlled emissive uses, which are declining, and for the uncontrolled feedstock uses, which grew rapidly over the last few decades but have recently stabilized. Future emission trends will largely depend on the extent to which HFC-23 is destroyed by HCFC-22 production facilities and the amount of HCFC-22 produced.
- **Future emissions of HFCs, HCFCs, and CFCs contribute approximately 60, 9, and 3 cumulative Gt CO₂-equivalent emissions, respectively, from 2020 to 2060 in the baseline scenario.** Of the 60 Gt CO₂-eq emissions from HFCs, 53 arise from future production. For reference, cumulative CO₂ emissions from fossil fuel usage are projected over this time period to be 1,700 Gt CO₂ in the RCP-6.0 scenario and 760 Gt CO₂ in the RCP-2.6 scenario. The total radiative forcing from CFC and HCFCs and their HFC replacements is projected to continue to increase gradually for the next decade or two. After that point, the ODS and HFC restrictions of the Montreal Protocol, if adhered to, ensure a continued decline in total RF from ODSs and their replacements through the rest of the century.
- **Global warming potentials, global temperature change potentials, and ozone depletion potentials of hundreds of HCFCs are presented, most for the first time in an assessment.** This comprehensive assessment includes all the HCFCs listed under Annex C, Group I of the Montreal Protocol, many of which did not have estimated GWPs at the time of the signing of the Kigali Amendment.

Updates on impacts of climate gases and other processes on future stratospheric ozone

In this section, we summarize potentially important impacts on the future of the ozone layer that could result from anthropogenic activity not associated with ODS production or consumption and not controlled by the Montreal Protocol. As noted above, a major issue is that uncertainties in future changes in the ozone layer will be influenced more by uncertainties in CO₂, CH₄, and N₂O levels than by uncertainties in the levels of ODSs, especially as we

¹ UNEP 2013. Drawing Down N₂O to Protect Climate and the Ozone Layer. A UNEP Synthesis Report. United Nations Environment Programme (UNEP), Nairobi, Kenya.

approach the 1980 values of EESC. Increases in greenhouse gas concentrations are predicted to lead to increases in upper-stratospheric ozone at all latitudes, with a more complex pattern of ozone changes in the lower stratosphere, including a decrease in low latitudes due to changes in dynamics and transport. These processes are discussed in detail in **Chapters 3 and 4**. Note that natural forces such as large explosive volcanic eruptions could also adversely affect ozone recovery over the next decade, while ODS levels remain high.

- **The wide range of possible future levels of CO₂, CH₄, and N₂O represents an important limitation to making accurate projections of the ozone layer.** Global mean warming as well as stratospheric cooling will drive ozone changes through both atmospheric circulation and chemistry. Future ozone levels depend on the path of greenhouse gas and aerosol emissions as well as the sensitivity of the climate system to these emissions. Future ODS atmospheric concentrations are more certain than atmospheric concentrations of climate forcing emissions, as long as there is adherence to the Montreal Protocol. This chapter considers various climate scenarios, using the Representative Concentration Pathways (RCPs) adopted by the IPCC for its Fifth Assessment Report (AR5). The Paris Agreement, with a stated objective to limit globally averaged warming to less than 2°C, requires emissions closest to RCP-2.6, the lowest emission scenario of all the RCP scenarios.
- **Intentional long-term geoengineering applications that substantially increase stratospheric aerosols to mitigate global warming by reflecting sunlight would alter stratospheric ozone.** The estimated magnitudes and even the sign of ozone changes in some regions are uncertain because of the high sensitivity to variables such as the amount, altitude, geographic location and type of injection, and the halogen loading. An increase of stratospheric sulfate aerosol burden in amounts sufficient to substantially reduce global radiative forcing would delay the recovery of the Antarctic ozone hole. Much less is known about the effects on ozone from geoengineering solutions using non-sulfate aerosols.
- **Rocket launches presently have a small effect on total stratospheric ozone (much less than 0.1%).** Space industry developments indicate that rocket emissions may increase more significantly than reported in the previous Assessment. Their impacts will depend on rocket design (particularly the altitude of emissions), launch vehicle sizes, launch rates, spaceport locations, and fuel types. Important gaps remain in understanding rocket emissions and their combined chemical, radiative, and dynamical impacts on the global stratosphere and in projections of launch rates. These gaps limit the confidence level of predictions of present and future impacts of rocket emissions on stratospheric ozone and suggest periodic assessments are warranted. The lifetime of the most important rocket emissions is limited, and the stratospheric accumulation of rocket-emitted black carbon and alumina particles varies in correspondence with global launch rates and altitude of emissions.

Update on other environmental impacts of Montreal Protocol gases

Here, we refer to all gases controlled under the Montreal Protocol and its various Amendments, including the Kigali Amendment, as Montreal Protocol Gases.

- **There is increased confidence that trifluoroacetic acid (TFA) produced from degradation of HFCs, HCFCs, and HFOs will not harm the environment over the next few decades.** This assessment is based on the current estimates of future use of hydrocarbons, HCFCs, and HFOs. It is noteworthy that HFCs and HCFCs have atmospheric lifetimes long enough to globally distribute any TFA emissions, while HFOs have atmospheric lifetimes so short that TFA emissions are deposited near the point of emission. Periodic re-evaluation is prudent, given the uncertainties in the sources and sinks of TFA and because of its persistence in the environment.

Summary of the impacts of mitigation options and particular scenarios

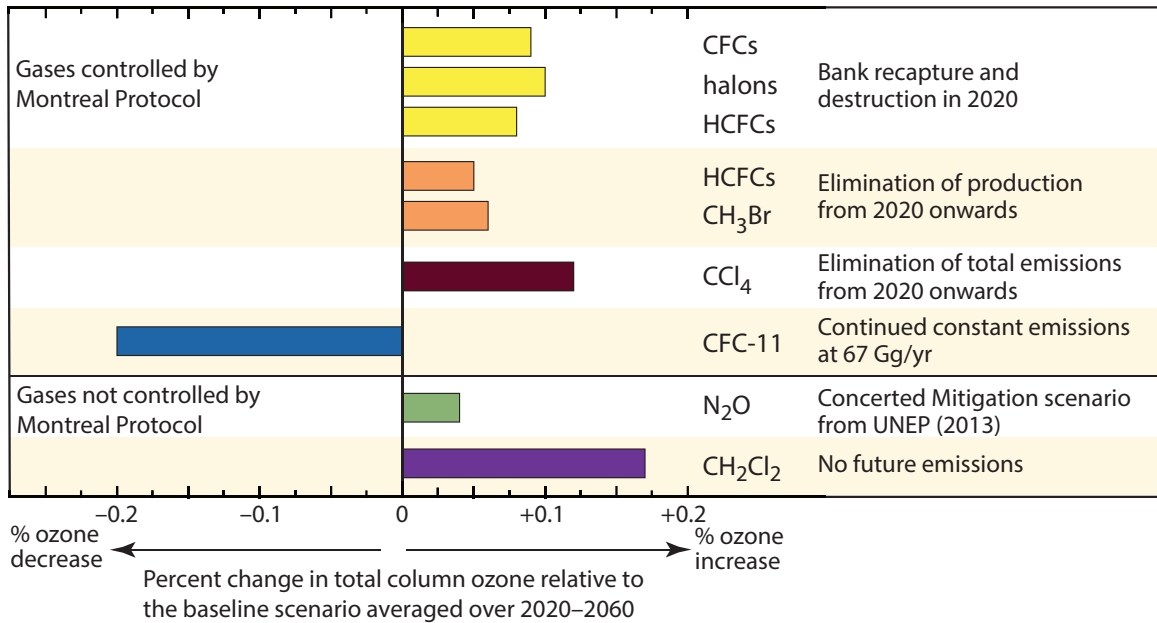
Figure 6-1 (also **Figure ES-9**) shows what ozone and climate-relevant changes could be avoided if various actions were taken. These changes are shown as the differences in global total column ozone averaged over 2020–2060 and in cumulative CO₂-equivalent emissions over 2020–2060 relative to the baseline (A1) scenario (which includes the Kigali Amendment for HFCs). The options available to hasten the recovery of the ozone layer are limited, mostly because actions that could help significantly have already been taken.

- For CFCs, halons, and HCFCs, the most effective mitigation option, not considering technical feasibility, is expanded bank recapture and destruction; elimination of HCFC production starting in 2020 would be somewhat less effective.
- For CH₃Br, elimination of production for currently uncontrolled quarantine and pre-shipment (QPS) applications is shown.
- For CCl₄, the impacts of total emissions elimination starting in 2020 are shown.
- For CH₂Cl₂, an uncontrolled ozone-depleting gas whose exact sources are unknown, we show that immediate emissions elimination would have a greater positive impact on total column ozone than total emissions elimination of CCl₄.
- For N₂O, the impacts of the Concerted Mitigation average scenario from UNEP (2013) are shown, compared to the RCP-6.0 scenario. The Concerted Mitigation scenario was developed by averaging the four published mitigation scenarios (RCP-2.6, SRES B2, and scenarios 4 and 5 from Davidson, 2012) that lead to lower N₂O emissions in 2050 than were experienced in 2005.
- For HFCs, the impact of a hypothetical complete global phaseout of production (excluding HFC-23) starting in 2020 is shown. As discussed in **Chapter 2**, for this scenario the surface temperature contribution of the HFC emissions would stay below 0.02 °C for the entire 21st century and beyond.

Further detail on these options and scenarios is given in **Section 6.4** and **Table 6-5**.

All the scenarios discussed above hasten the ozone layer recovery (CFCs, halons, HCFCs, CH₃Br, CCl₄, CH₂Cl₂ and N₂O) and reduce warming (HFCs, CFCs, halons, HCFCs, CCl₄, and N₂O). An additional scenario for emissions that may result from a violation of the Montreal Protocol is shown, namely continuing unexplained emissions of CFC-11 at 67 Gg yr⁻¹, which is the average calculated annual emission from atmospheric concentration observations over 2002–2016. This scenario leads to more ozone depletion and climate warming. Avoiding this scenario would have a larger positive impact on future ozone than any of the other mitigation options considered here.

Change in Ozone in Response to Alternative Scenarios



Change in GWP-Weighted Emissions in Response to Alternative Scenarios

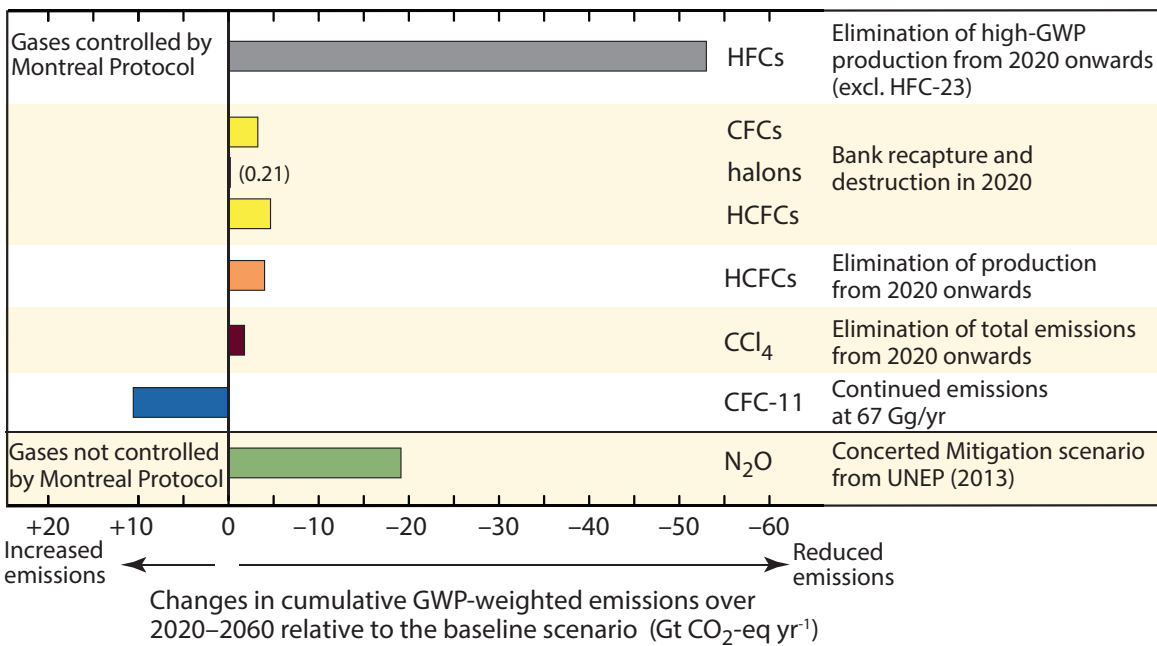


Figure 6-1. Ozone and climate-relevant impacts of alternative future scenarios compared with the baseline scenario. The climate-relevant metric is chosen to be the integrated GWP-weighted emission from 2020 to 2060, and the ozone-relevant metric is the percentage change in total column ozone averaged over 2020 to 2060. A decrease in total ozone and an increase in GWP-weighted emissions occur when future emissions are higher than in the baseline scenario for the compounds considered. Numerical values of these changes are shown in **Table 6-5**.

CHAPTER 6

SCENARIOS AND INFORMATION FOR POLICYMAKERS

6.1 INTRODUCTION

The World Meteorological Organization (WMO) Ozone Assessments have reported on the ozone layer and related processes since the 1980s. Since 1989, the Assessments have focused on reviewing progress of the control measures introduced under the 1987 Montreal Protocol and its subsequent Amendments and adjustments. The Protocol is widely acknowledged to have been highly successful, resulting in striking reductions in the total amount of ODSs in the atmosphere (see **Chapter 1**) and more recently in an upturn in upper-stratospheric ozone levels (**Chapter 3**), giving confidence in the projections that ozone will recover sometime around mid-century at mid-latitudes and the Arctic, and somewhat later for the Antarctic. In addition, it was shown around a decade ago that the Montreal Protocol and its Amendments and adjustments had contributed more to climate change mitigation than any other existing international agreement at that time (Velders et al., 2007).

In this chapter, we focus on possible options and scenarios to aid policymakers in decisions related to protecting stratospheric ozone and minimizing effects on climate from ODS halocarbons and their replacements. As production and consumption of controlled ODSs have continued to decline, options for reducing their future emissions have become somewhat more limited but still exist and with significant potential for ozone and climate protection. One potentially important new result is a slower decline in CFC-11 atmospheric concentrations than projected in the last Assessment; the implications of this result are discussed in **Section 6.4**. Also, growth in very short-lived substances, such as CH_2Cl_2 , and other compounds not covered by the Protocol (e.g., N_2O) could have important effects on the future evolution of stratospheric ozone.

A major new development relating to policy is the Kigali Amendment to the Montreal Protocol, which introduces controls on HFCs. HFCs are replacement compounds that have only small effects on ozone depletion. However, many of these compounds in

current commercial use are strong greenhouse gases and therefore affect climate. The Kigali Amendment comes into force on January 1, 2019, as it has now been ratified by the threshold 20 parties to the Montreal Protocol. This chapter summarizes the projected impacts of the Kigali Amendment on climate (which are discussed in detail in **Chapter 2**) and also examines some other processes and policies unrelated to Montreal Protocol gases, including impacts of proposed stratospheric aerosol geoengineering interventions that might alter stratospheric ozone.

6.1.1 Summary of Findings from the Previous Ozone Assessment

Chapter 5 of the previous Assessment evaluated the impacts of various hypothetical policy options for reducing future emissions of ODSs, including elimination of production and bank recapture and destruction (Harris and Wuebbles et al., 2014). Updates to Ozone Depletion Potentials (ODPs), Global Warming Potentials (GWPs) and, for the first time in an Ozone Assessment, Global Temperature change Potentials (GTPs), were also presented. The main findings were

- Emissions from the 2015 ODS banks through to 2050 were projected to lead to greater future ozone depletion and climate forcing than those caused by future ODS production. Halon banks were projected to contribute most to ozone depletion, while CFC and HCFC banks were expected to contribute most in terms of GWP-weighted emissions.
- The impact on the recovery of stratospheric ozone of further policy actions on ODSs that had already been controlled was becoming smaller, but if all ODS emissions ceased (including from banks), then the return to 1980 mid-latitude equivalent effective stratospheric chlorine (EESC) values would be brought forward by about 11 years from the baseline scenario of 2047.
- Global ozone was expected to increase to above pre-1980 levels due to future projected increases

in carbon dioxide (CO₂) and methane (CH₄), which act to increase globally averaged ozone.

- Future CCl₄ emissions remained more uncertain than for other ODSs due to incomplete understanding of the current budget—with likely missing source(s)—but were expected to remain an important factor in the evolution of EESC.
- There was still insufficient research available to confidently compare the options of mitigating emissions of anthropogenic very short-lived substances (VSLs) with those of the longer-lived ODSs, but VSLs were expected to play a relatively larger role in future ozone depletion if long-lived controlled halocarbons followed their projected decline.
- Quarantine and pre-shipment (QPS) uses of CH₃Br—which are exempted uses not controlled by the Montreal Protocol—constituted an annual consumption that was larger than that from uses controlled by the Protocol. The elimination of future emissions from QPS uses would have brought forward the date of EESC return to 1980 levels by 1.1 years relative to the baseline scenario.
- The direct radiative forcing (RF) from ODS halocarbons (CFCs, halons, and HCFCs) in 2014 was about 0.33 W m⁻² and near its expected peak. The RF was projected to decrease to about 0.20 W m⁻² by 2050 and to near 0.10 W m⁻² by 2100, assuming continued compliance with the Montreal Protocol.
- While HFCs constituted less than 1% of the RF on climate (0.02 W m⁻²), if the mix of HFCs remained unchanged, increasing demand would have implied a radiative forcing for HFCs as high as 0.4 W m⁻² by 2050. Replacement of the current mix of high-GWP HFCs with low-GWP compounds was projected to have the potential to lead to a decrease in the projected RF possibly by as much as 0.07 W m⁻² by 2030 relative to the baseline scenario. HFC banks were also stated to be an important consideration when estimating the impact of HFC mitigation on future climate change.
- If (hypothetical) geoengineering of the climate system via anthropogenic increases of stratospheric sulfate aerosols were to occur within the

next few decades, it could deplete stratospheric ozone, with the largest effects in the polar regions, although quantitative studies were limited.

Since the last Assessment, in addition to peer-reviewed publications, several reports have addressed topics of direct interest for this chapter:

- The SPARC report, *Solving the Mystery of Carbon Tetrachloride* (SPARC, 2016). This report identifies four specific emission pathways for CCl₄, which have not been well quantified by previous Ozone Assessments, and shows that these pathways, combined with revised lifetime estimates for CCl₄, result in a reduced discrepancy between known atmospheric sources and sinks. These pathways are (1) fugitive emissions from incineration, feedstock usage, and process agents; (2) unreported non-feedstock emissions during production of chlorinated methanes and perchloroethylene; (3) unreported inadvertent emissions during the production and use of chlorine gas; and (4) legacy emissions from contaminated land areas.
- Reports produced by the UNEP Technology and Economic Assessment Panel (TEAP). These reports continue to assess the technological and economic possibilities for phasing in commercially available replacements for ODSs (e.g., UNEP, 2016). This provides key information on the technical feasibility of scenarios considered in this chapter that assume reductions in future production or the capture and destruction of banks.

6.1.2 Key Issues to Be Addressed in This Assessment

The majority of this chapter is dedicated to assessing the potential future impacts of a number of ozone-relevant processes and activities on ozone depletion and climate forcing, in order to aid policy decisions regarding stratospheric ozone protection and related climate issues. Simple, well-established metrics are used to provide information about the effect of emissions from human activity on stratospheric ozone and climate. Ozone metrics include Ozone Depletion Potentials (ODPs) and equivalent effective stratospheric chlorine (EESC). Climate metrics used are Global Warming Potentials (GWPs), Global Temperature change Potentials (GTPs), and radiative

forcing (RF). GWPs and GTPs are presented for an extensive set of less common HCFCs for the first time and are updated for other HCFCs and HFCs in Group I of Annexes A, C, and F of the Kigali Amendment. New ozone and climate metrics for short-lived halolefins, which are characterized by very small ODPs, GWPs, and GTPs, are also reported.

New scenarios that incorporate previously reported bottom-up bank estimates, the latest ODS mixing ratio observations, and reported production are generated in this chapter, and the potential impacts on future ozone depletion and climate forcing are calculated. These scenarios investigate effects of hypothetical changes in emissions and are illustrative of potential mitigation actions. For the first time, projections of an anthropogenic VSLs (CH_2Cl_2) are incorporated into these scenarios. The impact of future HFC abundances on climate forcing, with regard to the Kigali Amendment (**Section 6.2.1.2**), is also assessed, using the scenarios presented in **Chapter 2**.

Consistent with **Chapters 3** and **4** in this Assessment in their analyses of future projections of ozone, we use the Representative Concentration Pathway (RCP) 6.0 scenario (IPCC, 2013) as the baseline emission scenario for CO_2 , CH_4 , and N_2O . The sensitivity of the projected impacts of these greenhouse gases on stratospheric ozone is investigated by additionally using the RCP2.6, RCP4.5, and RCP8.5 scenarios. Our primary reason for using a variety of future greenhouse gas (GHG) scenarios is to assess the range of ozone impacts of the compounds relative to those controlled under the Montreal Protocol. The RCP2.6 scenario is the one that most closely complies with the stated goal of the Paris Agreement to hold “the increase in the global average temperature to well below 2°C above pre-industrial levels and pursuing efforts to limit the temperature increase to 1.5°C above preindustrial levels” (IPCC, 2013a). It should be noted that a new group of scenarios (Shared Socioeconomic Pathways, or SSPs) has recently been developed. The SSPs are based on alternative socioeconomic projections that could arise from plausible major global developments (O’Neill et al., 2017; Riahi et al., 2017). This new scenario framework, established by the climate change research community, will be used for the new generation of earth system models as part of the Coupled Model Intercomparison Project Phase 6 (CMIP6). Here, in common with the rest of this Assessment, we

use the RCP scenarios that were adopted by the IPCC for its Fifth Assessment Report (IPCC, 2013b).

In common with previous Assessments, this chapter also assesses some other potential influences on stratospheric ozone that do not involve the emission of chlorine- and bromine-containing source gases, including deliberate climate intervention and rockets. Here, and elsewhere in the chapter, key gaps in our understanding that prevent a firm assessment of future ozone levels are identified.

6.2 ISSUES OF POTENTIAL IMPORTANCE TO STRATOSPHERIC OZONE AND CLIMATE

6.2.1 Halocarbons Controlled Under the Montreal Protocol

Implementation of the Montreal Protocol controls has resulted in significantly lower EESC than would otherwise have occurred (WMO, 2014, and preceding reports) as well as significant reductions in radiative forcing of climate change. The majority of ODSs that were originally controlled under the Montreal Protocol are now declining in the atmosphere. The atmospheric abundance of CFCs has declined substantially (**Chapter 1**) mainly due to their substitution by HCFCs, HFCs, and not-in-kind (NIK) solutions including non-fluorinated compounds; although some CFCs, notably CFC-11, have not dropped as quickly as expected over the last few years, and the reasons for this are not well understood. The observed rate of decline of atmospheric CCl_4 also remains slower than predicted, and there is new understanding of potential additional sources that include by-product emissions from chloromethane and perchloroethylene plants, although a discrepancy between sources and sinks still exists. **Section 6.4** discusses the implications of these uncertainties on future EESC.

Atmospheric CH_3Br results from both natural and anthropogenic emissions, the latter mainly from its use as a fumigant. The atmospheric abundance of CH_3Br has continued to decline, most likely due to the phase-out (completed in 2015) of controlled industrial production and consumption (**Chapter 1**). Critical use exemptions (CUEs) for the controlled uses, applied for by developed countries since 2005 and by developing countries since 2015, have declined dramatically from

their peak in 2005 of 21.8 Gg yr⁻¹ and now represent only a small fraction (<10% or 0.7 Gg) of annual use of CH₃Br. Quarantine and pre-shipment (QPS) uses of CH₃Br, which are not controlled by the Montreal Protocol, have remained relatively stable over the last decade and in 2016 constituted an annual consumption of 8.4 Gg.

HCFCs, which are transitional replacement compounds, are still increasing in the atmosphere, although growth rates have slowed in response to their phaseout schedules, which were established first in 1992 with an accelerated phaseout established in 2007 (Harris and Wuebbles et al., 2014). In non-Article 5 countries, HCFC production started decreasing around 2000, well before the phaseout schedule started in 2004, whereas the production of HCFCs in Article 5 parties continued to rise until 2012 and started decreasing just when the phaseout schedule went into effect in 2013 (UNEP, 2017). The consumption of HCFCs in Asia in Article 5 parties in 2015 accounts for the majority of global consumption at around 70%. Thus, for achieving further global HCFC emissions reductions, complying with or even accelerating the earlier phaseout schedule (by promoting the replacement of HCFCs by low-GWP fluorinated compounds or non-fluorinated compounds and other NIK solutions) in Asia plays an important role in reducing future HCFC emissions. An important source of emissions not controlled by the Montreal Protocol is emissions from banked ODSs, mainly from uses such as refrigerants and foams. If no further policy actions for banked ODSs are considered in Article 5 parties, especially in Asia, emissions from banked HCFCs will become larger than those of banked CFCs (Daniel et al., 2011). Thus, banked HCFCs will be a major source of both ODSs and climate emissions in the coming decades. Effective measures for reducing emissions from banked HCFCs are recovery and destruction from banked ODSs when equipment that uses refrigerants and foams is disposed, together with appropriate management for reducing leakage during the operation of such equipment (Box 5-1 of Harris and Wuebbles et al., 2014). In **Section 6.4** we discuss the effect on future EESC and ozone of policy options that include reducing HCFC leakage by bank recapture and destruction and eliminating production of HCFCs.

Halons are particularly important to ozone depletion because they contain bromine, which is roughly 60 times more effective at depleting ozone than chlorine. However, because of their smaller atmospheric concentrations, halons influence climate to a much smaller degree than other ODSs such as CFCs, HCFCs, and CCl₄. In Harris and Wuebbles et al. (2014), future leakage of halons from their banks was found to be the largest contributor to ozone depletion through to 2050. While, for the Assessments, we assume that bank capture is 100% effective, in reality the accessibility and profitability of the various banks are important factors in destroying emissions; for example, halon bank capture from fire-fighting equipment for use in new aircraft where alternatives are not available is generally much more cost effective than CFC and HCFC bank capture from foams used in home insulation where alternatives are widely available.

6.2.1.1 REPLACEMENT COMPOUNDS

The reduction in ODS emissions has occurred as a result of NIK technology; containment, recovery, and recycling actions; and replacement by compounds that do not have significant ODPs. Examples of NIK technology include mechanical pumps or hydrocarbons to replace ODS propellants in consumer and commercial applications, CO₂ or hydrocarbons to replace ODSs in foam-blowing applications, and ammonia in industrial refrigeration. Ammonia and the hydrocarbons used (ethane, propane, and butane) do not have any significant impact on stratospheric ozone or radiative forcing of climate change. Of the in-kind replacement compounds, HFCs are by far the most important (for climate; they are non-ozone depleting), with HFC-134a accounting for the majority of HFC production, emissions, atmospheric concentration, and radiative forcing (see **Chapter 2**). Oxygenated compounds (e.g., hydrofluoroethers) have found use in niche applications. The decreased use of CFCs, and now HCFCs, has resulted in increased HFC use, particularly in the refrigeration and air conditioning sectors and, to a lesser degree, in the foam and fire protection sectors. Annual global production of CFCs peaked in the late 1980s (UNEP, 2017), HCFC production peaked in the late 2000s (UNEP, 2017), and HFC production and emissions continue to increase (McCulloch and Midgley, 2001; Velders et al., 2015a) (see also **Chapters 1** and **2**). As

will be discussed in **Section 6.2.6**, the atmospheric degradation of HFCs neither contributes significantly to tropospheric ozone formation nor yields products that pose a significant known risk to human or ecosystem health.

HFCs typically have lower GWPs than the CFCs and HCFCs they have replaced. Yet, some HFCs such as HFC-23 (GWP = 12,400), HFC-143a (GWP = 3,170), and HFC-125 (GWP = 4,800), and to a lesser extent HFC-134a (GWP = 1,300), have high GWPs. While the current contribution of HFCs to radiative forcing of climate is small at approximately 0.02 W m^{-2} (see **Chapter 2**), the potential future growth in the emissions of high-GWP HFCs has given rise to concerns about their possible future climate impact (UNEP, 2011; Velders et al., 2009; Velders et al., 2015b; Velders et al., 2012; WMO, 2011; 2014; Wuebbles et al., 2013) and to the Kigali Amendment of the Montreal Protocol discussed in the next section.

To minimize ozone layer depletion and have minimal impact on climate, ODS replacements need to have low ODPs and low GWPs. Meeting such conditions requires replacement compounds to not contain chlorine or bromine, have short lifetimes, and/or have weak infrared (IR) absorption cross-sections.

Halogenated alkenes (halogenated olefins, HFOs) such as HFO-1234yf, HFO-1234ze(E), HCFO-1233zd(Z), and HCFO-1233zd(E) are commercially important short-lived replacement compounds (Brown, 2009; Burkholder et al., 2015; Wallington et al., 2010; 2017). Members of this class of compounds have low ODPs and GWPs (**Appendix A**) and have been developed for use as refrigerants, aerosol propellants, degreasing agents, and foam-blowing agents (Burkholder et al., 2015; Wallington et al., 2017). HFOs can be used on their own or as blends with HFCs. A number of other short-lived compounds have also been proposed as replacements for long-lived ODSs and HFCs (see **Chapter 1**).

The energy efficiency of the equipment used can also be very important to the indirect impact of replacement compounds on climate forcing. In fact, for some applications, the indirect impact on climate through energy efficiency can be far more important than the direct impact through emissions of the gas itself, as discussed below and in **Chapter 2**.

6.2.1.2 KIGALI AMENDMENT

The Kigali Amendment comes into force on January 1, 2019, as it has now been ratified by the threshold 20 parties to the Montreal Protocol. Under Annex F, it includes 18 controlled HFC substances and forms a framework of regulations in 4 country groupings; the main non-Article 5 (non-A5) parties, other non-A5 parties, Group I A5 parties, and Group II A5 parties. It subsumes all current policies for HFCs. Unlike the current restriction of ODSs listed in the Montreal Protocol, rather than aim for a complete phaseout, the amendment aims to achieve 80–85% phaseout of production and consumption of HFCs compared to baseline levels. The amendment aims to implement the phasedown of HFC production and consumption starting in 2019 for most developed countries, in 2024 for most developing countries, and in 2028 for some developing countries. The Amendment also mandates that HFC-23 emissions should be destroyed to the extent practicable by all countries.

The Kigali Amendment will significantly limit the future production and consumption of HFCs. Under the current control measures, emissions of HFCs are projected to peak around 2035, about a decade after the peak in global production and consumption, due to gradual emissions from refrigeration and air-conditioning equipment (so-called banks). The HFC bank, therefore, represents a substantial source of emissions and radiative forcing after production is phased down (Velders et al., 2014). Emissions of HFC-23 (formed as a by-product of HCFC-22 manufacture, see **Section 6.2.1.3**) should also be significantly limited. The contribution of HFCs (excluding HFC-23) to the global average surface temperature change is projected to reach a maximum—assuming compliance with the Kigali Amendment—of around 0.07°C by 2060, after which it decreases slowly to about 0.06°C by 2100 (**Chapter 2**). Without Kigali, surface temperature warming from HFCs might have been as high as 0.3°C – 0.5°C by 2100 (**Chapter 2**). Of course, adjustments to the HFC control schedules analogous to historical adjustments to the ODS control schedules could substantially reduce the climate impact.

The Kigali Amendment regulations mandate not only different phasedown schedules of production and consumption (for the different country groupings) but also different settings of base year and baseline

expressed in CO₂ equivalents. The baselines in non-A5 parties are set based on historical data of HFCs (2011–2013) plus 15% of the baseline consumption of HCFCs, whereas the baselines in A5 parties are set at the average amounts of HFCs from 2020 to 2022 in Group I countries, and the average amounts of HFCs from 2024 to 2026 in Group II countries, plus 15% of the baseline consumption of HCFCs for both groups (Chapter 2, Table 2-3). Thus, the effects of emissions reductions due to the Kigali Amendment will depend on the levels of baseline consumption in A5 parties even before the phasedown schedule starts, which in turn depends on incentives to reduce the consumption of HFCs and promote the replacement to non-fluorinated compounds.

Options are available to accelerate the phasedown schedule and provide additional avoided GWP-weighted emissions of HFCs, including use of technologically feasible low-GWP alternatives in place of high-GWP HFCs in refrigeration and air-conditioning equipment during the phasedown (Xu et al., 2013). Additional benefits of the Kigali Amendment could be gained via the development of more energy-efficient equipment that uses these low-GWP replacements, since the CO₂ emissions resulting from the energy used by the equipment are important contributors to the total climate impact related to refrigerant use (e.g., Shah et al., 2015).

6.2.1.3 HFC-23

HFC-23 is formed as a by-product at the reactor stage of the manufacture of HCFC-22. Atmospheric emissions can be avoided if HCFC-22 production is managed for better containment and if the HFC-23 is incinerated. Incineration projects in developing countries have been supported through the Clean Development Mechanism (CDM) of the Kyoto Protocol (<http://cdm.unfccc.int>), allowing a significant fraction of the HFC-23 produced in HCFC-22 facilities to be incinerated during the period 2006–2013. Despite these mitigation efforts, there has been a resurgence in emissions since 2009 (Rigby et al., 2014), with emissions in 2013–2015 similar to or slightly higher than in 2006, when CDM-facilitated destruction had yet to be fully implemented (Simmonds et al., 2018). This increase in emissions is attributed mainly to the fact that no new CDM projects were awarded after 2009, while HCFC-22 production for feedstock use in

non-Annex 1 countries (mainly China) was increasing, including from plants that did not have abatement technology (Fang et al., 2014; Simmonds et al., 2018). The Montreal Protocol regulates for dispersive uses of HCFC-22 (such as refrigerants and foams), which are being reduced. However, around half of the current production of HCFC-22 is for feedstock uses (Miller et al., 2010; WMO, 2014) (such as fluorine-contained resin and components of sophisticated technologies), which are uncontrolled. Total HCFC-22 production increased rapidly in the past few decades but has recently stabilized (Miller et al., 2010), showing that expansion of feedstock use has not matched the decrease in emissive uses and indeed also appears to have stabilized over the last few years.

The Kigali Amendment mandates all HCFC-22 producing facilities to collect and destroy the emitted HFC-23 by-product “to the extent practicable,” although reduction schedules and frameworks are still under discussion. The emission reductions can be gained for most developing countries because many companies set up destruction facilities under the CDM. However, although the incremental cost of HFC-23 destruction is far less than the price paid by the CDM, the cost for renewal of the destruction facilities and operating the incineration may be an issue for some developing countries. In summary, emissions of HFC-23 are expected to be reduced under the full implementation of the Kigali Amendment, assuming declines mandated by the Protocol outpace any increases in HCFC-22 production. However, the future trajectory of HFC-23 emissions is uncertain and depends on the amount of HCFC-22 produced, the efficiency of avoiding unwanted HFC-23 by-products, and whether the amount of HFC-23 incinerated increases or decreases.

6.2.2 Breakdown Products

The atmospheric degradation of HCFCs, HFCs, and HFOs is initiated by reaction with OH radicals leading to the formation of halogenated carbonyl compounds, which undergo further oxidation to yield HF, HCl, CO₂, and, in some cases, trifluoroacetic acid (TFA) (Burkholder et al., 2015; Calvert et al., 2008; IPCC/TEAP, 2005; Wallington et al., 1994; WMO, 2011, 2014). The photochemical ozone creation potentials of HCFCs, HFCs, and HFOs are very small, and tropospheric ozone formation resulting from their

degradation is of negligible importance (Hayman and Derwent, 1997; Luecken et al., 2010; Wallington et al., 2015; WMO, 2011, 2014). The additional burden of HF, HCl, and CO₂ at the concentrations expected from atmospheric degradation of HCFCs, HFCs, and HFOs is of no consequence.

TFA is a product of the atmospheric degradation of HCFC-123 and several commercially important ODS replacement compounds such as HFC-134a, HFO-1234yf, and HFC-227ea. HFO-1234yf has five times the TFA breakdown products than the HFC-134a it replaces in mobile air conditioners. TFA is a ubiquitous natural component of the hydrosphere, with many sources beyond the halocarbons controlled under the Montreal Protocol (e.g., Scheurer et al., 2017). It is present in ocean water, even at great depths and in remote locations, at a concentration of approximately 200 ng/l (Solomon et al., 2016). In surface freshwater, TFA levels are typically 10–300 ng l⁻¹. TFA is stable in the environment and accumulates in terminal water bodies such as salt lakes. TFA levels in the Dead Sea have been reported to be 6,400 ng l⁻¹ (Boutonnet et al., 1999). Currently, the oxidation of HFC-134a makes the largest contribution from ODS replacements to TFA formation. The global background atmospheric concentration of HFC-134a is approximately 100 ppt. Assuming a 7–20% molar yield of TFA (Wallington et al., 1996), rainout as the sole atmospheric fate of TFA, and annual global precipitation of 5×10^{17} liters Warneck and Williams (2012) give an estimate of 20–50 ng l⁻¹ for the current average TFA concentration in global precipitation resulting from HFC-134a degradation. Local concentrations will be higher or lower than the global average depending on local precipitation volumes and photochemical activity. The concentrations of TFA observed in rainwater typically substantially exceed those that can be accounted for by HFC-134a degradation, indicating the presence of significant sources other than HFC degradation (Frank et al., 1996; McCulloch and Lindley, 2003; Wu et al., 2014a, b). HFC-134a is currently being replaced by HFO-1234yf in applications such as mobile air conditioners. HFO-1234yf has a higher, 100%, molar TFA yield and degrades more rapidly and closer to its emission sources than HFC-134a with 20% molar TFA yield. Luecken et al. (2010), Russell et al. (2012), Henne et al. (2012), Kazil et al. (2014), and Wang et al. (2018) have estimated TFA concentrations

in rainwater resulting from future use of HFO-1234yf and report similar findings. Average concentrations in rainwater are projected to be of the order of 1,000 ng l⁻¹. Regions with lower rainfall have higher concentrations but lower total deposition. Increases in TFA levels in terminal water bodies in North America of 1,000–15,000 ng l⁻¹ with a maximum of 200,000 ng l⁻¹ in the Sonoran Desert were projected in a modeling study of 50 years of future HFO-1234yf use (Russell et al., 2012).

It has been shown recently that the reaction of Criegee intermediates with TFA in the gas phase is extremely rapid (Chhantyal-Pun et al., 2017). Criegee intermediates are present in the atmosphere as a result of the reaction of ozone with alkenes and play an important role in atmospheric chemistry over landmasses with vegetation, where biogenic emissions of alkenes (e.g., isoprene and terpenes) are significant and ozone is available. Reactive loss of TFA via reaction with Criegee intermediates could be an important loss mechanism for TFA, and it has not been accounted for in atmospheric models of TFA deposition. Inclusion of this new gas-phase chemistry in atmospheric models could decrease the projected deposition of TFA over landmasses (by as much as a factor of two) (Chhantyal-Pun et al., 2017).

The effects of TFA on human and ecosystem health resulting from the use of compounds regulated under the Montreal Protocol have been assessed by Solomon et al. (2016). Mammals are insensitive to TFA (Boutonnet et al., 1999), and plants and other animals have a high tolerance to TFA. Solomon et al. (2016) tested a worst-case scenario with upper-limit TFA levels estimated for the future use of HFC-134a, HFO-1234yf, HFC-143a, and HFC-227ea through the year 2050 and selecting the most sensitive biological endpoints for different species. The no-observed-effect-concentrations for aquatic organisms considered by Solomon et al. (2016) were in the range 3×10^7 – 2.4×10^9 ng l⁻¹, with an outlier at 1.2×10^5 ng l⁻¹. Risks for humans, terrestrial vertebrates, plants exposed via soil, and aquatic plants and animals were assessed to be de minimis (Solomon et al., 2016). Risks for organisms in salt lakes and playas were not assessed because there are no data on the toxicity of TFA for such organisms. It was noted that future increases in TFA levels resulting from ODS replacement degradation in salt lakes will be small compared to the

existing burden of other natural salts in such locations (Solomon et al., 2016). The large body of published field measurements, toxicological studies, modeling studies, and environmental assessments point to a clear conclusion: The current and estimated future concentrations of TFA and its salts resulting from degradation of HCFCs, HFCs, and HFOs do not pose any known significant risk to human or ecosystem health (Solomon et al., 2016).

6.2.3 Very Short-Lived Substances (VSLs; Biogenic and Anthropogenic)

VSLs have not been controlled by the Montreal Protocol since it has been mistakenly assumed they have a negligible impact on stratospheric ozone due to their short atmospheric lifetimes and/or because they are dominated by biogenic sources. Previous Assessments had considered *n*-propyl bromide as an ODS with a latitude-dependent ODP. Since the last Assessment, a number of new studies predict a significant impact of VSLs on ozone as discussed below.

Chlorinated VSLs are predominantly anthropogenic in origin (**Chapter 1**). They currently contribute only a small fraction (<10%) to total stratospheric chlorine but are becoming more relevant for stratospheric ozone due to increased emissions of CH_2Cl_2 , which is used as an industrial solvent, as a blowing agent in the production of foam plastics, and as a feedstock or by-product in the production of other chemicals (Campbell and Shende, 2005; Simmonds et al., 2006). Surface concentrations have increased by around 8% (2.85 ppt) per year between 2004 and 2014 (Hossaini et al., 2017). Assuming this mean growth rate continues linearly, Hossaini et al. (2017) predict that CH_2Cl_2 could delay the return of total lower stratospheric Cl_y to pre-1980 levels by 15–17 years, and by 2050, reduce annual mean ozone concentrations in the lower stratosphere by 6%—effects that are much larger than the influence of potentially eliminating future small levels of production or emission of CFCs and HCFCs. In **Section 6.4** we examine the effects of eliminating emissions of CH_2Cl_2 on future ozone and the influence of different RCPs and varying OH levels on projections of the impact of CH_2Cl_2 on future ozone.

Biogenic VSLs—mainly CHBr_3 and CH_2Br_2 —account for an appreciable fraction (~30%) of total stratospheric bromine. The majority of CHBr_3 and

CH_2Br_2 emissions come from oceanic marine algae, mainly seaweeds (Carpenter and Liss, 2000). While most models currently assume fixed emissions or atmospheric mixing ratios of VSL Br (Hossaini et al., 2016), oceanic emissions may undergo future climate-induced or other anthropogenically induced changes. Changes in surface winds and sea surface temperature and removal of sea ice would likely increase the oceanic sea–air fluxes of VSL Br (Tegtmeier et al., 2015; Falk et al., 2017); however, possible changes in biological oceanic production are not sufficiently well understood. While currently believed to be small (Leedham et al., 2013), future anthropogenic emissions of VSL Br in the form of seaweed aquaculture have also been projected to substantially increase over the next years, particularly from Southeast Asia (Radulovich et al., 2015; WMO, 2014). The ODPs of VSLs are highly sensitive to growing emissions in this region (e.g., Tegtmeier et al., 2015).

The effectiveness of both brominated and chlorinated VSLs as ODSs depends not only on their emissions but also on chemical processing and the strength and location of convective transport (**Chapter 1**). In addition, the phaseout of the long-lived chlorinated source gases under the Montreal Protocol and the resulting decline in stratospheric chlorine mean that bromine-mediated O_3 destruction via the $\text{BrO} + \text{ClO}$ catalytic cycle will decrease over the 21st century. However, there is not currently a consensus on whether the combination of these factors causes a delay in the return of Antarctic ozone to pre-1980 levels due to bromine VSLs. Falk et al. (2017) find that changes in atmospheric chemistry and transport and a decrease of anthropogenic chlorine may result in a decrease in the total amount of stratospheric Br_y VSLs and its impact on ozone during the 21st century, despite increasing VSL Br emissions. In contrast, Tegtmeier et al. (2015) project a 31% increase of the ODP-weighted emissions of CHBr_3 by 2100, compared to present values under the RCP8.5 scenario, due to a larger convective updraft mass flux in the upper troposphere and increasing emissions, offset by less effective catalytic ozone destruction. Fernandez et al. (2017) find that VSL Br chemistry affects the depth and duration of the Antarctic ozone hole and will dominate Antarctic ozone seasonality by 2100, but that its inclusion in a global model does not result in a significant delay to the modelled ozone return date to 1980 levels.

Conversely, Yang et al. (2014) and Oman et al. (2016) derived an increase of between 7 and 10 years in the return date when VSLs Br are included.

In summary, emissions of VSLs Br from seaweed farming and from physical sea–air exchange may increase in the future, but overall changes in VSLs Br emissions from these combined effects, along with potential climate-induced changes in natural oceanic production, are not known to any degree of certainty. Whether increased future VSLs Br emissions would actually lead to a delay in O₃ recovery is also highly uncertain, with contrasting results due to structural differences between models and internal model variability.

Previous Assessments have concluded that iodine chemistry likely has a negligible role in determining levels of stratospheric ozone, based on available remote-sensing measurements of iodine in the lowermost stratosphere. Saiz-Lopez et al. (2015) however calculate that significant levels of total reactive iodine, between two and five times larger than the currently assumed upper limits, can be injected into the stratosphere and exert an ODP similar to, or even larger than, that of VSLs Br. There are currently no projections of how iodinated VSLs might affect the future evolution of the stratospheric ozone layer, although oceanic iodine emissions are predicted to have increased over the 20th century due to increases in surface ozone concentrations (Sherwen et al., 2017).

6.2.4 The Key Climate Gases: Carbon Dioxide, Methane, and Nitrous Oxide

The most important drivers of climate change over the last century are the well-mixed greenhouse gases (GHGs) carbon dioxide (CO₂), methane (CH₄), and nitrous oxide (N₂O), with HFCs as a growing new threat to climate as a consequence of its widespread use as a transitional substitute for ODSs. With atmospheric lifetimes of a decade or more, these gases are circulated and mixed around the globe to yield small inter-hemispheric gradients. The atmospheric abundances and associated radiative forcings on climate from these gases have increased substantially in the industrial era (see **Chapters 1, 3, and 5**). Future changes in halogen concentrations will take place against the backdrop of the changes occurring in the climate and in the chemical and radiative effects

of these GHGs. The Paris Agreement within the United Nations Framework Convention on Climate Change (UNFCCC) enhances previous UNFCCC targets for reducing overall climate forcing, starting in the year 2020, and aims to limit the global average temperature increase this century to well below 2°C above preindustrial levels and to pursue efforts to limit the temperature increase to 1.5°C. Within the Agreement, each country determines its own contribution towards the global goals, called Nationally Determined Contributions (NDCs). One key aspect for the Montreal Protocol is that the Paris Agreement does not give stringent guidance on the levels of the most important climate gases for stratospheric ozone, namely CH₄ and N₂O. Changing concentrations of CH₄ and N₂O can significantly affect the amounts of hydrogen oxides (HO_x) and nitrogen oxides (NO_x) concentrations in the stratosphere, which also affect the concentration and distribution of ozone. The NO_x produced from dissociation of N₂O decreases stratospheric ozone, while CH₄ can lead to regions of net ozone production, particularly in the troposphere, and to regions of depletion, but in the global average leads to additional ozone. The continuing increase in the global CO₂ concentration and, to a lesser degree, the increase in global CH₄ concentration also have important effects on stratospheric ozone through cooling of the stratosphere, which slows the ozone chemical loss rates. The resulting climate change from increasing GHGs also strengthens the stratospheric Brewer–Dobson circulation (BDC), which will redistribute ozone (see **Chapter 5**).

Future ozone levels will be strongly dependent on the actual future emissions and concentrations of these climate gases. Once the NDCs of the major countries are available beyond the current estimates of 2030, going out to mid-century or beyond, it will be possible to better estimate the impact of the Paris Agreement on the future state of the ozone layer and also better determine the dates for the return of the ozone layer to its 1980 values. As shown in Rogelj et al. (2016), the initial NDCs do not hold globally averaged temperature increases below 2°C, and so further reductions in projected GHG emissions, with associated different impacts on stratospheric ozone, are expected if climate actions are taken to meet the Paris Agreement. **Section 6.4** examines how the changing concentrations of these gases according to selected RCPs

adopted by the IPCC for its Fifth Assessment Report (IPCC, 2013b) could affect future changes in ozone relative to the changing emissions and concentrations of halogens. Of the RCPs, the RCP2.6 scenario is the closest one holding global temperature increase below 2°C (IPCC, 2013a).

6.2.5 Deliberate Climate Intervention

6.2.5.1 GEOENGINEERING VIA STRATOSPHERIC SULFATE AEROSOL MODIFICATIONS

Increasing the burden of stratospheric aerosols, also called stratospheric aerosol geoengineering, has been proposed as a method to increase the reflectivity of Earth's atmosphere in order to counteract some effects of climate change. The most discussed application is using the continuous injection of SO₂ (or H₂SO₄) into the tropical stratosphere. Despite similarities to short-term impacts of volcanic eruptions, the impact of geoengineering strategies on the climate system would be different, since they would have to be applied over an extended period of time to continuously cool Earth's surface. The increase in stratospheric aerosol surface area density (SAD) as a result of increasing sulfur injections over a continuous time period would increase surface cooling, but it would also cause an increase in heterogeneous ozone loss cycles involving reactive chlorine (ClO_x), bromine (BrO_x), and hydrogen (HO_x) (see **Appendix 6A**). On the other hand, the reduction of nitrogen oxides through increasing heterogeneous reactions (mostly important in the tropical mid-stratosphere) could actually increase ozone and counteract a potential decrease in tropical column ozone as the result of projected increasing GHGs. These chemical effects of geoengineering on ozone would be reduced by the end of the 21st century because of the projected future decrease in ODSs and consequent halogen activation through heterogeneous reactions.

In addition to chemical changes, an increased stratospheric aerosol burden could also cause larger dynamical changes, including heating of the lower tropical stratosphere and a speedup of the BDC, including changes in tracer transport towards high latitudes, which in part would counteract the change in ozone due to chemistry (**Appendix 6A**). For large injection amounts, this may even cause an increase in column ozone in the Northern Hemisphere (NH) winter mid-latitudes compared to a non-geoengineering

scenario (Tilmes et al., 2018). Changes in tracer transport and UV as a result of changes in column ozone and aerosol scatter may also increase tropospheric methane lifetime (Visoni et al., 2017b), may alter stratosphere-to-troposphere exchange of ozone and other tracers (Xia et al., 2017), and would weaken the tropospheric jet streams (Richter et al., 2018). The potential heating of the tropopause may further cause a significant increase in stratospheric water vapor, impacting radiation and chemistry.

Column ozone changes as the result of stratospheric aerosol geoengineering therefore depends on the injection amount, timing (ODS loading), and injection strategy (influencing aerosol size and location; **Appendix 6A**). Relatively small and constant injections of 2.5–4 Tg S yr⁻¹ between 2020 and 2070, which would result in 0.5°C of surface cooling, are calculated to lead to an approximately 4% reduction in the global stratospheric column ozone for 2020 and only 1% reduction by 2070 (Pitamy et al., 2014; Xia et al., 2017). Much larger injection amounts that would lead to a surface temperature cooling of around 2°C in 2040–2050, based on a single model study, would result in reductions in column ozone of 28–40% in October over Southern Hemisphere (SH) high latitudes and 8–18% for NH high latitudes in March, with varying values depending on the injection altitude (Tilmes et al., 2018). Injections closer to the tropopause cause a stronger dynamical response and could result in up to an 8% increase in column ozone in NH winter mid- and high latitudes. A single modeling transient simulation based on RCP8.5 greenhouse gas forcings with continuously increasing SO₂ injections between 2020 and 2099 and decreasing ODSs would result in approximately constant change in column ozone in high polar latitudes (20–23% in October over the SH and 10–12% in March over the NH polar latitudes) and slightly larger (3–5%) column ozone values compared to non-geoengineering conditions for tropics and winter northern mid-latitudes by the end of the 21st century (Richter et al., 2018).

Use of Other Aerosols

The use of high refractive index solid particles such as Al₂O₃, TiO₂, and CaCO₃ have been suggested as stratospheric aerosol geoengineering options with lower stratospheric heating and lower surface areas

for heterogeneous reactions than sulfate aerosols (Dykema et al., 2014; Keith et al., 2016). Limited heating in the stratosphere and reduced reactivity of the particles may change the dynamical response compared to sulfate aerosols. Based on simple 2-D model simulations, Keith et al. (2016) estimate that a radiative forcing of -1 W m^{-2} achieved using stratospheric injection of CaCO_3 particles could result in a 3.8% increase in global column ozone. Estimated aerosol properties and uptake rates still need to be confirmed

by lab studies. Impacts on chemistry and dynamics in comprehensive earth system models have not been investigated.

6.2.5.2 GEOENGINEERING VIA SOLAR IRRADIANCE REDUCTION

Other geoengineering activities proposed to help counteract climate change via solar radiation management involve modifying Earth's energy balance by

Box 6-1. Stratospheric Aerosol Geoengineering

Climate geoengineering via reduction of incoming solar radiation is a strategy to deliberately mitigate some of the effects of anthropogenic global warming (Crutzen, 2006). Since it does not address the cause of climate change (the increase in greenhouse gases) it could be only a temporary solution to help reduce the worst impacts, including heat waves, floods, sea level rise, etc., until decarbonization has effectively stabilized the climate (Tilmes et al., 2016; Wigley, 2006). Stratospheric aerosol geoengineering is a proposed method to reflect incoming shortwave solar radiation to cool Earth's surface, also called solar radiation management. The idea of this approach is to inject aerosols or gases that form aerosols (most studies have performed calculations for sulfur dioxide [SO_2]) into the tropical stratosphere. These are distributed around the globe within approximately 1–2 months, similar to what has been observed after large volcanic eruptions. The continuous injection of SO_2 or aerosols is assumed to form a persistent aerosol layer that achieves a certain amount of global cooling, with a cooling efficiency reaching up to 1°C per $10 \text{ TgSO}_2 \text{ yr}^{-1}$ injections (Pierce et al., 2011; Kravitz et al., 2018), although with potentially reduced efficiency with increasing injection amounts (Niemeier and Schmidt, 2017). Earth system models have a range of approximately a factor of three in the forcing efficiency per injection amount, which depends on the aerosol microphysical descriptions and radiation scheme, as well as feedbacks including changes in ice clouds and assumptions regarding levels of other greenhouse gases (Vioni et al., 2017). There is large uncertainty in the regional impacts of stratospheric aerosol geoengineering. The following is a brief overview of currently known potential benefits, side effects, and risks (Robock, 2016).

Benefits: Earth system models have shown that globally averaged temperatures can be balanced (Kravitz et al., 2013), extreme temperatures and large precipitation events can be reduced (Curry et al., 2014), aridity can be reduced (Tilmes et al., 2016), and the melting of the Arctic sea ice can be significantly slowed or even reversed (Kravitz et al., 2017). The cooling of Earth's surface via stratospheric aerosol geoengineering has potential positive impacts on air quality (Xia et al., 2017) and agriculture and crop yields (Pongratz et al., 2012). Limited investigation also suggests surface ozone levels could decline (Eastham et al., 2018; Xia et al., 2017), which would lead to health benefits. A potential decrease in column ozone may be beneficial if it counteracts the increasing column ozone above preindustrial levels from a projected super recovery. Strategically placed injections may reverse the shortening of the Quasi-Biennial Oscillation (QBO) period from increasing greenhouse gases in the future (Richter et al., 2018). Changes in direct to diffuse radiation ratio have been shown to be beneficial for plant growth and may have other benefits for the biosphere (Xia et al., 2016). The strong cooling potential of stratospheric aerosols would allow for a quick response to sudden climate changes, and the relatively short lifetime of stratospheric sulfate aerosols of about 2 years would allow for a phaseout of geoengineering in a short time if required. The approach would not largely change ocean acidification but may reduce the bleaching of coral reefs (Zhang et al., 2017).

Box 6-1, continued.

Side Effects: Models show that past or present-day climate conditions cannot be perfectly restored with geo-engineering and that, depending on how it is implemented, it may lead to unintended side effects. Models agree that cooling Earth's surface via shortwave radiation (as opposed to mitigating the heating caused by increased trapping of longwave radiation) slows the hydrological cycle, which leads to reductions in global precipitation (Tilmes et al., 2013). While the largest reductions occur over the oceans, this method may lead to a disruption of the monsoonal precipitation. Other side effects include significant heating in the tropical stratosphere, a substantial increase in stratospheric water vapor, a strengthening of the polar night jets, and a weakening of subtropical jets and tropospheric storm tracks (Tilmes et al., 2018; Richter et al., 2018). Changes in stratosphere–troposphere exchange may impact tropospheric ozone and methane lifetimes (Visioni et al., 2017b). Enhanced sulfur deposition resulting from injections was shown to be unimportant (Kravitz et al., 2009). Changes in stratospheric ozone, including the delay of the recovery of ozone at high altitudes and the potential increase of ozone for some regions and seasons, and changes in aerosols impact surface ultraviolet (UV) radiation. Substantial changes in UV, either increased or decreased from pre-ozone hole values, may be harmful for life on Earth. Further, potential side effects include changes in ocean currents, carbon budget, effects on land and ocean biosphere, energy production for solar generators, and visible astronomy. New strategies are being currently developed that aim to reduce some of these side effects (Kravitz et al., 2017).

Risks: Attempting to offset elevated global temperatures requires consistent injections until greenhouse gases are sufficiently reduced. Depending on the pathway, this approach may require hundreds of years of application (Tilmes et al., 2016). A sudden termination of such an application would lead to significant climate change within 10 years after the termination (Jones et al., 2013). Uncertainties regarding future climate change mean that the injection amounts may be higher than anticipated. There are other possible risks that are not included in the models, for example, impacts on the biosphere and continued sea level rise. Additionally, feedback processes might be larger than model predictions, and the current model parameterizations might not be correct in a “geo-engineered” world. Technical injection strategies have not been developed to date, and the required costs would depend on many factors (McClellan et al., 2012).

reflecting sunlight before it enters Earth's atmosphere (e.g., Early, 1989; Seifritz, 1989; Angel, 2006). Recent model studies investigating the stratospheric response in the Geoengineering Model Intercomparison Project (GeoMIP) G1 experiment computed a global ozone increase of 2–8% throughout most of the stratosphere due to a 4% reduction in the total solar irradiance (TSI), with a global total column ozone increase of 1.6% (Jackman and Fleming, 2014; Nowack et al., 2016). This resulted in up to a 20% reduction in local UV radiation, with potential adverse effects on life on Earth, including vitamin-D deficiency and an increase in tropospheric ozone. The main drivers of the ozone increase were reductions in atomic oxygen and temperature caused by the 4% TSI decrease, which subsequently slowed the ozone photochemical loss rates. Reductions in stratospheric water vapor and atomic oxygen excited state, O(¹D), also contributed

to the ozone enhancement by decreasing odd hydrogen concentrations and therefore the HO_x-ozone loss rates.

6.2.6 Other Potential Influences on Stratospheric Ozone

Emissions from Rockets

Since WMO (2014), the orbital launch rate has increased by about a factor of two (Doncaster et al., 2016; FAA, 2016). Recent developments suggest that rocket launches and emissions will continue to increase and possibly accelerate. New space systems, such as reusable and heavy-lift launch vehicles and communication satellite constellations using thousands of satellites in low earth orbit, have emerged (Klinkrad, 2017; Pelton and Jacque, 2016). Maturation of these

systems ensures that launch emissions will increase in coming years. Detailed scenarios of future launch emissions based on known, likely, or speculative future space transportation requirements have not been developed.

Studies of the atmospheric impacts of rockets have primarily focused on stratospheric chemical perturbations associated with the various components of rocket engine emissions. In particular, ozone loss caused by solid rocket motors (ammonium perchlorate oxidizer) occupies the greatest portion of the literature, as summarized in Harris and Wuebbles et al. (2014). Existing model predictions are necessarily incomplete, however, because they do not account for the several types of fuels used by the space industry or the rapid evolution in the global space launch industry and because of the sparsity of new research using modern models that couple atmospheric radiation and chemistry.

For several decades (1981–2011), the Space Shuttle was the largest single rocket emission source, and research focused on its solid rocket motor emissions. After the Space Shuttle ended service in 2011, solid rocket motor emissions from other launch vehicles (Ariane V, Vega, and others) have increased such that solid rocket motor emissions into the stratosphere ($\sim 4 \text{ Gg yr}^{-1}$) have remained nearly constant over the past decade. Global models (Voigt et al., 2013), using prescribed HCl and alumina aerosol emissions, generally agree that as recently as a few years ago, solid rocket motor emissions produce a global total column ozone loss of about 0.03%, approximately equally partitioned between HCl gas-phase reactions and alumina surface heterogeneous chlorine activation reactions. The alumina surface heterogeneous contribution is not well understood, however. Two microphysical parameters, acknowledged as poorly understood in Daniel et al. (2011), determine the magnitude of the alumina impact. These are (1) the size distribution of emitted alumina (specifically, the submicron mode mass fraction, which determines steady-state stratospheric alumina surface area density) and (2) the chlorine activation rate constant. Models have tended to adopt values representative of lower bounds for these parameters. Extrapolations of model results to parameter upper bounds suggest that alumina-related global ozone loss could be a factor of 10 larger than the widely assumed value of 0.03% (Voigt et al., 2013).

No research has been done since WMO (2014) to conclusively eliminate the possibility of upper-bound submicron mass fraction or chlorine activation rate.

Ross and Sheaffer (2014) considered the radiative effects of the black carbon (BC; i.e., “soot”) and alumina aerosol components of rocket emissions and noted that coupling between radiative and chemical impacts presents a potentially important path for ozone loss from rocket emissions. BC emissions from kerosene-fueled rockets have a relatively long stratospheric lifetime (~ 3 years) and accumulate in the upper stratosphere (Ross et al., 2010). This BC scatters and absorbs incoming solar radiation, possibly increasing stratospheric temperatures and thereby accelerating the rate of ozone-destroying chemical reactions. Models of BC-based geoengineering (Kravitz et al., 2012) and limited nuclear exchanges (Mills et al., 2014) can be viewed as analogues to rocket BC emissions, though scaled up by orders of magnitude. Downward extrapolations using these models suggest that stratospheric heating in the present-day rocket BC accumulation (Ross et al., 2010) could produce global ozone loss comparable to that purely from chemical loss from solid rocket motors. The fraction of global launches using propellants that have a relatively large BC emission index (mainly kerosene) has trended upward in recent years, increasing the steady-state BC accumulation. Indirect ozone loss caused by stratospheric heating associated with rocket BC emissions has yet to be studied using the required coupled chemistry and climate models.

Larson et al. (2017) modeled the impact of hydrogen-fueled rockets emitting only water vapor (typically, propellants emit $\sim 400 \text{ g [H}_2\text{O]}$ per kg of fuel). They found global ozone loss from rocket H_2O emissions to be three orders of magnitude less than from an equivalent emission from solid rocket motors. The present water vapor component of rocket emissions produces ozone loss less than 0.0001%. Even under the most expansive plausible launch growth scenario, ozone loss from hydrogen-fueled rockets does not become significant.

Larson et al. (2017) also examined ozone loss caused by spacecraft descent from orbit. Intense atmospheric heating in the mesospheric portion of the reentry corridor produces NO_x , which while not directly emitted is a source arising from rocket activity. Larsen et al.

Table 6-1. Atmospheric lifetimes, fractional halogen release factors, and Ozone Depletion Potentials (ODPs) for long-lived halocarbons. In this Assessment, lifetimes are based on SPARC (2013) and SPARC (2016). Fractional release factors (mid-latitude conditions) used in this Assessment are from Newman et al. (2007), with ODPs calculated using the fractional release values from Laube et al. (2013), shown in parentheses. Lifetime uncertainties are based on SPARC (2013) lifetimes as evaluated by Velders and Daniel (2014); the uncertainty associated with the CCl₄ lifetime has not been updated for the revised lifetime and so is left blank. See Chapter 1 for further discussion on atmospheric lifetimes.

| Halocarbon | Atmospheric Lifetime (years) | | Lifetime Uncertainty (1σ) | Fractional Release Factors | ODPs | |
|----------------------------------|------------------------------|------------------|---------------------------|----------------------------|--------------------------------|--------------------------------|
| | WMO (2014) | This Assessment | | | WMO (2014) and this Assessment | This Assessment Recommendation |
| Annex A-I | | | | | | |
| CFC-11 | 52 | 52 | ±22% | 0.47 | 1.0 | 1.0 |
| CFC-12 | 102 | 102 | ±15% | 0.23 | 0.73 (0.81) | 1.0 |
| CFC-113 | 93 | 93 | ±17% | 0.29 | 0.81 (0.82) | 0.8 |
| CFC-114 | 189 | 189 | ±12% | 0.12 | 0.50 | 1.0 |
| CFC-115 | 540 | 540 | ±17% | 0.04 | 0.26 | 0.6 |
| Annex A-II | | | | | | |
| halon-1301 | 72 | 72 | ±13% | 0.28 | 15.2 (19.0) | 10.0 |
| halon-1211 | 16 | 16 | ±29% | 0.62 | 6.9 (7.7) | 3.0 |
| halon-2402 | 28 | 28 | ±19% | 0.65 | 15.7 | 6.0 |
| Annex B-II | | | | | | |
| CCl ₄ | 26 ^a | 32 | | 0.56 | 0.87 (0.87) | 1.1 |
| Annex B-III | | | | | | |
| CH ₃ CCl ₃ | 5.0 ^b | 5.0 ^b | ±3% | 0.67 | 0.14 (0.17) | 0.1 |
| Annex C-I | | | | | | |
| HCFC-22 | 12 | 12 | ±16% | 0.13 | 0.034 (0.024) | 0.055 |
| HCFC-123 | 1.3 | 1.3 | | | 0.02 ^c | 0.02 |
| HCFC-124 | 5.9 | 5.9 | | | 0.022 ^c | 0.022 |
| HCFC-141b | 9.4 | 9.4 | ±15% | 0.34 | 0.102 (0.069) | 0.11 |
| HCFC-142b | 18 | 18 | ±14% | 0.17 | 0.057 (0.023) | 0.065 |
| HCFC-225ca | 1.9 | 1.9 | | | 0.025 ^c | 0.025 |
| HCFC-225cb | 5.9 | 5.9 | | | 0.033 ^c | 0.033 |
| Annex E | | | | | | |
| CH ₃ Br | 0.8 ^d | 0.8 ^d | ±17% | 0.60 | 0.57 | 0.6 |
| Others | | | | | | |
| halon-1202 | 2.5 | 2.5 | ±33% | 0.62 | 1.7 | |
| CH ₃ Cl | 0.9 ^e | 0.9 ^e | ±18% | 0.44 | 0.015 | |

Notes:

- ^a The partial lifetime for CCl₄ is 44 years for atmospheric loss (from SPARC, 2013) and is assumed to be 183 years for oceanic loss (Butler et al., 2016) and 375 years for soil loss for a total lifetime of 32 years (see **Chapter 1**).
- ^b The partial lifetime for CH₃CCl₃ is 5 years for atmospheric loss (from SPARC, 2013).
- ^c ODPs taken from Papanastasiou et al. (2018).
- ^d The total lifetime for CH₃Br is 1.5 years for atmospheric loss (from SPARC, 2013), 3.1 years for oceanic loss, and 3.3–3.4 years for soil loss.
- ^e The partial lifetime for CH₃Cl is 1.3 years for atmospheric loss (from SPARC, 2013) and 3 years for oceanic and soil losses.

(2017) modeled the NO_x emission for spacecraft re-
turning from orbit, finding ozone column loss would
not exceed 0.1% at a rate of 10⁵ reentries per year. For
comparison, the present reentry rate (including large
space debris) is less than 10² per year so that current
ozone loss from reentry NO_x emissions is inferred to
be less than 0.0001%.

6.3 METRICS FOR CHANGES IN OZONE AND CLIMATE

6.3.1 Metrics for Changes in Ozone

The two primary metrics for studies of stratospheric
ozone are equivalent effective stratospheric chlorine
(EESC) and Ozone Depletion Potentials (ODPs).
An updated analysis of ODPs was given in the last
Assessment (see Section 5.3 and especially Box 5-2
in Harris and Wuebbles et al. (2014) for the basic
description of the EESC and ODP concepts; see also
Tables 5-2 and 5-3 in that Assessment for the derived
values of ODPs). Uncertainty estimates of the ODPs
were also included in Table 5-2, and to our knowl-
edge, have not been updated. A discussion of the
uncertainties associated with ODPs and EESC from a
variety of sources can be found in Velders and Daniel
(2014). Semi-empirical ODPs (see Box 5-2 in Harris
and Wuebbles et al., 2014) and EESC take advantage
of observations to determine fractional release factors
(FRFs), which quantifies how much of a trace gas is
broken down by the time it reaches a particular re-
gion of the stratosphere. **Section 6.4** and **Chapter 1**
describe a recent update to the FRF formalism for
chlorine- and bromine-containing compounds. This
leads to relatively minor changes in FRFs, and thus
to semi-empirical ODPs, and to more significant
changes in calculated EESC. This update does not,

however, affect model-calculated ODPs. Relative to
the last Assessment, the only lifetime change for the
most important long-lived halocarbons is for CCl₄.
As discussed in **Chapter 1**, the CCl₄ lifetime has
been updated from 26 to 32 years, leading to a 23%
increase in its ODP (**Table 6-1** and **Appendix A**). It is
also important to recognize that ODPs can depend on
the background atmosphere. Revell et al. (2015) have
confirmed that this is especially the case for nitrous
oxide (N₂O), where ODP values are likely to be larger
(by as much as a factor of two depending on levels
of chlorine and methane in the stratosphere) for 2100
than in the present day.

In addition to the updates above, there are only a few
new studies of ODPs since WMO (2014), primarily
for compounds considered to play a relatively minor
role in ozone depletion. The discussion of these fol-
lows below in two parts, for long-lived gases (atmo-
spheric lifetimes greater than 1 year) and for short-
lived gases. Overall, the findings for ODPs are similar
to prior Assessments, but this Assessment includes
ODP estimates for a few additional compounds.

Long-Lived Gases

Davis et al. (2016), using the NASA Goddard two-di-
mensional chemistry-climate model, evaluated the
atmospheric lifetimes, ODPs, and GWPs for several
CFCs not previously examined, namely CFC-112,
CFC-112a, CFC-113a, and CFC-114a. The first ob-
servations of the small atmospheric concentrations
of CFC-112, CFC-112a, and CFC-113a were report-
ed by Laube et al. (2014), along with budget analy-
ses with emission sources dating back to the 1960s
(see **Chapter 1**). The first long-term measurements
of CFC-114 and CFC-114a, separately (Laube et al.,

2016), have also been reported since WMO (2014). As expected, the ODPs for these CFCs are quite large: 0.98, 0.86, 0.73, and 0.72 for CFC-112, CFC-112a, CFC-113a, and CFC-114a, respectively.

Short-Lived Gases

Wallington et al. (2015) analyzed the atmospheric chemistry for a number of different short chain haloolefins; however, only HCFO-1233zd(E) (26-day lifetime using a simple scaling relative to global-averaged OH (hydroxyl) concentrations) and HCFO-1233zd(Z) (12-day lifetime) had non-zero ODPs, and these were already included in Harris and Wuebbles et al. (2014) based on the earlier study by Patten and Wuebbles (2010). Patten and Wuebbles (2010), using a three-dimensional atmospheric chemistry-climate model, found an atmospheric lifetime of 40 days (for emissions assumed to be on all landmasses from 30°N to 60°N) and an ODP of 0.00034 for HCFO-1233zd(E) and an atmospheric lifetime of 13 days and an ODP of <0.00034 for HCFO-1233zd(Z). In a new study updating the reaction rates, Sulbaek Andersen et al. (2017) found a slightly smaller lifetime for HCFO-1233zd(E) of 36 days and reduced the ODP to 0.00030 for the same emissions assumptions as made in Patten and Wuebbles (2010). As emphasized in prior assessments, ODPs for very short-lived substances (VSLs) that contain bromine or chlorine are strongly dependent on the geographic location and season of emission. Therefore, it is important to provide the emissions assumptions when reporting VSL ODP derivations. Although ODP-weighted emissions have been used for some time in analyses of long-lived gases, Tegtmeier et al. (2015) extend this approach to short-lived compounds through analyses of CHBr₃ emissions from the ocean by accounting for the area-based variations in ODPs and emissions. They found that ODP-weighted emissions of CHBr₃ were about 9% of the total ODP-weighted emissions by the long-lived halogenated ODPs and that they are expected to grow over the rest of the century due to climate change.

Indirect ODPs

As strong radiative forcers, HFCs increase tropospheric and lower-stratospheric temperatures, thereby enhancing ozone-destroying catalytic cycles and

modifying the atmospheric circulation. These changes lead to a weak indirect depletion of stratospheric ozone. Incorporating the interactions between chemistry, radiation, and dynamics, model-calculated ODPs for HFC-32, HFC-134a, HFC-125, HFC-143a, and HFC-23 range from 0.39×10^{-3} to 30.0×10^{-3} (Hurwitz et al., 2015). These values are approximately 100 times larger than previous ODP estimates, which were based solely on the direct chemical potential to deplete ozone via catalytic loss cycles that involve fluorine (Ravishankara et al., 1994). Nevertheless, their total projected impact on globally averaged total ozone from HFCs remains less than 0.1 DU (Dobson unit) by 2050 (Hurwitz et al., 2016), even for the high-growth HFC scenario from Velders et al. (2015).

6.3.2 Metrics for Changes in Climate

Radiative forcing (RF), Global Warming Potentials (GWPs), and Global Temperature change Potentials (GTPs) are the primary metrics used to consider the climate effects of halocarbons and other gases. An updated analysis of GWPs and GTPs was given in the last Assessment (see section 5.3 and especially Box 5-3 in Harris and Wuebbles et al. (2014) for the basic description of the GWP and GTP concepts; Table 5A-1 in that Assessment gives the derived values of GWPs and GTPs from IPCC, 2013b). Table 5-5 in Harris and Wuebbles et al. (2014) provides an update for a number of halocarbons based on the updated SPARC (2013) lifetimes, while Section 5.3.2 (and Tables 5-6 and 5-7) discuss uncertainties in the GWP and GTP derivations. Shortcomings of using RF, GWPs, and GTPs as proxies for climate response have been studied extensively and are summarized in Chapter 8 of IPCC (2013b). More recent work has examined how the GWP concept can be appropriately used to compare different climate-forcing agents (Allen et al., 2016).

In this Assessment, updates for many GWPs and GTPs are provided. **Table 6-2** presents values for selected long-lived ODSs and HFCs, following the approach used in IPCC AR5 (2013b) that is currently being used by policymakers. This Assessment also includes GWPs and GTPs for the 274 HCFCs in Annex C of the Montreal Protocol (**Appendix A**). These values are potentially useful as the Parties continue the process of phasing out HCFC production and consumption; many of them are provided for the first time in

an assessment. The new values are based on estimates of lifetimes and calculations of infrared absorption characteristics (Papanastasiou et al., 2018). Because these quantities are not experimentally measured, the metrics calculated from this information typically have larger uncertainties associated with them than those based on laboratory measurements.

As in the last Assessment, these metrics were calculated based on the evaluation and assessment of IPCC (Myhre et al., 2013), with updates based on Etminan et al. (2016). The new analyses by Etminan et al. (2016) include shortwave effects not adequately considered previously; these affect the radiative forcing efficiency and GWP for CH₄ but have no significant effects on the GWPs for other compounds. Also shown are the atmospheric lifetimes and radiative efficiencies used in these analyses. As in WMO (2014) and IPCC (2013b), the CO₂ radiative efficiencies (and hence the GWPs and GTPs) of non-CO₂ greenhouse gases presented in **Table 6-2** and **Appendix A** are calculated with a CO₂ level corresponding to 391 ppm.

The following discusses the few new studies of GWPs and GTPs (based on updates to atmospheric lifetimes or new radiative efficiencies for the compounds in question) that have been published since WMO (2014) in two parts: long-lived gases (atmospheric lifetimes greater than 1 year) and short-lived gases. Overall, with the exception of the values for CH₄, there have been minor changes in the derived GWPs and GTPs for the compounds evaluated.

Long-Lived Gases

As mentioned above (**Section 6.3.1**), Davis et al. (2016) have provided 100-year GWP values for CFCs that have not previously received much attention: CFC-112, CFC-112a, CFC-113a, and CFC-114a. Lu et al. (2017) updated analyses of the radiative forcing for NF₃ and derived GWPs and GTPs for 20- and 100-year integrations. Their GWP and GTP values are smaller than those derived previously by IPCC (2013b), primarily due to their derivation of a smaller radiative efficiency. In contrast, a study by Totterdill et al. (2016) found a 25% larger radiative efficiency for NF₃ than IPCC (2013b) and therefore larger GWP and GTP values.

Short-Lived Gases

Most of the new analyses since WMO (2014) of short-lived halocarbons have been associated with short-lived haloolefins, which generally have extremely small GWP values. A short description is provided of some of the key studies. Wallington et al. (2015), along with their analyses of ODPs, provide estimated GWPs for a number of HCFOs, all having 100-year GWPs of 1 or less. Sulbaek Andersen et al. (2017) derive GWP values for HCFO-1233zd(E) of 19, 5, and 1 for 20-, 100- and 500-year time horizons, respectively, using the radiative forcing three-dimensional modeling studies from Wuebbles et al. (2013) for emissions assumed to be distributed across all landmasses from 30°N to 60°N; these GWPs are larger than prior values but reasonable for the assumed landmass emissions. Orkin et al. (2014) examined the photochemical properties of HCFO-1233zd(Z) and estimated an atmospheric lifetime of 46 days assuming a well-mixed distribution (which would be very unlikely for such a short-lived gas) and a relatively small 100-year GWP of 14 (but this again reflects an even distribution of the concentration of the gas).

Climate Carbon-Cycle Feedbacks

New studies of the Climate–Carbon cycle Feedbacks (CCFs) on GWPs and GTPs show the potential importance of accounting for these feedbacks with an explicit CCF model rather than with a linear feedback approach, especially for long-time horizons (Stern and Johansson, 2017). While values of GWPs and GTPs change less than 10% for all well-mixed greenhouse gases when the time horizon is limited to 100 years or less, the values for long time horizons, such as 500 years, can be substantially lower (by up to 30% for the GWP and up to 90% for the GTP) with the explicit CCF model than with the linear feedback approach. This Assessment does not account for the CCF effects in the values of GWPs and GTPs presented here.

Indirect GWPs

There are multiple types of indirect (100-yr) GWPs that have been discussed in the literature. Usually, these relate to the chemical impact a source gas has on other gases and their subsequent climate forcing. One indirect effect that has been shown to be important

Table 6-2. Lifetimes, radiative efficiencies, direct global warming potentials (GWPs), and Global Temperature change Potentials (GTPs) for selected gases (based on a radiative efficiency for CO₂ based on [CO₂] = 391 ppm). The CO₂ AGWPs^a for the 20- and 100-yr time horizons are 2.495 x 10⁻¹⁴ and 9.171 x 10⁻¹⁴ W yr (m² kg)⁻¹; the CO₂ AGTPs^a for the 20-, 50-, and 100-yr time horizons are 6.841 x 10⁻¹⁶, 6.167 x 10⁻¹⁶, and 5.469 x 10⁻¹⁶ K kg⁻¹. GTPs for the 50-yr time horizon are not included in this table but may be found in Appendix A.

| Industrial Designation or Common Name | Lifetime (years) | GWP 20-yr | GWP 100-yr | GTP 20-yr | GTP 100-yr |
|---------------------------------------|------------------|-----------|------------|-----------|------------|
| Annex A-I | | | | | |
| CFC-11 | 52 | 7,090 | 5,160 | 7,160 | 2,920 |
| CFC-12 | 102 | 10,800 | 10,300 | 11,300 | 8,590 |
| CFC-113 | 93 | 6,560 | 6,080 | 6,830 | 4,860 |
| CFC-114 | 189 | 7,710 | 8,580 | 8,180 | 8,530 |
| CFC-115 | 540 | 5,780 | 7,310 | 6,210 | 8,290 |
| Annex A-II | | | | | |
| halon-1301 | 72 | 7,930 | 6,670 | 8,160 | 4,700 |
| halon-1211 | 16 | 4,590 | 1,750 | 3,950 | 300 |
| halon-2402 | 28 | 3,920 | 2,030 | 3,730 | 615 |
| Annex B-II | | | | | |
| CCl ₄ | 32 | 3,790 | 2,110 | 3,670 | 750 |
| Annex B-III | | | | | |
| CH ₃ CCl ₃ | 5 | 555 | 153 | 300 | 21 |
| Annex C-I | | | | | |
| HCFC-22 | 12 | 5,310 | 1,780 | 4,230 | 265 |
| HCFC-141b | 9.4 | 2,590 | 800 | 1,900 | 114 |
| HCFC-142b | 18 | 5,140 | 2,070 | 4,530 | 390 |
| Annex E | | | | | |
| CH ₃ Br | 0.8 | 7.6 | 2 | 2.4 | <1 |
| Others | | | | | |
| halon-1202 | 2.5 | 720 | 196 | 285 | 27 |
| CH ₃ Cl | 0.9 | 16 | 4.3 | 5.1 | <1 |
| HFC-23 | 228 | 11,085 | 12,690 | 11,825 | 13,150 |
| HFC-32 | 5.4 | 2,530 | 705 | 1,440 | 90 |
| HFC-125 | 30 | 6,280 | 3,450 | 6,040 | 1,180 |
| HFC-134a | 14 | 3,810 | 1,360 | 3,170 | 215 |
| HFC-143a | 51 | 7,050 | 5,080 | 7,110 | 2,830 |
| HFC-152a | 1.6 | 545 | 148 | 190 | 21 |
| HFC-227ea | 36 | 5,250 | 3,140 | 5,140 | 1,260 |
| HFC-245fa | 7.9 | 2,980 | 880 | 2,040 | 124 |

Notes:

^a From the mass of the atmosphere (5.135 x 10¹⁸ kg; Trenberth and Smith, 2005), average molecular mass of dry air (28.964 g mol⁻¹; Warneck and Williams, 2012), and molecular mass of CO₂ (44.01 g mol⁻¹) the conversion factor 1 ppm CO₂ = 7.803 x 10¹² kg is derived. This conversion factor can be used to convert the CO₂ AGWPs and AGTPs given above to units of per ppm rather than per kg.

results from the destruction of stratospheric ozone by the ODSs. Because ozone is a greenhouse gas itself, destruction of ozone will lead to a cooling influence on climate. For gases like the halons, this indirect effect is actually larger than, and opposite in sign to, the direct forcing caused by the presence of the halons themselves. There have been no new studies updating this indirect effect for the ODSs, so we update them here (**Table 6-3**) only for the revised CO₂ AGWP (absolute GWP, which is the radiative forcing integrated over a given time horizon, resulting from a pulse emission of the gas) and the updated lifetime of CCl₄.

As interest in shorter-lived compounds replacing longer-lived greenhouse gases has grown, the importance of identifying the degradation products of these compounds and understanding the physical properties of the products has been pointed out. This is another situation in which the indirect GWP can actually be larger than the direct GWP of an emitted compound (Bravo et al., 2011; Jubb et al., 2015).

6.4 SCENARIOS AND SENSITIVITY ANALYSES

6.4.1 Tools Used in Analyses of Ozone and Climate Effects

In this chapter, as in the past two Ozone Assessments (WMO, 2011, 2014), we use two primary tools to compare the climate and ozone impacts of various future scenarios. The first is a simple box model (Harris and Wuebbles et al., 2014), which allows for the calculation of the ozone metrics EESC and ODP-weighted emissions and of the climate metrics RF (radiative forcing) and GWP-weighted emissions (100-yr time horizon). EESC has been shown to be a reasonable proxy for the amount of stratospheric ozone depletion caused by a given abundance of a long-lived ODS (Daniel et al., 2010), and RF is a quantity that describes the energy imbalance often due to the presence of some compound in the atmosphere, and is roughly proportional to the global average surface temperature change it will produce (Myhre et al., 2013). The second evaluation tool used in this chapter is the NASA/Goddard Space Flight Center (GSFC) 2-D coupled chemistry–radiation–dynamics model (Fleming et al., 2011) driven with mixing ratio boundary conditions calculated from the box model. Earlier versions

of this model were also used in Daniel and Velders, et al. (2011) and Harris and Wuebbles et al. (2014). The inclusion of the 2-D model allows us to compare impacts of the long-lived ODSs that are controlled by the Montreal Protocol with the impacts of CO₂, CH₄, and N₂O as well as with very short-lived (VSLS) compounds like CH₂Cl₂. The GSFC 2-D model compares well with observations and with the 3-D Goddard Earth Observing System Chemistry Climate Model (GEOSCCM) in simulating temperature and various transport-sensitive features in the meridional plane, such as the horizontal and vertical gradients of long-lived stratospheric tracers and age of air (Fleming et al., 2011; SPARC, 2013). Projections of future ozone using this 2-D model are also in very good agreement with those of more complex 3-D models used in **Chapters 3, 4, and 5** of this Assessment to examine the impacts of various processes and emissions on ozone and climate (see **Appendix 6A**). 3-D models provide our best understanding of chemical, dynamical, and radiative processes and how they interact to explain the past and future state of the atmosphere. However, these models take large amounts of computer time, which makes evaluation of many dozens of alternative scenarios impractical. Thus, in this chapter, we do not use any 3-D model calculations.

RF is calculated throughout this chapter as it was in Harris and Wuebbles et al. (2014), using the radiative efficiencies found in the **Appendix Table A-1**. EESC is also calculated as in WMO (2014) and is used as the basis for comparison of different scenarios (**Section 6.4.3.1**). However, we also discuss calculations of EESC using the updated approach of Ostermoller et al. (2017) and Engel et al. (2017). The fundamental advance in these papers is the recognition that the difference between the average age of ODSs that have dissociated and the average age of inert tracers can be important to the estimated amount of Cl_y and Br_y in the stratosphere and thus for EESC. They demonstrate that the use of mean age of air in the calculation of both fractional release and in EESC (Newman et al., 2007) leads to a bias in those quantities. The impact of the updated theoretical approach on calculated fractional release factors (FRFs) is not large overall, but it does alter the FRF of a few compounds (Engel et al., 2017). The effect on the change to polar EESC is also not particularly large since the average age of the dissociated ODSs

Table 6-3. Indirect GWPs from ozone depletion (direct forcing from ODSs, themselves, is not included). Approach is taken from Daniel et al. (1995), assuming a radiative forcing due to ozone depletion in 2011 of -0.15 W m^{-2} (IPCC, 2013b). Uncertainty in this radiative forcing leads to an uncertainty in these GWPs of $\pm 100\%$. Direct GWPs are shown for comparison.

| GAS | Indirect GWP 100-yr | Direct GWP 100-yr |
|----------------------------------|---------------------|-------------------|
| CFC-11 | -2,860 | 5,160 |
| CFC-12 | 2,050–2,050 | 10,300 |
| CFC-113 | -2,180 | 6,080 |
| CFC-114 | -880 | 8,580 |
| CFC-115 | -210 | 7,310 |
| HCFC-22 | -98 | 1,780 |
| HCFC-123 | -35 | 80 |
| HCFC-124 | -45 | 530 |
| HCFC-141b | -250 | 800 |
| HCFC-142b | -160 | 2,070 |
| CH ₃ CCl ₃ | -310 | 153 |
| CCl ₄ | -2,610 | 2,110 |
| CH ₃ Br | -1,210 | 2 |
| halon-1211 | -18,500 | 1,750 |
| halon-1301 | -46,100 | 6,670 |
| halon-2402 | -44,800 | 2,030 |
| HCFC-225ca | -39 | 127 |
| HCFC-225cb | -58 | 525 |

are generally not too different from the mean age of an inert tracer. At mid-latitudes, on the other hand, the new approach leads to significantly older effective ages for dissociated ODSs than for an inert tracer in many cases, assumed to be three years here and in previous Assessments (WMO, 2007, 2011, 2014).

The return of EESC to 1980 levels continues to be a useful metric to compare future scenarios. It is important to recognize, however, that relatively small changes in stratospheric chlorine and bromine loading (i.e., EESC) can lead to large changes in this return

time because of how gradually EESC is declining in the baseline scenario. It is also important to recognize that while numerous sources of uncertainty, particularly in atmospheric lifetimes, limit our ability to pinpoint the return of EESC to 1980 levels to within 25–40 years (95% confidence interval) (Velders and Daniel, 2014), this metric can be used meaningfully to compare differences in return dates of various scenarios, assuming that the relative atmospheric lifetimes, production, and bank estimates of different substances or groups of substances are well defined.

6.4.2 Baseline Scenario for Ozone and Climate

Future atmospheric concentrations of ODSs depend on the amount emitted to the atmosphere and the rate at which destruction occurs. The destruction rate can change over time due to changes in atmospheric circulation, changes in solar irradiances at the relevant wavelengths, or changes in reactive chemicals like OH, O(1D), and atomic chlorine. Release to the atmosphere depends on multiple factors, which can include the amount released during and after production, whether production is ultimately for use as a feedstock or for dispersive uses, and on the rate at which the ODS is released from existing applications, also called banks.

Because of inherent uncertainties in these sources and sinks, it is not possible to perfectly predict future ODS concentrations. Therefore, the baseline (A1) scenario should be considered a plausible future pathway, and not the most likely future pathway in some statistical sense. In fact, here and in Chapter 1 we show the extent to which historical observations have differed from the baseline scenario projections of past Assessments. It is also important to keep in mind that the purpose of the projections in this chapter is not for them to serve as predictions, but instead to be used to evaluate the impact of potential policy options regarding the future production and consumption of various ODSs as well as emissions from banks.

The baseline scenario in this Assessment has been developed using the same methodology as has been used in the past several Assessments (WMO, 2007, 2011, 2014). Observations from **Chapter 1** are used to constrain the mixing ratios over the time period when they are available, which is generally from around 1980 through 2016. Before this time period, mixing ratios are taken from the previous Assessment (Harris and Wuebbles et al., 2014), except for CFC-114 (see discussion below). The recent mixing ratios are used in conjunction with the bottom-up bank estimates for 2008 (UNEP, 2009) and the annual production reported to the Ozone Secretariat to estimate bank values through the beginning of 2016 using the relationship

$$B_{i+1} = B_i + P_i - E_i$$

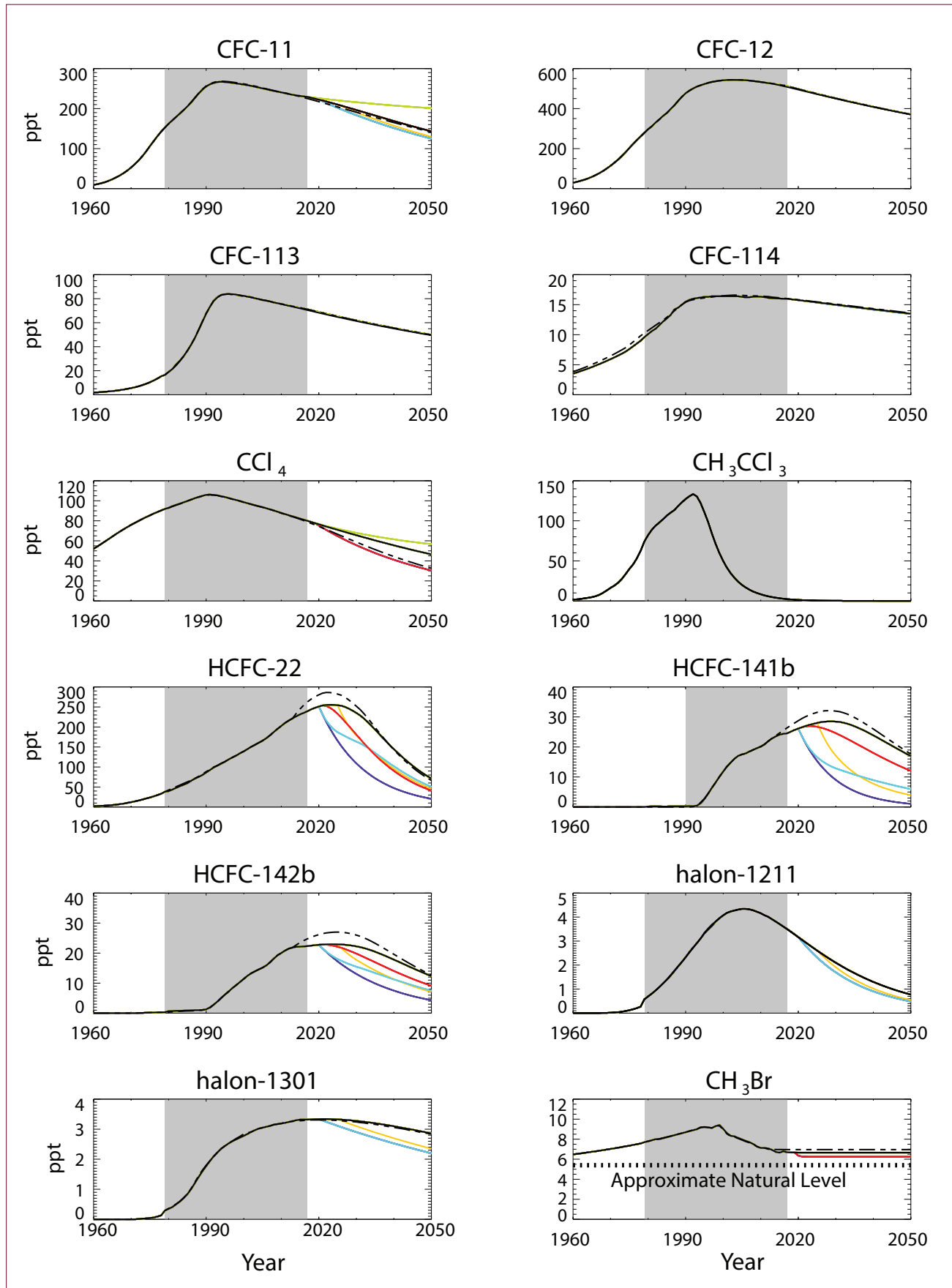
where B_i is the bank at the beginning of year i , and P_i and E_i are the production and emission, respectively,

throughout year i . Knowing the annual emissions and bank values allow for a calculation of the bank fraction that is annually released over the past several years. The annual release fractions, averaged over the last 7 years, are then assumed to remain constant in the future; by assuming that future production is equal to what is permitted by the fully adjusted and amended Montreal Protocol and that this is added to the banks, these release fractions can be used to estimate future annual emissions.

Table 6-4 contains the long-lived ODS mixing ratios for the baseline scenario, and Figure 6-2 includes a comparison of the current baseline scenario with the baseline scenario from WMO (2014). Many of the current projections remain very similar to the previous ones (e.g., CFC-12, CFC-113, and CFC-114 and halons 1211 and 1301). Such agreement is to be expected since our understanding of global lifetimes for most of the compounds has not changed, there has been no reported production to UNEP for CFCs and halons, and we continue to assume the same 2008 bank levels as in Harris and Wuebbles et al. (2014). There has been a slight downward revision in the CFC-114 mixing ratios from 1979 through the mid-1980s because of recent additions of firm data to the historical record (**Chapter 1**) (Laube et al., 2014). Thus, CFC-114 mixing ratios preceding the atmospheric measurement record have been scaled by a constant factor (0.92) to avoid a discontinuity in 1979. **Figure 6-2** also shows how the individual mixing ratios change in the different alternative scenarios. For the scenarios shown, the HCFCs show much more dependence on future emissions than do the CFCs in relation to their current atmospheric concentrations, but CFC emissions, in particular those from the CFC-11 banks, remain significant.

The CCl_4 projection in the current Assessment is higher than in Harris and Wuebbles et al. (2014) because emissions are assumed to decline at a rate of $2.5\% \text{ yr}^{-1}$ rather than the $6\% \text{ yr}^{-1}$ assumed in Harris and Wuebbles et al. (2014). There is substantial inter-annual variability in the emission trend, but the updated rate is more consistent with the long-term trend over the last two decades.

HCFC projections are similar to those of the previous Assessment (Harris and Wuebbles et al., 2014), although the three major HCFCs shown in **Figure 6-2**



all have concentrations somewhat lower for the next few years, owing to recent growth in concentrations that was less than projected previously and to the fact that reported production over the past few years has been less than was assumed in Harris and Wuebbles et al. (2014).

CH₃Br projections are developed by calculating the total atmospheric loss of CH₃Br (using the approach used in Table 1-4 of Carpenter and Reimann et al., 2014) with a global atmospheric lifetime of 0.8 years, and assuming equivalent total atmospheric emissions. (Note that the baseline scenario of the previous Assessment assumed a global atmospheric CH₃Br lifetime of 0.75 years as in WMO, 2011). All emissions, including QPS and CUE emissions, are assumed to continue at the 2016 level indefinitely into the future. This is a minor difference from the baseline scenario of the last Assessment, where CUE emissions were assumed to be zero after 2012. This change makes little difference to the calculations since production under CUE has continued to decline and was less than a tenth of production for QPS in 2016.

A lower assumed total atmospheric emission is the primary reason for a slight lowering of future CH₃Br atmospheric concentrations in the baseline scenario when compared with the previous Assessment (6.7 ppt currently relative to the previous 7.0 ppt). Note that the CH₃Br budget continues to have a significant imbalance between sources and sinks, and there is a large uncertainty in both terms (WMO, 2014). The key issue, however, is the level of anthropogenic production and consumption that could be controlled, if desired, which is well defined. We also note that (continued) reduction in the global atmospheric mole fraction of CH₃Br leads to an increase in the net sea-air flux of CH₃Br, which can somewhat dampen

policy actions taken to reduce anthropogenic emissions. While the ocean response to recent and predicted future changes in atmospheric CH₃Br is now very small (resulting in a calculated increase in net ocean emissions according to the budget terms of Carpenter and Reimann et al. (2014) of ~0.4 Gg yr⁻¹ from 2012 to 2016), we note that since the mid-1990s, the net ocean source has likely increased by ~10 Gg yr⁻¹ (Hu et al., 2012; WMO, 2014).

The baseline scenario for HFCs is taken directly from **Chapter 2** and includes global control measures introduced by the Kigali Amendment and other regional and national actions. In order to estimate the impact of the Kigali actions, we use the reference scenarios for HFCs developed in Velders et al. (2015a), which are projections without consideration of specific global control measures. These HFC scenarios are discussed in detail in **Chapter 2, Section 2.5.1**.

Potentially, one of the more important differences from projections of previous Assessments is that CFC-11 has declined more slowly than projected for a number of years, and the discrepancy has increased since 2012. While this is not apparent from **Figure 6-2** due to the large scale on the y-axis, it has the potential to be important and will be discussed later in **Section 6.4.3**. We continue to treat CFC-11 emission in the baseline scenario as has been done in previous Assessments, i.e., as arising solely from its banks. This does lead to a higher implied annual bank release fraction, since the ratio of emissions to bank size has gone up substantially since 2013.

In addition to evaluating the impact of future ODS emissions and concentrations, we use the 2-D model to examine the impact of future concentrations of N₂O, CH₄, and CO₂, as well as of short-lived halocarbon (i.e., CH₂Cl₂) emissions, on stratospheric ozone.

Figure 6-2. Comparison of long-lived halocarbon mixing ratios in the current baseline scenario (shown as solid black curve) with those from the baseline scenario of WMO (2014) (dot-dashed black line); future mixing ratio projections for the “no emission from 2020 onward” (dark blue), “bank capture and destruction in 2020” (cyan), “bank capture and destruction in 2025” (yellow), and “no production from 2020 onward” (red) scenarios. Shaded regions represent the time periods when mixing ratios are constrained to observational estimates (see **Chapter 1**). The approximate natural concentration of CH₃Br is noted by the dotted blue line in the lower right-hand panel (see **Chapter 1**). The green curves for CFC-11 and CCl₄, respectively, show concentrations for scenarios in which annual emissions remain at 67 Gg yr⁻¹ of CFC-11 and 33 Gg yr⁻¹ of CCl₄.

Table 6-4. Mixing ratios (ppt) of the ODSs considered in the baseline scenario. Values are for the beginning of the corresponding year. Shaded areas indicate when the mixing ratio values are forced to equal global average estimates inferred from observations (see Chapter 1).

| Year | CFC-11 | CFC-12 | CFC-113 | CFC-114 | CFC-115 | CCl ₄ | CH ₃ CCl ₃ |
|------|--------|--------|---------|---------|---------|------------------|----------------------------------|
| 1955 | 3.3 | 14.3 | 1.3 | 2.4 | 0.0 | 42.3 | 0.1 |
| 1960 | 9.5 | 29.5 | 1.9 | 3.5 | 0.0 | 52.1 | 1.5 |
| 1965 | 23.5 | 58.8 | 3.1 | 4.6 | 0.0 | 64.4 | 4.7 |
| 1970 | 52.8 | 114.3 | 5.5 | 5.9 | 0.2 | 75.9 | 16.3 |
| 1975 | 106.1 | 203.1 | 10.4 | 7.6 | 0.6 | 85.5 | 40.0 |
| 1980 | 162.4 | 296.6 | 19.0 | 10.1 | 1.6 | 93.0 | 82.3 |
| 1981 | 170.7 | 311.3 | 21.5 | 10.6 | 1.9 | 94.6 | 89.0 |
| 1982 | 179.4 | 329.6 | 25.3 | 11.0 | 2.2 | 96.0 | 93.9 |
| 1983 | 187.6 | 345.4 | 28.5 | 11.6 | 2.4 | 97.2 | 97.8 |
| 1984 | 196.4 | 362.8 | 32.0 | 12.2 | 2.8 | 98.5 | 102.1 |
| 1985 | 205.6 | 378.1 | 36.8 | 12.7 | 3.1 | 99.8 | 106.6 |
| 1986 | 215.4 | 397.2 | 41.9 | 13.3 | 3.5 | 101.1 | 110.2 |
| 1987 | 226.5 | 415.9 | 47.4 | 14.2 | 3.9 | 102.7 | 113.3 |
| 1988 | 237.6 | 437.9 | 54.2 | 14.5 | 4.3 | 103.7 | 118.3 |
| 1989 | 247.5 | 458.8 | 61.1 | 15.0 | 4.8 | 104.9 | 122.9 |
| 1990 | 255.2 | 476.2 | 67.7 | 15.5 | 5.2 | 106.0 | 127.2 |
| 1991 | 260.6 | 489.6 | 73.3 | 15.8 | 5.7 | 106.2 | 130.7 |
| 1992 | 264.0 | 500.6 | 78.4 | 16.0 | 6.1 | 105.8 | 133.3 |
| 1993 | 266.3 | 510.1 | 81.3 | 16.1 | 6.5 | 105.3 | 130.4 |
| 1994 | 266.9 | 516.3 | 83.1 | 16.2 | 6.9 | 104.4 | 122.1 |
| 1995 | 266.3 | 522.4 | 83.7 | 16.3 | 7.2 | 103.8 | 110.6 |
| 1996 | 265.2 | 528.5 | 83.8 | 16.3 | 7.5 | 102.8 | 98.2 |
| 1997 | 264.2 | 533.0 | 83.6 | 16.4 | 7.7 | 101.8 | 84.1 |
| 1998 | 262.8 | 536.3 | 83.2 | 16.4 | 7.9 | 100.8 | 71.1 |
| 1999 | 261.5 | 539.1 | 82.7 | 16.4 | 8.0 | 99.8 | 59.5 |
| 2000 | 259.9 | 541.2 | 82.1 | 16.4 | 8.1 | 98.6 | 49.7 |
| 2001 | 258.4 | 542.9 | 81.8 | 16.4 | 8.2 | 97.6 | 41.5 |
| 2002 | 256.7 | 543.6 | 81.2 | 16.4 | 8.3 | 96.6 | 34.5 |
| 2003 | 254.5 | 543.6 | 80.4 | 16.4 | 8.3 | 95.6 | 28.8 |
| 2004 | 252.5 | 543.5 | 79.6 | 16.4 | 8.3 | 94.6 | 24.0 |
| 2005 | 250.5 | 542.7 | 78.9 | 16.3 | 8.3 | 93.7 | 20.0 |
| 2006 | 248.4 | 541.8 | 78.4 | 16.2 | 8.4 | 92.6 | 16.7 |

| | HCFC-22 | HCFC-141b | HCFC-142b | halon-1211 | halon-1202 | halon-1301 | halon-2402 | CH ₃ Br | CH ₃ Cl |
|--|---------|-----------|-----------|------------|------------|------------|------------|--------------------|--------------------|
| | 1.0 | 0.0 | 0.0 | 0.00 | 0.00 | 0.00 | 0.00 | 6.3 | 491.3 |
| | 2.1 | 0.0 | 0.0 | 0.00 | 0.00 | 0.00 | 0.00 | 6.5 | 510.3 |
| | 4.9 | 0.0 | 0.0 | 0.00 | 0.00 | 0.00 | 0.00 | 6.7 | 528.1 |
| | 12.1 | 0.0 | 0.0 | 0.02 | 0.00 | 0.00 | 0.02 | 7.0 | 539.9 |
| | 23.8 | 0.0 | 0.2 | 0.12 | 0.01 | 0.04 | 0.06 | 7.4 | 545.8 |
| | 39.6 | 0.2 | 0.7 | 0.70 | 0.01 | 0.35 | 0.15 | 7.8 | 548.4 |
| | 43.8 | 0.2 | 0.7 | 0.82 | 0.01 | 0.41 | 0.17 | 7.9 | 548.6 |
| | 48.0 | 0.2 | 0.8 | 0.94 | 0.01 | 0.50 | 0.19 | 8.0 | 548.9 |
| | 52.0 | 0.2 | 0.8 | 1.09 | 0.01 | 0.59 | 0.21 | 8.0 | 549.1 |
| | 55.6 | 0.2 | 0.8 | 1.25 | 0.01 | 0.71 | 0.23 | 8.1 | 549.3 |
| | 59.7 | 0.2 | 0.9 | 1.40 | 0.01 | 0.84 | 0.25 | 8.2 | 549.4 |
| | 65.6 | 0.2 | 0.9 | 1.56 | 0.02 | 1.01 | 0.27 | 8.3 | 549.5 |
| | 71.1 | 0.2 | 1.0 | 1.75 | 0.02 | 1.21 | 0.30 | 8.4 | 549.6 |
| | 75.1 | 0.2 | 1.0 | 1.94 | 0.02 | 1.41 | 0.32 | 8.5 | 549.7 |
| | 80.2 | 0.2 | 1.1 | 2.13 | 0.02 | 1.60 | 0.35 | 8.6 | 549.8 |
| | 86.3 | 0.3 | 1.3 | 2.33 | 0.02 | 1.77 | 0.38 | 8.7 | 549.8 |
| | 92.5 | 0.3 | 1.9 | 2.55 | 0.02 | 1.94 | 0.40 | 8.8 | 549.9 |
| | 98.8 | 0.3 | 2.8 | 2.74 | 0.03 | 2.10 | 0.42 | 8.9 | 549.9 |
| | 103.3 | 0.5 | 3.9 | 2.92 | 0.03 | 2.23 | 0.44 | 9.0 | 549.9 |
| | 108.4 | 1.3 | 5.0 | 3.11 | 0.03 | 2.35 | 0.46 | 9.2 | 550.0 |
| | 113.2 | 2.6 | 6.2 | 3.32 | 0.04 | 2.44 | 0.47 | 9.2 | 560.9 |
| | 119.0 | 4.5 | 7.2 | 3.48 | 0.04 | 2.53 | 0.48 | 9.2 | 544.9 |
| | 123.7 | 6.4 | 8.4 | 3.63 | 0.04 | 2.60 | 0.48 | 9.1 | 535.0 |
| | 128.4 | 8.2 | 9.3 | 3.81 | 0.04 | 2.66 | 0.49 | 9.3 | 555.4 |
| | 134.3 | 10.1 | 10.4 | 3.95 | 0.05 | 2.72 | 0.49 | 9.4 | 563.3 |
| | 139.1 | 11.8 | 11.4 | 4.07 | 0.05 | 2.78 | 0.49 | 9.0 | 552.6 |
| | 144.7 | 13.5 | 12.4 | 4.17 | 0.04 | 2.84 | 0.49 | 8.6 | 540.2 |
| | 150.5 | 14.8 | 13.3 | 4.23 | 0.04 | 2.91 | 0.49 | 8.3 | 536.3 |
| | 155.4 | 16.1 | 13.9 | 4.27 | 0.04 | 2.97 | 0.49 | 8.3 | 541.5 |
| | 160.5 | 17.0 | 14.6 | 4.31 | 0.04 | 3.02 | 0.48 | 8.1 | 536.4 |
| | 165.7 | 17.5 | 15.2 | 4.34 | 0.03 | 3.05 | 0.48 | 8.0 | 538.7 |
| | 171.9 | 17.9 | 15.9 | 4.34 | 0.03 | 3.08 | 0.48 | 7.8 | 537.1 |

| Year | CFC-11 | CFC-12 | CFC-113 | CFC-114 | CFC-115 | CCl ₄ | CH ₃ CCl ₃ | |
|------|--------|--------|---------|---------|---------|------------------|----------------------------------|--|
| 2007 | 246.2 | 539.8 | 77.7 | 16.3 | 8.4 | 91.5 | 14.0 | |
| 2008 | 244.1 | 537.6 | 76.9 | 16.3 | 8.4 | 90.3 | 11.7 | |
| 2009 | 242.2 | 535.5 | 76.1 | 16.4 | 8.4 | 89.1 | 9.9 | |
| 2010 | 240.4 | 532.8 | 75.7 | 16.3 | 8.4 | 87.9 | 8.3 | |
| 2011 | 238.4 | 530.2 | 75.0 | 16.3 | 8.4 | 86.7 | 6.9 | |
| 2012 | 236.4 | 527.7 | 74.4 | 16.1 | 8.4 | 85.5 | 5.8 | |
| 2013 | 234.4 | 524.8 | 73.7 | 16.1 | 8.4 | 84.5 | 4.8 | |
| 2014 | 232.9 | 521.9 | 73.0 | 16.1 | 8.4 | 83.3 | 4.0 | |
| 2015 | 231.7 | 519.1 | 72.4 | 16.0 | 8.5 | 82.3 | 3.4 | |
| 2016 | 230.3 | 515.9 | 71.7 | 16.0 | 8.5 | 81.1 | 2.7 | |
| 2017 | 229.2 | 512.6 | 71.2 | 16.0 | 8.5 | 79.9 | 2.3 | |
| 2018 | 227.0 | 507.6 | 70.4 | 15.9 | 8.5 | 78.8 | 1.8 | |
| 2019 | 224.8 | 502.6 | 69.7 | 15.8 | 8.5 | 77.8 | 1.5 | |
| 2020 | 222.5 | 497.7 | 68.9 | 15.8 | 8.5 | 76.7 | 1.2 | |
| 2021 | 220.1 | 492.9 | 68.2 | 15.7 | 8.5 | 75.6 | 1.0 | |
| 2022 | 217.6 | 488.1 | 67.4 | 15.6 | 8.5 | 74.5 | 0.8 | |
| 2023 | 215.1 | 483.3 | 66.7 | 15.5 | 8.5 | 73.4 | 0.7 | |
| 2024 | 212.5 | 478.6 | 66.0 | 15.5 | 8.5 | 72.3 | 0.6 | |
| 2025 | 209.9 | 473.9 | 65.3 | 15.4 | 8.5 | 71.2 | 0.5 | |
| 2030 | 196.4 | 451.2 | 61.9 | 15.0 | 8.5 | 65.9 | 0.2 | |
| 2035 | 182.6 | 429.7 | 58.6 | 14.6 | 8.5 | 60.7 | 0.1 | |
| 2040 | 168.9 | 409.1 | 55.6 | 14.2 | 8.4 | 55.8 | 0.0 | |
| 2045 | 155.7 | 389.5 | 52.7 | 13.9 | 8.4 | 51.1 | 0.0 | |
| 2050 | 143.1 | 370.9 | 49.9 | 13.5 | 8.3 | 46.7 | 0.0 | |
| 2055 | 131.2 | 353.2 | 47.3 | 13.2 | 8.2 | 42.6 | 0.0 | |
| 2060 | 120.0 | 336.3 | 44.8 | 12.8 | 8.2 | 38.8 | 0.0 | |
| 2065 | 109.7 | 320.2 | 42.5 | 12.5 | 8.1 | 35.2 | 0.0 | |
| 2070 | 100.1 | 304.9 | 40.3 | 12.2 | 8.0 | 31.9 | 0.0 | |
| 2075 | 91.3 | 290.3 | 38.1 | 11.8 | 8.0 | 28.9 | 0.0 | |
| 2080 | 83.2 | 276.4 | 36.1 | 11.5 | 7.9 | 26.1 | 0.0 | |
| 2085 | 75.7 | 263.2 | 34.3 | 11.2 | 7.8 | 23.6 | 0.0 | |
| 2090 | 68.9 | 250.6 | 32.5 | 10.9 | 7.7 | 21.3 | 0.0 | |
| 2095 | 62.7 | 238.6 | 30.8 | 10.6 | 7.7 | 19.2 | 0.0 | |
| 2100 | 57.0 | 227.2 | 29.2 | 10.4 | 7.6 | 17.2 | 0.0 | |

| | HCFC-22 | HCFC-141b | HCFC-142b | halon-1211 | halon-1202 | halon-1301 | halon-2402 | CH ₃ Br | CH ₃ Cl |
|--|---------|-----------|-----------|------------|------------|------------|------------|--------------------|--------------------|
| | 179.1 | 18.5 | 16.9 | 4.32 | 0.03 | 3.11 | 0.47 | 7.7 | 542.0 |
| | 187.3 | 19.1 | 18.1 | 4.28 | 0.03 | 3.15 | 0.47 | 7.5 | 544.7 |
| | 195.2 | 19.6 | 19.3 | 4.22 | 0.02 | 3.17 | 0.46 | 7.3 | 543.0 |
| | 202.5 | 20.1 | 20.0 | 4.16 | 0.02 | 3.19 | 0.46 | 7.1 | 539.1 |
| | 210.0 | 20.9 | 20.8 | 4.08 | 0.02 | 3.21 | 0.45 | 7.1 | 534.7 |
| | 216.0 | 21.9 | 21.5 | 4.01 | 0.02 | 3.24 | 0.44 | 7.1 | 535.8 |
| | 221.4 | 22.8 | 21.8 | 3.91 | 0.02 | 3.27 | 0.44 | 6.9 | 542.3 |
| | 226.5 | 23.5 | 22.1 | 3.81 | 0.02 | 3.30 | 0.43 | 6.7 | 538.7 |
| | 231.5 | 24.1 | 22.2 | 3.71 | 0.01 | 3.32 | 0.42 | 6.7 | 546.0 |
| | 235.3 | 24.4 | 22.2 | 3.61 | 0.01 | 3.32 | 0.42 | 6.8 | 555.3 |
| | 239.3 | 24.5 | 22.3 | 3.51 | 0.01 | 3.32 | 0.41 | 6.8 | 550.6 |
| | 244.0 | 25.1 | 22.5 | 3.40 | 0.01 | 3.33 | 0.40 | 6.7 | 539.5 |
| | 247.9 | 25.6 | 22.7 | 3.29 | 0.01 | 3.33 | 0.39 | 6.7 | 539.5 |
| | 251.1 | 26.1 | 22.8 | 3.17 | 0.00 | 3.34 | 0.39 | 6.7 | 539.5 |
| | 253.7 | 26.6 | 22.9 | 3.06 | 0.00 | 3.34 | 0.38 | 6.7 | 539.5 |
| | 255.0 | 27.0 | 22.9 | 2.94 | 0.00 | 3.34 | 0.37 | 6.7 | 539.5 |
| | 255.5 | 27.4 | 22.9 | 2.83 | 0.00 | 3.34 | 0.37 | 6.7 | 539.5 |
| | 255.2 | 27.7 | 22.9 | 2.72 | 0.00 | 3.33 | 0.36 | 6.7 | 539.5 |
| | 254.3 | 28.0 | 22.9 | 2.61 | 0.00 | 3.33 | 0.35 | 6.7 | 539.5 |
| | 235.0 | 28.5 | 22.2 | 2.10 | 0.00 | 3.28 | 0.31 | 6.7 | 539.5 |
| | 193.4 | 26.9 | 20.5 | 1.66 | 0.00 | 3.20 | 0.28 | 6.7 | 539.5 |
| | 144.6 | 23.9 | 17.8 | 1.30 | 0.00 | 3.10 | 0.25 | 6.7 | 539.5 |
| | 103.1 | 20.4 | 15.0 | 1.01 | 0.00 | 2.98 | 0.22 | 6.7 | 539.5 |
| | 71.1 | 16.9 | 12.3 | 0.77 | 0.00 | 2.86 | 0.19 | 6.7 | 539.5 |
| | 48.1 | 13.8 | 9.9 | 0.59 | 0.00 | 2.73 | 0.17 | 6.7 | 539.5 |
| | 32.2 | 11.2 | 7.9 | 0.44 | 0.00 | 2.60 | 0.15 | 6.7 | 539.5 |
| | 21.5 | 8.9 | 6.2 | 0.34 | 0.00 | 2.46 | 0.13 | 6.7 | 539.5 |
| | 14.2 | 7.1 | 4.9 | 0.25 | 0.00 | 2.33 | 0.11 | 6.7 | 539.5 |
| | 9.4 | 5.6 | 3.8 | 0.19 | 0.00 | 2.20 | 0.10 | 6.7 | 539.5 |
| | 6.2 | 4.5 | 2.9 | 0.14 | 0.00 | 2.08 | 0.08 | 6.7 | 539.5 |
| | 4.1 | 3.5 | 2.2 | 0.10 | 0.00 | 1.96 | 0.07 | 6.7 | 539.5 |
| | 2.7 | 2.8 | 1.7 | 0.08 | 0.00 | 1.84 | 0.06 | 6.7 | 539.5 |
| | 1.8 | 2.2 | 1.3 | 0.06 | 0.00 | 1.73 | 0.05 | 6.7 | 539.5 |
| | 1.2 | 1.7 | 1.0 | 0.04 | 0.00 | 1.62 | 0.05 | 6.7 | 539.5 |

RCP6.0 is used in the baseline scenario, with sensitivity calculations performed using RCP2.6, RCP4.5, and RCP8.5 scenarios. While the specific RCP does not affect conclusions regarding the importance of the various ODS emission sources to future ozone depletion, the wide range of concentrations of N_2O , CH_4 , and CO_2 across the RCPs can lead to a rather large difference in the date when global column ozone returns to 1980 levels.

Given the multiple sources of CH_2Cl_2 (Leedham Elvidge et al., 2015) and continued variability in growth rates, we assume that it is reasonable to project constant emissions forward; thus, the baseline for CH_2Cl_2 maintains current atmospheric mixing ratios into the future. We note, however, that there are major uncertainties in future emissions of CH_2Cl_2 due to a lack of bottom-up information on its industrial sources. A constant stratospheric VSL Br of 5 ppt is used in all the 2-D model runs.

6.4.3 Alternative Future Scenarios

As in past Assessments, we consider multiple alternative future sensitivity cases to assess which emission sources are responsible for the projected concentrations of the various ODSs and of EESC. This information can inform policy discussions by quantifying the effects of various potential policy controls.

Zero-emission scenarios are run for all ODSs, both individually and collectively, and assume no future anthropogenic emission into the atmosphere from any source; thus, the future concentrations are governed exclusively by the current concentrations and the global lifetimes. These scenarios represent minimum concentrations that can be achieved through direct controls, assuming the lifetimes used in the model are accurate and unchanging. There are also scenarios in which there is continued production into the future as allowed by the Montreal Protocol but current banks are eliminated, and other scenarios in which current banks continue to emit into the future but future production is eliminated. None of these alternative scenarios is presented as a likely, or even necessarily a possible, future path. Instead, they are meant as sensitivity studies, which can aid in determining the impact of some lesser reduction. For example, if 10% of the CFC bank were captured and destroyed in 2020, the magnitude of the impact is expected to be

about 10% of the effect of the case considered here, in which the entire CFC bank in 2020 was captured and destroyed. There is a slight nonlinearity introduced tied to the return of EESC to 1980 levels, because a larger mitigation will cause EESC to cross below the 1980 threshold sooner, thus changing the ending time of the integration. The time when emissions occur can also lead to a response that does not scale linearly. Thus, for example, some metrics for the combined impact of a zero-production scenario with a zero-bank scenario are not expected to be exactly the same as the metrics for a zero-emission scenario.

Designing the alternative scenarios for most ODSs is relatively straightforward since they are entirely, or almost entirely, emitted from human activity. CH_3Br is an exception. As discussed previously, the key aspect to evaluating the controllable contribution of CH_3Br to stratospheric bromine and ozone depletion is the amount that is emitted from human activity in comparison to natural emissions. As in previous Assessments, we consider emissions from QPS (7.3 Gg yr^{-1} in 2016) and CUE (0.7 Gg yr^{-1} in 2016) to be the controllable emissions. We do not consider emissions from indoor or outdoor biomass burning as being controllable, nor do we consider any potential emissions reduction from leaded gasoline, due to its small estimated contribution to total emissions.

As stated above, the concentration of CFC-11 has not dropped as quickly as expected over the last few years or as quickly as it had been dropping over the preceding ten years. This observation is particularly unexpected because reported global production of the CFCs, in total, has been below zero (i.e., more destruction than production) since 2010 (UNEP, 2017). This discrepancy could be attributed to several potential causes: (1) a circulation change that resulted in lower natural loss rates; (2) increased emission from existing equipment; or (3) emissions from production that have not been reported to the Ozone Secretariat for allowed uses as feedstock or process agents or from illegal uses for new equipment or to service existing equipment. Identifying the underlying cause(s) is key to quantifying the potential implication for ozone depletion. If, for example, a temporary circulation change is entirely responsible for the slower decline, there is little long-term impact. While atmospheric circulation changes have likely played a role, 3-D models cannot explain the observed atmospheric concentrations without

emission increases after 2012 (Montzka et al., 2018). An abrupt and substantial increase in emissions from existing banks, required to solely explain the observations, is considered highly unlikely: While building demolition may lead to increasing CFC-11 emissions as the insulating foams in the buildings are destroyed, such emissions are expected to ramp up slowly and to primarily occur in developed countries, which is not shown by the observations (Montzka et al., 2018). These lines of evidence suggest the possibility that the emissions could be related to unreported production (Montzka et al., 2018). Thus, we have included an additional sensitivity case in which we assume the future emissions of CFC-11 do not decline but remain at 67 Gg yr⁻¹, the average calculated top-down emissions over 2002–2016.

As discussed previously and in **Chapter 1**, new potential sources of CCl₄ emissions have been identified from industry and from legacy uses that are currently not captured in reporting to UNEP. There are also likely additional missing source(s). Given that future CCl₄ emissions remain uncertain, we have included an additional alternative scenario for CCl₄ in which current estimated top-down emissions (33 Gg yr⁻¹) remain constant indefinitely.

Projecting future CH₂Cl₂ emissions is one of the more uncertain aspects of the scenarios considered here. As discussed in **Chapter 1**, tropospheric mixing ratios of CH₂Cl₂ demonstrated strong growth from the early 2000s to around 2014. Growth has slowed since then, although growth rates continue to be highly variable. A potentially large source of CH₂Cl₂ is as a co-product of CHCl₃ manufacture, which is used almost entirely for HCFC-22 production (Oram et al., 2017). Oram et al. (2017) calculate that around 715 kt of CH₂Cl₂ (in 2015) could be produced in association with HCFC-22 production in China, of which ~455 Gg (nearly half of estimated global CH₂Cl₂ annual emissions) could be used for emissive applications. If indeed CH₂Cl₂ production is closely linked to the demand for HCFC-22, then its emissions could decline in the future, as long as noncontrolled feedstock production of HCFC-22 does not outweigh declines in controlled HCFC-22 emissions mandated by the Montreal Protocol. However, the variable growth rates of CH₂Cl₂ and the lack of a definitive understanding of its global budget mean that reliable projections are currently not possible. Thus,

we develop two alternative scenarios for CH₂Cl₂, intended as sensitivity studies to examine the potential influence on stratospheric O₃: (1) continued strong growth in emissions, assuming that surface mole fractions grow consistently at 2.85 ppt per year (the mean rate observed during 2004–2014 as in scenario 1 from Hossaini et al., 2017), and (2) immediate cessation of emissions.

It is important to recognize that N₂O remains the most significant ODP-weighted emission among all the ODSs. Thus, even though N₂O is not controlled under the Montreal Protocol, we run two mitigation scenarios to compare with the ODS emission cases. These alternative scenarios will also have climate implications because N₂O is a long-lived greenhouse gas. The two scenarios are unchanged from Harris and Wuebbles et al. (2014). In one, all future anthropogenic emissions are eliminated, and in the other, the average of the “concerted mitigation” scenarios from UNEP (2013) is assumed. These scenarios are RCP2.6, SRES B2, and scenarios 4 and 5 from Davidson (2012). Future assumptions in these scenarios vary, but as an example, scenario 4 in Davidson (2012) considered improved agricultural efficiency and emissions reductions of 50% in the transportation/industrial sectors and from biomass burning relative to a baseline scenario in 2050. Scenario 5 incorporates scenario 4 assumptions, as well as a reduction in meat consumption.

Policy options can be directly compared with the baseline scenario of this Chapter (**Table 6-5**) using: (1) the return of EESC to 1980 levels, (2) integrated EESC above 1980 levels, (3) integrated ODP- and (4) GWP-weighted ODS emissions from 2020 through 2060, and (5) integrated ozone depletion. As in past Assessments, 1980 is the reference year—identified as a time when the return of EESC or global column ozone to levels experienced then signifies an important milestone in moving towards recovery. It is important to recognize, however, that even when EESC or global column ozone returns to 1980 levels, there will almost certainly be differences in the ozone spatial distribution both for the total column as well as in the vertical profile. These differences are unavoidable as long as greenhouse gases like CO₂, CH₄, and N₂O remain perturbed from their 1980 levels. The actual year of return to 1980 global column ozone also will depend on natural variations (e.g., in meteorology and atmospheric circulation) that can affect ozone,

Table 6-5. Comparison of scenarios and cases^a: the year when EESC^b drops below the 1980 value for both mid-latitude and Antarctic vortex, and integrated EESC differences (mid-latitude case) relative to the baseline (A1) scenario^c. Also shown are changes in integrated ODP- and GWP-weighted emissions and, for selected cases, integrated global ozone depletion for 2020–2060. Future changes in CH₄ and CO₂ may also significantly alter ozone levels, potentially by amounts larger than any of the cases considered in this table.

| Scenario and Cases | Percent Difference in Integrated EESC Relative to Baseline Scenario for the Mid-latitude Case | | Year When EESC is Expected to Drop Below 1980 Value | | Change in Cumulative ODP-Weighted Emission: 2020–2060 | Change in Cumulative GWP-Weighted Emission: 2020–2060 | Percent Difference in Integrated O ₃ Depletion ^g : 2020–2060 |
|--|---|------------------------------|---|--------|---|---|--|
| | Mid-latitude ^{c,d} | | Antarctic Vortex ^d | | (Million tons CFC-11-eq) | (Billion tons CO ₂ -eq) | |
| | $\int_{1980}^{\chi} EESC dt$ | $\int_{2020}^{\chi} EESC dt$ | | | | | |
| Scenarios | | | | | | | |
| A1: Baseline scenario | 0.0 | 0.0 | 2049.4 | 2075.7 | 0.00 | 0.0 | 0.00 |
| Cases^a of zero production from 2020 onward of: | | | | | | | |
| P0: All ODS | -4.2 | -19.1 | 2044.6 | 2070.3 | -0.88 | -5.8 | -0.21 |
| CFCs | -0.0 | -0.0 | 2049.4 | 2075.7 | -0.00 | -0.0 | -0.00 |
| Halons | -0.0 | -0.0 | 2049.4 | 2075.7 | -0.00 | -0.0 | -0.00 |
| HCFCs | -0.8 | -3.9 | 2048.6 | 2075.3 | -0.12 | -4.0 | -0.05 |
| CH ₃ Br for QPS and CUE ^h | -1.5 | -6.8 | 2048.2 | 2074.2 | -0.18 | -0.0 | -0.06 |
| CCl ₄ | -2.2 | -9.9 | 2046.6 | 2072.3 | -0.59 | -1.8 | -0.17 |
| Cases^a of zero emissions from 2020 onward of: | | | | | | | |
| E0: All ODS (does not include N ₂ O) | -8.0 | -36.8 | 2039.6 | 2064.2 | -2.30 | -13.9 | -0.48 |
| CFCs | -1.7 | -7.9 | 2047.3 | 2073.2 | -0.62 | -3.3 | -0.09 |
| Halons | -2.2 | -9.9 | 2047.1 | 2073.0 | -0.61 | -0.2 | -0.10 |
| HCFCs | -2.4 | -11.0 | 2047.5 | 2074.7 | -0.30 | -8.7 | -0.12 |
| CCl ₄ ⁱ | -2.2 | -9.9 | 2046.6 | 2072.4 | -0.59 | -1.8 | -0.12 |
| CH ₃ CCl ₃ | -0.0 | -0.0 | 2049.4 | 2075.7 | -0.00 | -0.0 | -0.00 |
| CH ₃ Br for QPS and CUE ^h | -1.5 | -6.8 | 2048.2 | 2074.2 | -0.18 | -0.0 | -0.06 |
| Total anthropogenic N ₂ O ^j | - | - | - | - | -5.25 | -81.8 | -0.45 |
| N ₂ O mitigation | - | - | - | - | -1.23 | -19.1 | -0.04 |

| Cases ^a of full recovery of the 2020 banks of: | | | | | | | |
|--|------|-------|--------|--------|-------|-------|-------|
| B0: All ODS | -5.1 | -23.2 | 2043.9 | 2069.7 | -1.42 | -8.1 | -0.27 |
| CFCs | -1.7 | -7.9 | 2047.3 | 2073.2 | -0.62 | -3.3 | -0.09 |
| Halons | -2.2 | -9.9 | 2047.1 | 2073.0 | -0.61 | -0.2 | -0.10 |
| HCFCs | -1.6 | -7.4 | 2048.3 | 2075.1 | -0.19 | -4.7 | -0.08 |
| Cases ^a of full recovery of the 2025 banks of: | | | | | | | |
| B1: All ODS | -3.1 | -14.1 | 2045.0 | 2070.6 | -1.09 | -6.9 | -0.18 |
| CFCs | -0.9 | -4.3 | 2047.9 | 2073.8 | -0.46 | -2.4 | -0.06 |
| Halons | -1.2 | -5.5 | 2047.7 | 2073.5 | -0.46 | -0.2 | -0.06 |
| HCFCs | -1.2 | -5.7 | 2048.1 | 2074.9 | -0.18 | -4.3 | -0.07 |
| Continued emission of CFC-11: | | | | | | | |
| Constant at 67 Gg yr ⁻¹ | +4.0 | +18.3 | 2056.7 | 2096.0 | +2.06 | +10.6 | +0.20 |
| Continued emission of CCl ₄ : | | | | | | | |
| | +0.9 | +4.0 | 2051.2 | 2080.6 | +0.42 | 1.3 | +0.05 |
| Cases relating to the VSLs CH ₂ Cl ₂ : | | | | | | | |
| No future anthropogenic emission | - | - | - | - | - | - | -0.17 |
| Increasing emission | - | - | - | - | - | - | +0.17 |

Notes:

- ^a Significance of ozone-depleting substances for future EESC were calculated in the hypothetical "cases" by setting production or emission to zero in 2020 and subsequent years or the bank of the ODS to zero in the year 2020 or 2025.
- ^b EESC is calculated as in WMO (2014).
- ^c EESC is integrated above the 1980 level and until it returns to this level, denoted as year "x"
- ^d For mid-latitude conditions, an average age of air of 3 years, corresponding fractional release values, and a bromine efficiency factor (alpha) of 60 are assumed. For Antarctic vortex conditions, an average age of air of 5.5 years, corresponding fractional release values, and an alpha value of 65 are assumed. In all cases, age spectra are applied as in Newman et al. (2007).
- ^e Semi-empirical ODPs from **Table 6-1**.
- ^f GWPs with 100-year time horizon (**Table 6-2**).
- ^g Integrated globally averaged total column ozone changes are taken from 2-D model runs described in this chapter.
- ^h It is assumed that 84% of production for QPS use is emitted to the atmosphere and that 65% of production under CUE is emitted (Harris and Wuebbles et al., 2014). The alternative scenario evaluated here includes elimination of emissions from both QPS use and under CUE. Note that emissions under CUE are 15 times smaller than emissions from QPS use in future years of the baseline scenario.
- ⁱ Banks are assumed to be zero. Emissions include uncertain sources such as possible fugitive emissions and unintended other emissions.
- ^j The integrated ODP- and GWP-weighted emissions correspond to the reduction of anthropogenic N₂O emissions from RCP6.0 to two mitigation cases (see text). The weaker "N₂O mitigation" scenario is only projected through 2050, so ODP- and GWP-weighted emissions are calculated for 2020–2050.

regardless of EESC levels and the amount of anthropogenic climate change.

6.4.3.1 STRATOSPHERIC OZONE IMPLICATIONS

We project that mid-latitude EESC will return to 1980 levels around 2049 and polar EESC will return around 2076 for the baseline scenario. This is almost 2 years later for mid-latitude EESC and slightly more than 2 years later for polar EESC when compared with the baseline scenario of WMO (2014). Both of these differences are primarily a result of higher concentrations of CCl_4 , which are caused primarily by slower projected decreases in future emissions. The difference in total EESC between the WMO (2014) baseline scenario and the current one is shown in **Figure 6-3**. The differences appear very small at the scale shown all the way to 2100.

The “No Future Emissions” scenario represents the fastest that EESC could recover, assuming no changes in lifetimes or fractional release values in the future. The close alignment of the “Zero 2020 Bank,” “Zero 2025 Bank,” and “No Future Production” cases demonstrates the comparable importance of current banks and future production when ODSs are examined together. If emissions were completely stopped in 2020, it could result in an earlier return of mid-latitude and polar EESC to 1980 levels by about a decade. However, for perspective, it is important to recognize the relatively small impacts that additional controls could have on ODSs when compared with what the Montreal Protocol has already accomplished (e.g., Figures 5-6 and 5-8 of Harris and Wuebbles et al., 2014).

As previously discussed, a new approach to calculate EESC (Engel et al., 2017) has been proposed, which

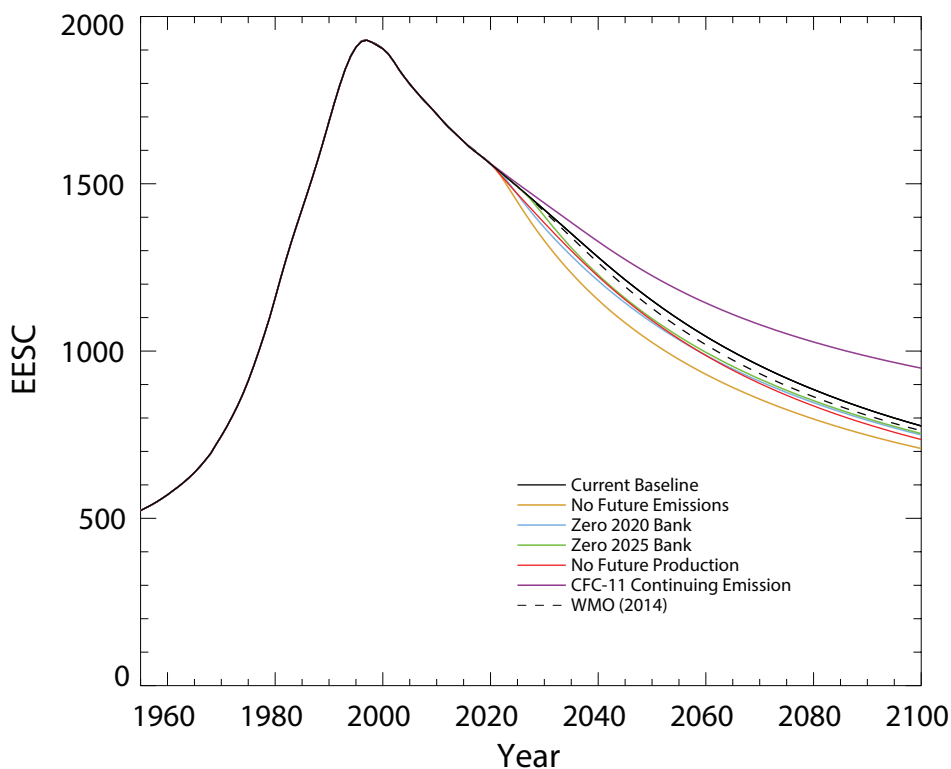


Figure 6-3. EESC for the current baseline scenario (mid-latitude conditions) compared with EESC from the WMO (2014) baseline scenario; also shown are the four major alternative scenarios that represent current mitigation examples considered in this Assessment, and a scenario that assumes a continuation of CFC-11 emissions through the end of the century at the level estimated over 2002–2016 (67 Gg yr^{-1}) (Montzka et al., 2018). All of the EESC curves are calculated using the approach from Newman (2007). The difference between the current baseline curve and the WMO (2014) curve is indistinguishable until after 2020.

differs from the methodology used in this chapter and in previous Assessments in that it attempts to account for the fact that the average age of air for source gases that have been dissociated in the stratosphere is longer than the average age of inert tracers in the same stratospheric location. For the scenarios considered in this chapter, the use of the new EESC approach leads to a delay in mid-latitude return to 1980 levels of about another decade, with a much smaller effect for polar EESC. Despite these quite large changes in the return dates for mid-latitude EESC, the relative importance of the various ODS emission sources to ozone depletion metrics changes little between the two approaches (cf. **Tables 6-5** and **6C-1**). For the rest of this chapter we will use the older EESC approach.

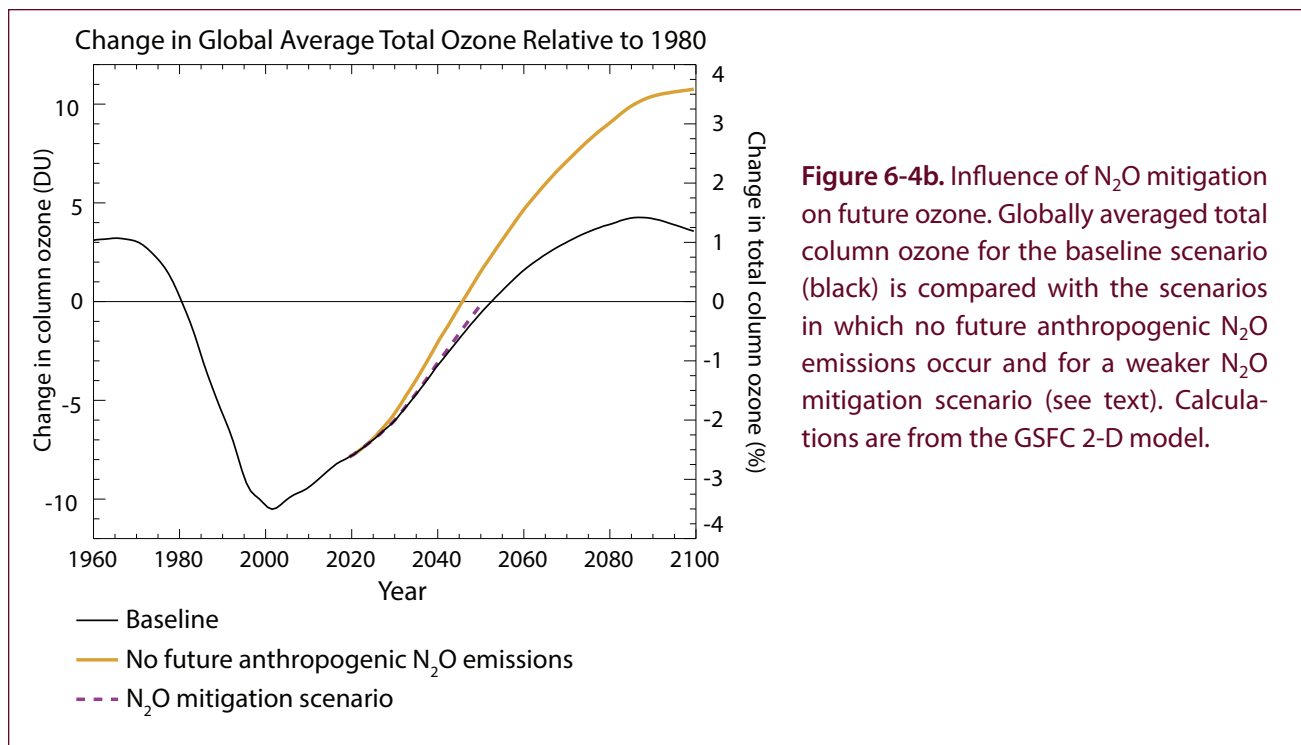
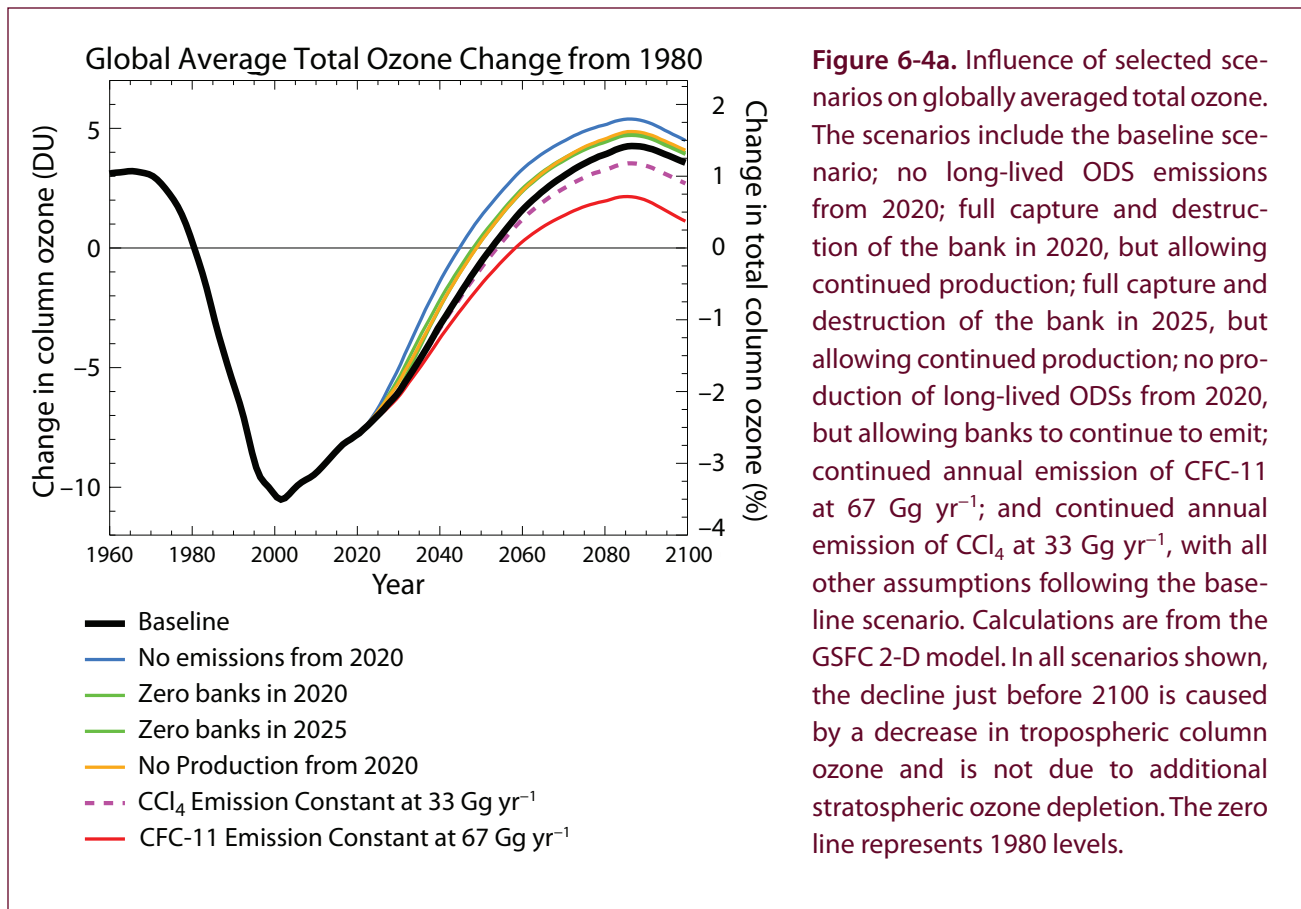
The importance of future emissions from CFCs, halons, HCFCs, CCl_4 , and CH_3Br (mainly from QPS) are all comparable, even more so than in the previous Assessment. As in WMO (2014), future emissions from CFCs and halons in the baseline scenario continue to arise entirely from the existing banks, while banks of CCl_4 and CH_3Br are assumed to be negligibly small, so future emissions for them arise exclusively from future production. Future HCFC emissions arise from both current banks as well as future projected production, with current banks contributing more than future production.

If the emissions indicated from the recent slowdown in the decline of CFC-11 concentrations continue into the future, the recovery of EESC and ozone will be delayed. As stated above, we have included a scenario in which CFC-11 emissions continue at 67 Gg yr^{-1} indefinitely. This is the level implied by atmospheric concentration trends over 2002–2016 if it is assumed that atmospheric dynamics played no role in the changing trends (Montzka et al., 2018) (**Chapter 1**). In this alternative scenario, the mid-latitude EESC return to 1980 levels is delayed by about 7 years, and polar EESC return is delayed by about 20 years. For context, the ODP-weighted CFC-11 emissions in this scenario exceed those of the baseline scenario by 2.1 million ODP-weighted tons over 2020–2060, thus almost doubling ODP-weighted emissions from the long-lived halocarbon ODSs over that period compared with the baseline scenario. Continuing emission of CCl_4 at 33 Gg yr^{-1} also has implications for ozone recovery: It delays the return of EESC to 1980 levels at mid-latitudes and in the Antarctic vortex

by ~2 years and ~5 years, respectively, relative to the baseline scenario.

Figure 6-4a compares the impact of selected scenarios on the globally averaged total column ozone as calculated with the 2-D model. As expected, the ozone response exhibits a roughly inverse relationship with the EESC curves shown in **Figure 6-3**. Continued CFC-11 emissions at 67 Gg yr^{-1} causes a change in ozone that grows over time and eventually leads to more ozone depletion than is caused by all future halocarbon ODS emissions in the baseline scenario. Shown in **Figure 6-4b** are the responses for the N_2O mitigation scenarios. N_2O exerts a similar ozone response to that shown in Harris and Wuebbles et al. (2014). After about 30 years, the impact of future anthropogenic N_2O emissions on ozone is larger than the combined impact of all future long-lived halogenated ODS emissions, and the N_2O influence continues to grow. The significance of N_2O is also apparent from its cumulative ODP- and GWP-weighted emissions shown in **Table 6-5**; the total N_2O anthropogenic emissions over 2020–2060 are more than two times that of the ODSs for ODP-weighted emissions, and six times for GWP-weighted emissions.

Figure 6-4c shows the impacts on ozone of the range of RCP scenarios (RCP2.6, 4.5, 6.0, and 8.5). The influences of CO_2 , CH_4 , and N_2O are shown, individually, by varying each one alone while holding the other two gases at 2015 levels. The baseline ODS scenario is used in all runs. The processes responsible for the ozone impacts of these greenhouse gases (GHGs) are discussed in **Chapter 3**. When compared with **Figure 6-4a**, it is apparent that the variations of each of these three gases across the RCP scenarios lead to a substantially wider range of possible future ozone levels than from the ODS scenarios alone. For example, the difference in global ozone in 2100 between the baseline ODS scenario and a scenario with no ODS emissions from 2020 is less than 1 DU (**Figure 6-4a**). This contrasts with differences of 11, 16, and 6 DU, due to differences in CO_2 , CH_4 , and N_2O , respectively, between the RCP2.6 and RCP8.5 scenarios. Thus, policies that affect the future evolution of these three GHGs in particular will be important for predicting how ozone will change. Furthermore, the potential increase of global ozone above preindustrial levels means that in the future, policy decisions that lead to less climate forcing and less ozone depletion may no



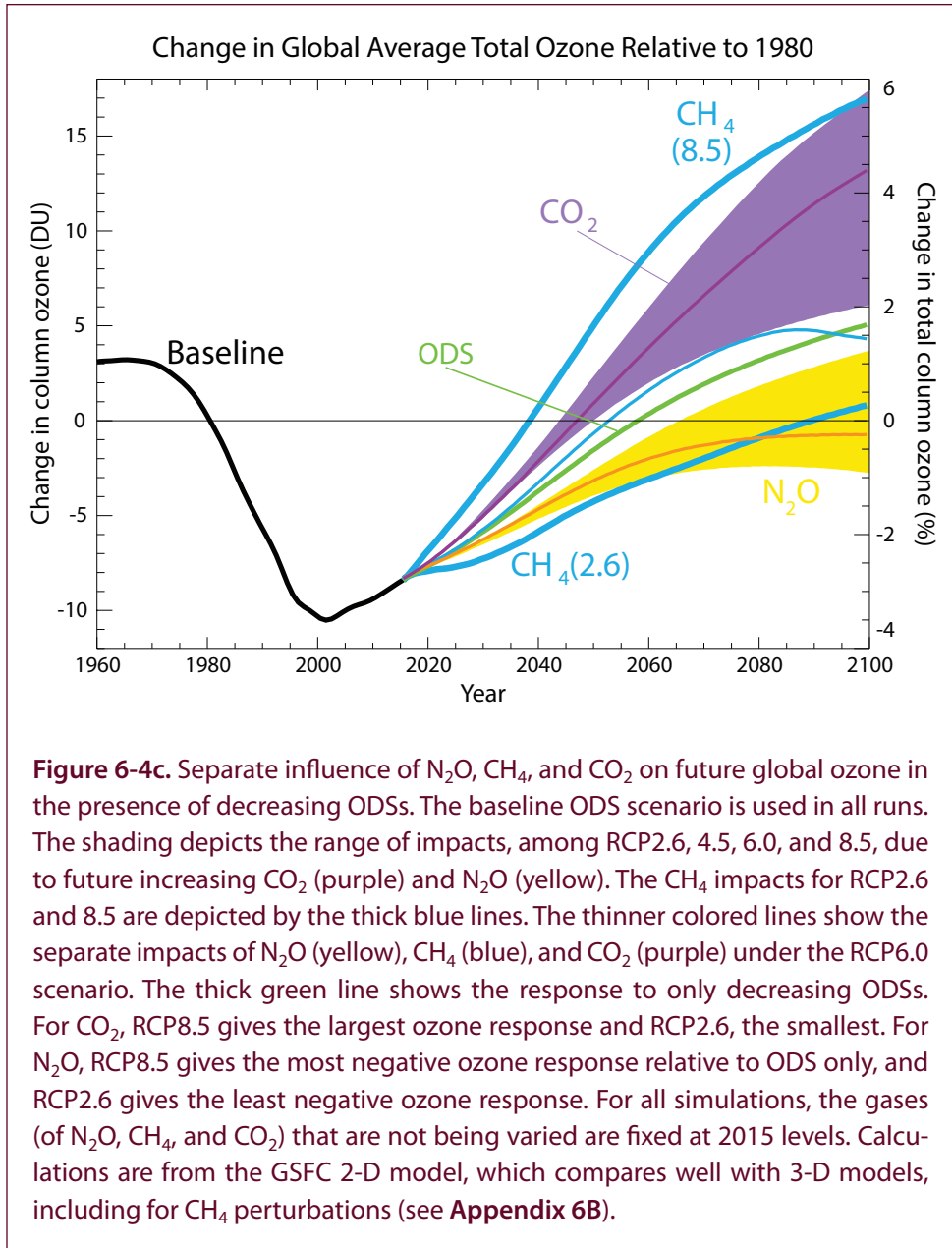


Figure 6-4c. Separate influence of N₂O, CH₄, and CO₂ on future global ozone in the presence of decreasing ODSs. The baseline ODS scenario is used in all runs. The shading depicts the range of impacts, among RCP2.6, 4.5, 6.0, and 8.5, due to future increasing CO₂ (purple) and N₂O (yellow). The CH₄ impacts for RCP2.6 and 8.5 are depicted by the thick blue lines. The thinner colored lines show the separate impacts of N₂O (yellow), CH₄ (blue), and CO₂ (purple) under the RCP6.0 scenario. The thick green line shows the response to only decreasing ODSs. For CO₂, RCP8.5 gives the largest ozone response and RCP2.6, the smallest. For N₂O, RCP8.5 gives the most negative ozone response relative to ODS only, and RCP2.6 gives the least negative ozone response. For all simulations, the gases (of N₂O, CH₄, and CO₂) that are not being varied are fixed at 2015 levels. Calculations are from the GSFC 2-D model, which compares well with 3-D models, including for CH₄ perturbations (see **Appendix 6B**).

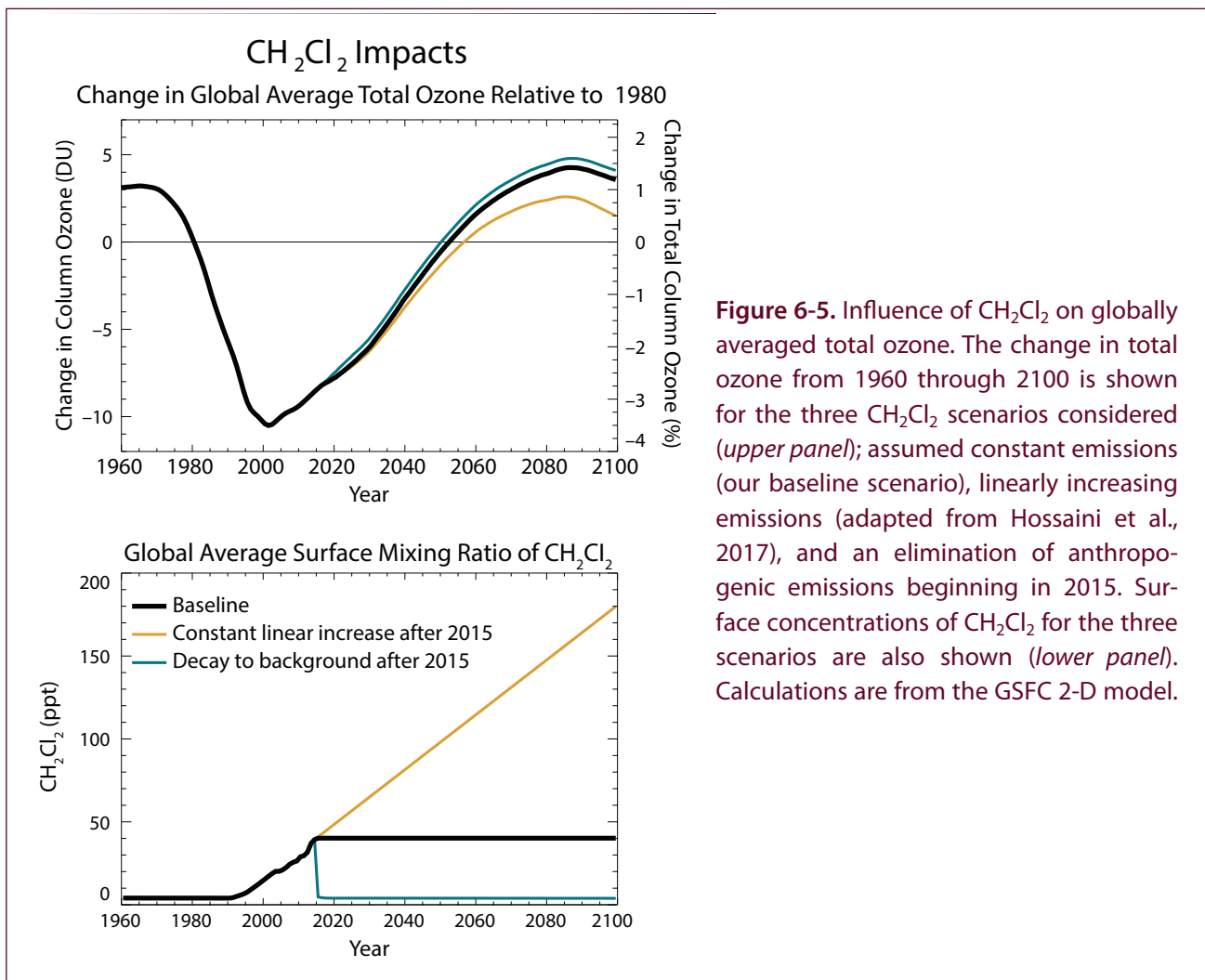


Figure 6-5. Influence of CH₂Cl₂ on globally averaged total ozone. The change in total ozone from 1960 through 2100 is shown for the three CH₂Cl₂ scenarios considered (*upper panel*); assumed constant emissions (our baseline scenario), linearly increasing emissions (adapted from Hossaini et al., 2017), and an elimination of anthropogenic emissions beginning in 2015. Surface concentrations of CH₂Cl₂ for the three scenarios are also shown (*lower panel*). Calculations are from the GSFC 2-D model.

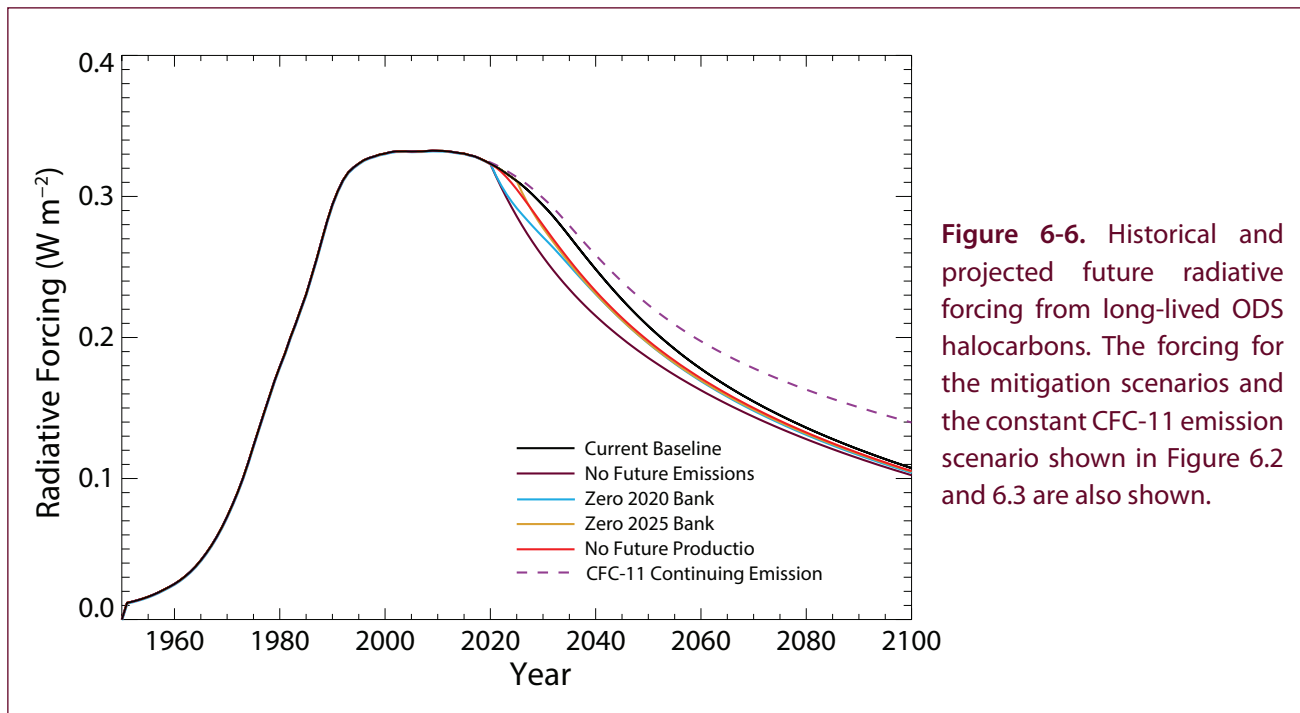
longer be considered a win-win proposition (Butler et al., 2016).

The two alternative scenarios for CH₂Cl₂, namely (1) continued strong growth in emissions and (2) immediate cessation of emissions, are shown in **Figure 6-5** along with its mixing ratios in the baseline scenario. Unlike the CFCs, CH₂Cl₂ has a short lifetime and thus responds rapidly to changes in emissions. If emissions quickly decrease in the future, the contribution of CH₂Cl₂ to stratospheric chlorine will also fall rapidly. Under scenario (1), the 2-D model predicts that integrated ozone depletion over 2020–2060 (shown in the final column of **Table 6-5**) would increase by even more than it would decrease if all future controlled ODS production were eliminated beginning in 2020. However, the continuing large variability in its surface abundances causes us to be unable to confidently predict future concentrations or to evaluate the plausibility of this scenario. If, on the other hand,

all anthropogenic emissions of CH₂Cl₂ had ceased in 2015, the effect on integrated ozone depletion from 2020–2060 would be about two-thirds of the effect of eliminating production of all controlled ODSs beginning in 2020.

6.4.3.2 CLIMATE IMPLICATIONS

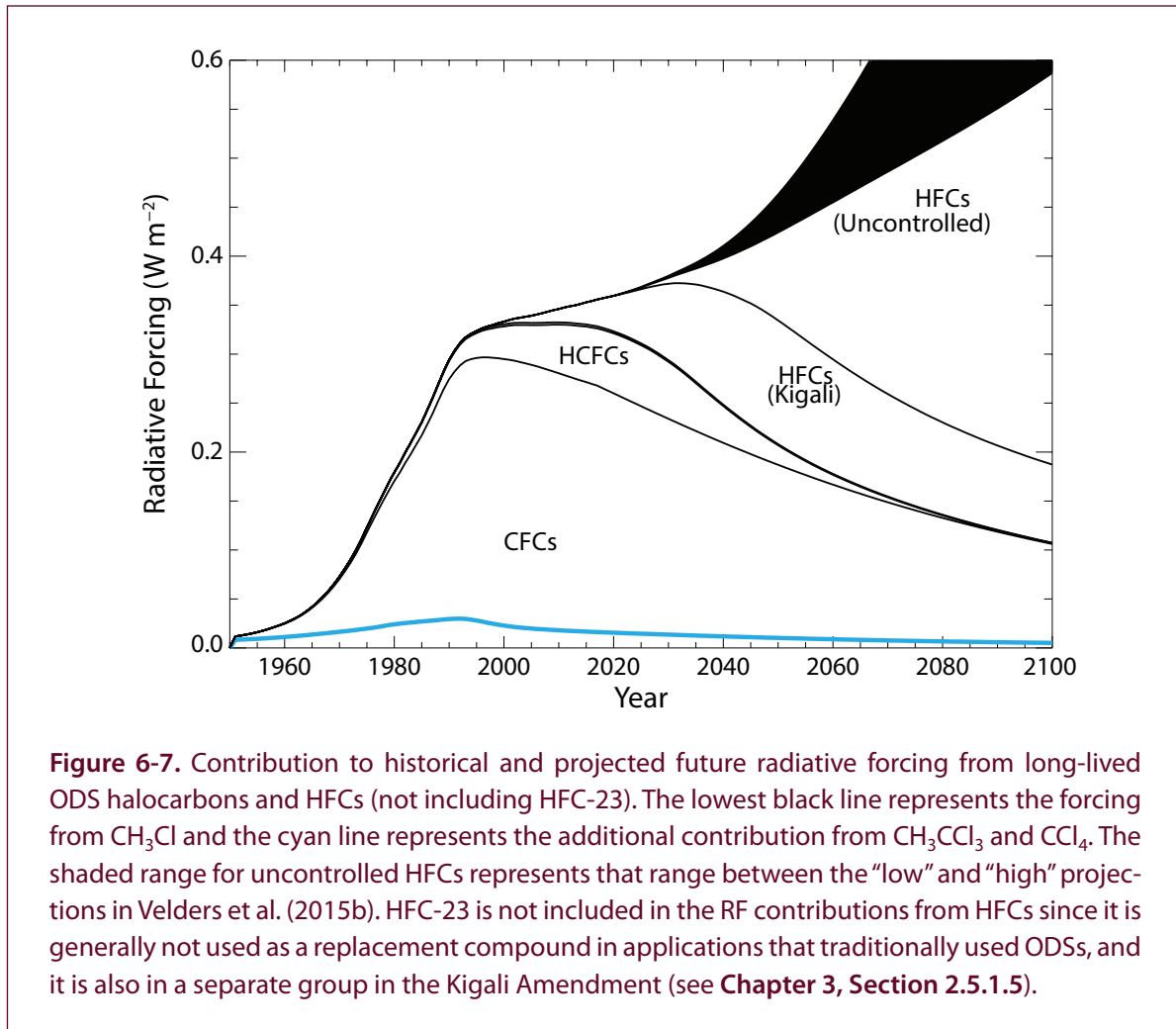
From the projections for 2020 through 2060, HCFC emissions contribute about two-thirds to the total GWP-weighted emissions for all ODSs (not including N₂O), with both future production and current banks playing comparable roles. Projected CFC banks in 2020 represent the next most important class of GWP-weighted emissions, contributing just over 20% of the total in the baseline scenario. If, however, unreported CFC-11 production is and continues to be an important factor, the GWP-weighted emissions of all the controlled ODSs from 2020 to 2060 would almost double compared with the baseline



scenario (assuming CFC-11 emissions continue at 67 Gg yr^{-1}), and CFCs would be the ODS group whose future emissions contribute most to climate change. Continuing CCl_4 emissions at 2016 levels lead to a much smaller additional climate impact. As a point of comparison, the amount of CO_2 emitted in 2015 from fuel combustion was 32 Gt CO_2 , and the sum from 2020 to 2060 in the RCP6.0 scenario is $1,700 \text{ Gt CO}_2$ (IEA, 2017), while the total CO_2 -equivalent emissions in the baseline scenario from ODSs controlled by the Montreal Protocol over 2020–2060 is projected to be $13.8 \text{ Gt CO}_2\text{-eq yr}^{-1}$.

As seen in **Figure 6-6**, the maximum difference in radiative forcing between the baseline scenario and the zero-emission scenario is less than 0.05 W m^{-2} , and by 2100, no ODS policy action could reduce ODS radiative forcing by as much as 0.01 W m^{-2} when compared with the baseline scenario, which assumes compliance with the Montreal Protocol. If there is not complete adherence to the Protocol, the RF would be expected to rise above the current baseline curve, with the actual RF path depending on the extent of the Montreal Protocol violation. If, for example, CFC-11 emissions were to continue at 67 Gg yr^{-1} indefinitely, RF would be 0.03 W m^{-2} higher in 2100 than in the baseline scenario (**Figure 6-6**).

Figure 6-7 shows the contribution of the various ODSs and their replacements, specifically HFCs, to future RF. The RF from CFCs has been declining since the latter half of the 20th century. The subsequent increase in the HCFC replacement compounds is projected to offset this decline through to about 2020. Once the transition to HFCs advances, the projected HFC concentration increases more than offset the decline in ODS RF for at least a decade. After that point, the HFC restrictions of the Kigali Amendment, if adhered to, ensure a continued decline in total RF from ODSs and their replacements through the rest of the century. This is one of the primary expected successes of the Kigali Amendment; in the absence of Kigali, there would have been a possibility that uncontrolled growth of HFCs could have led to increasing total RF through the end of the century. Our current projections suggest that the total RF from ODSs and their replacements will be below 0.2 W m^{-2} by the end of the century if there is global adherence to the Kigali Amendment, meaning the RF from all Montreal Protocol gases (ODSs and HFCs) would be only slightly higher than the RF of CFC-12, by itself, in the early 2000s, when it was at its peak concentration. Cumulative GWP-weighted HFC emissions under the Kigali Amendment (excluding HFC-23) are calculated to be $62\text{--}63 \text{ Gt CO}_2\text{-eq yr}^{-1}$ from 2020 to 2060 compared with potential emissions in the absence of



Kigali (baseline scenario of Velders et al., 2015b) over the same time period of 125–155 Gt CO_2 -eq yr^{-1} . A hypothetical immediate global phaseout of HFC production in 2020 could reduce these cumulative emissions to 9.5–9.6 Gt CO_2 -eq yr^{-1} , which represent continuing emissions from the banks. See **Chapter 2** for further discussion.

The climatic influence of the ODSs and their replacements are shown in comparison with the three dominant GHGs, CO_2 , CH_4 , and N_2O , in **Figure 6-8**. The figure demonstrates the large range in CO_2 -equivalent emissions and radiative forcing for these three climatologically important gases (using the RCP2.6 projection

as the minimum and the RCP8.5 projection as the maximum emissions scenario). The substantial benefit of the Kigali Amendment is apparent from the figure, in comparing the HFC curves without the Kigali Amendment (red dashed) with the Kigali curves (red solid). The sizable reduction in the climate impact of ODSs, in response to actions taken as a consequence of the Montreal Protocol, is also evident. In contrast, the relative reductions that can be made in future ODS and HFC emissions lead to a substantially smaller climate influence, assuming compliance with the Protocol.

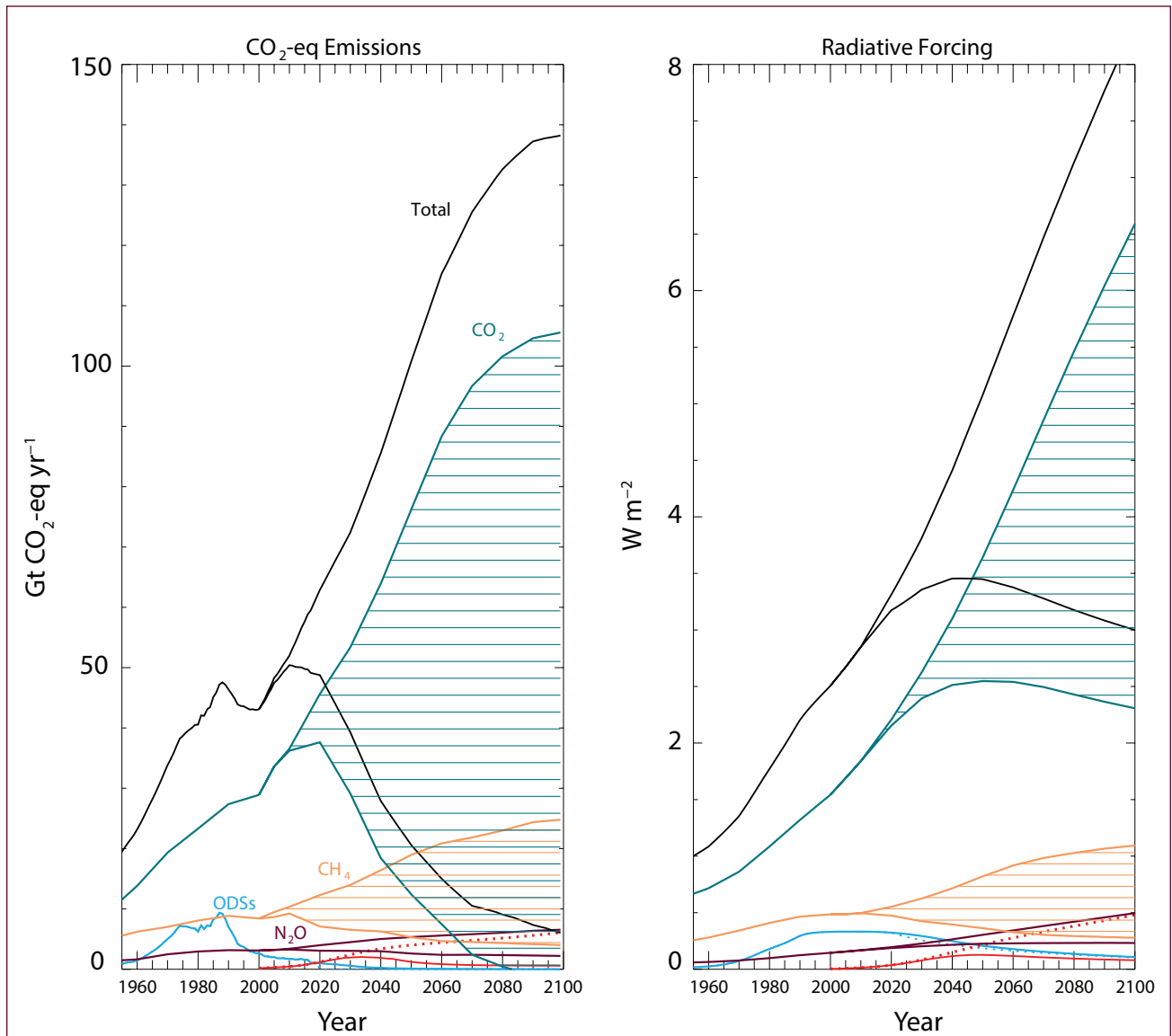


Figure 6.8. Emissions and radiative forcing of ODSs and HFCs compared to these quantities for the three long-lived greenhouse gases: CO₂, CH₄, and N₂O. Maximum (minimum) values for CO₂, CH₄, and N₂O represent the RCP8.5 (RCP2.6) future projections. The total represents the sum of all curves, with the maximum total including the baseline curves for ODSs and HFCs, and the RCP8.5 scenario for the other three greenhouse gases. The minimum total is the baseline ODS and HFC scenario and the RCP2.6 scenario for CO₂, CH₄, and N₂O. The HFC curves (red) are not labeled due to the lack of available space. The solid red curves are the baseline HFC scenario consistent with the Kigali Amendment and the dashed HFC curves represent the “low growth” future HFC scenario described in **Chapter 2** and is from Velders et al. (2015a). The dashed ODS curves represent the “no future ODS emission” scenario described in the text.

REFERENCES

- Allen, M.R., J.S. Fuglestedt, K.P. Shine, A. Reisinger, R.T. Pierrehumbert, and P.M. Forster, New use of global warming potentials to compare cumulative and short-lived climate pollutants, *Nat. Clim. Change*, 6 (8), 773–776, doi:10.1038/nclimate2998, 2016.
- Anderson, J.G., D.K. Weisenstein, K.P. Bowman, C.R. Homeyer, J.B. Smith, D.M. Wilmoth, D.S. Sayres, J.E. Klobas, S.S. Leroy, J.A. Dykema, and S.C. Wofsy, Stratospheric ozone over the United States in summer linked to observations of convection and temperature via chlorine and bromine catalysis, *Proc. Natl. Acad. Sci.*, 114 (25), E4905–E4913, doi:10.1073/pnas.1619318114, 2017.
- Angel, R., Feasibility of cooling the Earth with a cloud of small spacecraft near the inner Lagrange point (L1), *Proc. Natl. Acad. Sci.*, 103 (46), 17,184–17,189, doi:10.1073/pnas.0608163103, 2006.
- Aquila, V., C.I. Garfinkel, P.A. Newman, L.D. Oman, and D.W. Waugh, Modifications of the quasi-biennial oscillation by a geoengineering perturbation of the stratospheric aerosol layer, *Geophys. Res. Lett.*, 41 (5), 1738–1744, doi:10.1002/2013gl058818, 2014.
- Benduhn, F., J. Schallock, and M.G. Lawrence, Early growth dynamical implications for the steerability of stratospheric solar radiation management via sulfur aerosol particles, *Geophys. Res. Lett.*, 43 (18), 9956–9963, doi:10.1002/2016GL070701, 2016.
- Berthet, G., F. Jegou, V. Catoire, G. Krysztofiak, J.B. Renard, A.E. Bourassa, D.A. Degenstein, C. Brogniez, M. Dorf, S. Kreycky, K. Pfeilsticker, B. Werner, F. Lefevre, T.J. Roberts, T. Lurton, D. Vignelles, N. Begue, Q. Bourgeois, D. Daugeron, M. Chartier, C. Robert, B. Gaubicher, and C. Guimbaud, Impact of a moderate volcanic eruption on chemistry in the lower stratosphere: balloon-borne observations and model calculations, *Atmos. Chem. Phys.*, 17 (3), 2229–2253, doi:10.5194/acp-17-2229-2017, 2017.
- Boutonnet, J.C., P. Bingham, D. Calamari, C. de Rooij, J. Franklin, T. Kawano, J.M. Libre, A. McCulloch, G. Malinverno, J.M. Odom, G.M. Rusch, K. Smythe, I. Sobolev, R. Thompson, and J.M. Tiedje, Environmental risk assessment of trifluoroacetic acid, *Hum. Ecol. Risk Assess.*, 5 (1), 59–124, doi:10.1080/10807039991289644, 1999.
- Bravo, I., Y. Diaz-de-Mera, A. Aranda, E. Moreno, D.R. Nutt, and G. Marston, Radiative efficiencies for fluorinated esters: indirect global warming potentials of hydrofluoroethers, *Phys. Chem. Chem. Phys.*, 13 (38), 17185–17193, doi:10.1039/c1cp21874c, 2011.
- Brown, J., HFOs New, Low Global Warming Potential Refrigerants, *ASHRAE J.*, 51 (8), 22–29, 2009.
- Burkholder, J.B., R.A. Cox, and A.R. Ravishankara, Atmospheric degradation of ozone depleting substances, their substitutes, and related species, *Chem. Rev.*, 115 (10), 3704–3759, doi:10.1021/cr5006759, 2015.
- Butler, A.H., J.S. Daniel, R.W. Portmann, A.R. Ravishankara, P.J. Young, D.W. Fahey, and K.H. Rosenlof, Diverse policy implications for future ozone and surface UV in a changing climate, *Environ. Res. Lett.*, 11 (6), doi:10.1088/1748-9326/11/6/064017, 2016.
- Calvert, J.G., R.G. Derwent, J.J. Orlando, G.S. Tyndall, and T.J. Wallington, Mechanisms of atmospheric oxidation of the alkanes, 992 pp., Oxford University Press, New York, New York, 2008.
- Campbell, N., and R. Shende, HFCs and PFCs: Current and Future Supply, Demand and Emissions, plus Emissions of CFCs, HCFCs and Halons, in *Safeguarding the Ozone Layer and the Global Climate System: Issues Related to Hydrofluorocarbons and Perfluorocarbons*, edited by B. Metz, L. Kuijpers, S. Solomon, S.O. Andersen, O. Davidson, J. Pons, D. de Jager, T. Kestin, M. Manning, and L.A. Meyer, 403–436, Cambridge University Press, Cambridge, United Kingdom, 2005.
- Carpenter, L.J., and P.S. Liss, On temperate sources of bromoform and other reactive organic bromine gases, *J. Geophys. Res. Atmos.*, 105 (D16), 20539–20547, doi:10.1029/2000JD900242, 2000.
- Carpenter, L.J., and S. Reimann (Lead Authors), J.B. Burkholder, C. Clerbaux, B.D. Hall, R. Hossaini, J.C. Laube, and S.A. Yvon-Lewis, Update on Ozone-Depleting Substances (ODSs) and Other Gases of Interest to the Montreal Protocol, Chapter 1 in *Scientific Assessment of Ozone Depletion: 2014*, Global Ozone research and Monitoring Project–Report No. 55, World Meteorological Organization, Geneva, Switzerland, 2014.
- Chhantyal-Pun, R., M.R. McGillen, J.M. Beames,

- M.A.H. Khan, C.J. Percival, D.E. Shallcross, and A.J. Orr-Ewing, Temperature-dependence of the rates of reaction of trifluoroacetic acid with Criegee intermediates, *Angew. Chem. Int. Ed.*, *56*, 9044–9047, doi:10.1002/anie/201703700, 2017.
- Crutzen, P.J., Albedo enhancement by stratospheric sulfur injections: A contribution to resolve a policy dilemma?, *Climate Change*, *77*, 211–220, doi:10.1007/s10584-006-9101-y, 2006.
- Dai, Z., D.K. Weisenstein, and D.W. Keith, Tailoring meridional and seasonal radiative forcing by sulfate aerosol solar geoengineering, *Geophys. Res. Lett.*, *45*, 1030–1039, doi:10.1002/2017GL076472, 2018.
- Daniel, J.S., S. Solomon, and D.L. Albritton, On the evaluation of halocarbon radiative forcing and global warming potentials, *J. Geophys. Res. Atmos.*, *100* (D1), 1271–1285, doi:10.1029/94JD02516, 1995.
- Daniel, J.S., E.L. Fleming, R.W. Portmann, G.J.M. Velders, C.H. Jackman, and A.R. Ravishankara, Options to accelerate ozone recovery: ozone and climate benefits, *Atmos. Chem. Phys.*, *10*, 7697–7707, doi:10.5194/acp-7697-2010, 2010.
- Davidson, E.A., Representative concentration pathways and mitigation scenarios for nitrous oxide, *Environ. Res. Lett.*, *7*, doi:10.1088/1748-9326/7/2/024005, 2012.
- Davis, M.E., F. Bernard, M.R. McGillen, E.L. Fleming, and J.R. Burkholder, UV and infrared absorption spectra, atmospheric lifetimes, and ozone depletion and global warming potentials for CCl₂FCCl₂F (CFC-112), CCl₃CClF₂ (CFC-112a), CCl₃CF₃ (CFC-113a), and CCl₂FCF₃ (CFC-114a), *Atmos. Chem. Phys.*, *16* (12), 8043–8052, doi:10.5194/acp-16-8043-2016, 2016.
- Dhomse, S.S., D. Kinnison, M.P. Chipperfield, R.J. Salawitch, I. Cionni, M.I. Hegglin, N.L. Abraham, H. Akiyoshi, A.T. Archibald, E.M. Bednarz, S. Bekki, P. Braesicke, N. Butchart, M. Dameris, M. Deushi, S. Frith, S.C. Hardiman, B. Hassler, L.W. Horowitz, R.-M. Hu, P. Jöckel, B. Josse, O. Kirner, S. Kremser, U. Langematz, J. Lewis, M. Marchand, M.Y. Lin, E. Mancini, V. Marécal, M. Michou, O. Morgenstern, F.M. O'Connor, L. Oman, G. Pitari, D.A. Plummer, J.A. Pyle, L.E. Revell, E. Rozanov, R. Schofield, A. Stenke, K. Stone, K. Sudo, S. Tilmes, D. Visioni, Y. Yamashita, and G. Zeng, Estimates of ozone return dates from Chemistry-Climate Model Initiative simulations, *Atmos. Chem. Phys.*, *18* (11), 8409–8438, doi:10.5194/acp-18-8409-2018, 2018.
- Doncaster, B., J. Shulman, J. Bradford, and J. Olds, *SpaceWorks 2016 Nano/Microsatellite Market Forecast Report*, 20 pp., SpaceWorks Enterprises, Inc., Atlanta, Georgia, 2016.
- Douglass, A.R., R.S. Stolarski, S.E. Strahan, and L.D. Oman, Understanding differences in upper stratospheric ozone response to changes in chlorine and temperature as computed using CCM-Val-2 models, *J. Geophys. Res.*, *117* (D15), D16306, doi:10.1029/2012JD017483, 2012.
- Dykema, J.A., D.W. Keith, J.G. Anderson, and D. Weisenstein, Stratospheric controlled perturbation experiment: a small-scale experiment to improve understanding of the risks of solar geoengineering, *Phil. Trans. R. Soc. A* *372* (2031), doi:10.1098/rsta.2014.0059, 2014.
- Early, J.T., Space-based solar shield to offset greenhouse effect, *J. Br. Interplanet. Soc.*, *42* (12), 567–569, 1989.
- Eastham, S.D., D.W. Keith, and S.R.H. Barrett, Mortality tradeoff between air quality and skin cancer from changes in stratospheric ozone, *Environ. Res. Lett.*, *13*, doi:10.1088/1748-9326/aaad2e, 2018.
- Engel, A., H. Bonisch, J. Ostermoller, M.P. Chipperfield, S. Dhomse, and P. Jockel, A refined method for calculating equivalent effective stratospheric chlorine *Atmos. Chem. Phys.*, *18*, 601–619, doi:10.5194/acp-18-601-2018, 2018.
- English, J.M., O.B. Toon, and M.J. Mills, Microphysical simulations of sulfur burdens from stratospheric sulfur geoengineering, *Atmos. Chem. Phys.*, *12* (10), 4775–4793, doi:10.5194/acp-12-4775-2012, 2012.
- Etminan, M., G. Myhre, E.J. Highwood, and K.P. Shine, Radiative forcing of carbon dioxide, methane, and nitrous oxide: A significant revision of the methane radiative forcing, *Geophys. Res. Lett.*, *43*, 12614–12623, doi:10.1002/2016GL071930, 2016.
- FAA (Federal Aviation Administration), *Commercial Space Transportation Forecast, Executive Summary Report*, 177 pp., FAA Office of Commercial Space Transportation, Washington, D.C., 2016.
- Fahey, D.W., S.R. Kawa, E.L. Woodbridge, P. Tin, J.C. Wilson, H.H. Jonsson, J.E. Dye, D. Baumgardner, S. Borrmann, D.W. Toohey, L.M. Avallone,

- M.H. Proffitt, J. Margitan, M. Loewenstein, J.R. Podolske, R.J. Salawitch, S.C. Wofsy, M.K.W. Ko, D.E. Anderson, M.R. Schoeberl, and K.R. Chan, In situ measurements constraining the role of sulfate aerosols in mid-latitude ozone depletion, *Nature*, 363, 509–514, doi:10.1038/363509a0, 1993.
- Falk, S., B.M. Sinnhuber, G. Krysztofiak, P. Jokel, P. Graf, and S.T. Lennartz, Brominated VSLS and their influence on ozone under a changing climate, *Atmos. Chem. Phys.*, 17 (18), 11,313–11,329, doi:10.5194/acp-17-11313-2017, 2017.
- Fang, X.K., B.R. Miller, S.S. Su, J. Wu, J.B. Zhang, and J.X. Hu, Historical Emissions of HFC-23 (CHF₃) in China and Projections upon Policy Options by 2050, *Environ. Sci. Technol.*, 48 (7), 4056–4062, doi:10.1021/es404995f, 2014.
- Fernandez, R.P., D.E. Kinnison, J.-F. Lamarque, S. Tilmes, and A. Saiz-Lopez, Impact of biogenic very short-lived bromine on the Antarctic ozone hole during the 21st century, *Atmos. Chem. Phys.*, 17 (3), 1673–1688, doi:10.5194/acp-17-1673-2017, 2017.
- Fioletov, V.E., G.E. Bodeker, A.J. Miller, R.D. McPeters, and R. Stolarski, Global ozone and zonal total ozone variations estimated from ground-based and satellite measurements: 1964–2000, *J. Geophys. Res.*, 107 (D22), ACH21-1–ACH21-14, doi:10.1029/2001JD001350, 2002.
- Fiore, A.M., J.J. West, L.W. Horowitz, V. Naik, and M.D. Schwarzkopf, Characterizing the tropospheric ozone response to methane emission controls and the benefits to climate and air quality, *J. Geophys. Res.*, 113, D08307, doi:10.1029/2007JD009162, 2008.
- Fleming, E.L., C.H. Jackman, R.S. Stolarski, and A.R. Douglass, A model study of the impact of source gas changes on the stratosphere for 1850–2100, *Atmos. Chem. Phys.*, 11 (16), 8515–8541, doi:10.5194/acp-11-8515-2011, 2011.
- Froidevaux, L., J. Anderson, H.-J. Wang, R.A. Fuller, M.J. Schwartz, M.L. Santee, N.J. Livesey, H.C. Pumphrey, P.F. Bernath, J.M. Russell III, and M.P. McCormick, Global Ozone Chemistry And Related trace gas Data records for the Stratosphere (GOZCARDS): Methodology and sample results with a focus on HCl, H₂O, and O₃, *Atmos. Chem. Phys.*, 15 (18), 10,471–10,507, doi:10.5194/acp-15-10471-2015, 2015.
- Frank, H., A. Klein, and D. Renschen, Environmental trifluoroacetate, *Nature*, 382 (34), doi:10.1038/382034a0, 1996.
- Harris, N.R.P., and D.J. Wuebbles (Lead Authors), J.S. Daniel, J. Hu, L.J.M. Kuijpers, K.S. Law, M.J. Prather, and R. Schofield, Scenarios and Information for Policymakers, Chapter 5 in *Scientific Assessment of Ozone Depletion: 2014*, Global Ozone research and Monitoring Project–Report No. 55, World Meteorological Organization, Geneva, Switzerland, 2014.
- Hayman, G.D., and R.G. Derwent, Atmospheric chemical reactivity and ozone-forming potentials of potential CFC replacements, *Environ. Sci. Technol.*, 31 (2), 327–336, doi:DOI 10.1021/es950775l, 1997.
- Heckendorn, P., D. Weisenstein, S. Fueglistaler, B.P. Luo, E. Rozanov, M. Schraner, L.W. Thomason, and T. Peter, The impact of geoengineering aerosols on stratospheric temperature and ozone, *Environ. Res. Lett.*, 4 (4), 108, doi:10.1008/1748-9326/4/4/045108, 2009.
- Henne, S., D.E. Shallcross, S. Reimann, P. Xiao, D. Brunner, S. O’Doherty, and B. Buchmann, Future Emissions and Atmospheric Fate of HFC-1234yf from Mobile Air Conditioners in Europe, *Environ. Sci. Technol.*, 46 (3), 1650–1658, doi:10.1021/es2034608, 2012.
- Hossaini, R., P.K. Patra, A.A. Leeson, G. Krysztofiak, N.L. Abraham, S.J. Andrews, A.T. Archibald, J. Aschmann, E.L. Atlas, D.A. Belikov, H. Bonisch, L.J. Carpenter, S. Dhomse, M. Dorf, A. Engel, W. Feng, S. Fuhlbrugge, P.T. Griffiths, N.R.P. Harris, R. Hommel, T. Keber, K. Kruger, S.T. Lennartz, S. Maksyutov, H. Mantle, G.P. Mills, B.R. Miller, S.A. Montzka, F. Moore, M.A. Navarro, D.E. Oram, K. Pfeilsticker, J.A. Pyle, B. Quack, A.D. Robinson, E. Saikawa, A. Saiz-Lopez, S. Sala, B.M. Sinnhuber, S. Taguchi, S. Tegtmeier, R.T. Lidster, C. Wilson, and F. Ziska, A multi-model intercomparison of halogenated very short-lived substances (TransCom-VSLS): linking oceanic emissions and tropospheric transport for a reconciled estimate of the stratospheric source gas injection of bromine, *Atmos. Chem. Phys.*, 16 (14), 9163–9187, doi:10.5194/acp-16-9163-2016, 2016.
- Hossaini, R., M.P. Chipperfield, S.A. Montzka, A.A. Leeson, S.S. Dhomse, and J.A. Pyle, The increasing threat to stratospheric ozone from dichloro-

- methane, *Nature*, doi:10.1038/ncomms15962, 2017.
- Hu, L., S. Yvon-Lewis, Y.N. Liu, and T.S. Bianchi, The ocean in near equilibrium with atmospheric methyl bromide, *Global Biogeochem. Cycles*, 26, doi:10.1029/2011GB004272, 2012.
- Hurwitz, M.M., E.L. Fleming, P.A. Newman, F. Li, E. Mlawer, K. Cady-Pereira, and R. Bailey, Ozone depletion by hydrofluorocarbons, *Geophys. Res. Lett.*, 42, doi:10.1002/2015GL065856, 2015.
- Hurwitz, M.M., E.L. Fleming, P.A. Newman, F. Li, and Q. Liang, Early action on HFCs mitigates future atmospheric change, *Environ. Res. Lett.*, 11, doi:10.1008/1748-9326/11/11/114019, 2016.
- IEA (International Energy Agency), *Key World Energy Statistics 2017*, Paris, France, 2017.
- IPCC (Intergovernmental Panel on Climate Change), *Climate Change 2013: The Physical Science Basis: Contribution of Working Group I to the Fifth Assessment Report of the Intergovernmental Panel on Climate Change*, edited by T.F. Stocker, D. Qin, G.-K. Plattner, M. Tignor, S.K. Allen, J. Boschung, A. Nauels, Y. Xia, V. Bex, and P.M. Midgley, 1535 pp., Cambridge University Press, Cambridge, United Kingdom, 2013.
- IPCC/TEAP (Intergovernmental Panel on Climate Change, Technology and Economic Assessment Panel), *Special Report on Safeguarding the Ozone Layer and the Global Climate System: Issues Related to Hydrofluorocarbons and Perfluorocarbons*, 478 pp., Cambridge University Press, Cambridge, United Kingdom, doi:10.13140/2.1.4337.2161, 2005.
- Jackman, C.H., and E.L. Fleming, Stratospheric ozone response to a solar irradiance reduction in a quadrupled CO₂ environment, *Earth's Future*, 2, 331–340, doi:10.1002/2014EF000244, 2014.
- Jacob, D.J., *Introduction to Atmospheric Chemistry*, 266 pp., Princeton University Press, Princeton, New Jersey, 1999.
- Jones, A., J.M. Haywood, K. Alterskjaer, O. Boucher, J.N.S. Cole, C.L. Curry, P.J. Irvine, D.Y. Ji, B. Kravitz, J.E. Kristjánsson, J.C. Moore, U. Niemeier, A. Robock, H. Schmidt, B. Singh, S. Tilmes, S. Watanabe, and J.H. Yoon, The impact of abrupt suspension of solar radiation management (termination effect) in experiment G2 of the Geoengineering Model Intercomparison Project (GeoMIP), *J. Geophys. Res. Atmos.*, 118 (17), 9743–9752, doi:10.1002/jgrd.50762, 2013.
- Jubb, A.M., M.R. McGillen, R.W. Portmann, J.S. Daniel, and J.B. Burkholder, An atmospheric photochemical source of the persistent greenhouse gas CF₄, *Geophys. Res. Lett.*, 42 (21), 9505–9511, doi:10.1002/2015GL066193, 2015.
- Kawase, H., T. Nagashima, K. Sudo, and T. Nozawa, Future changes in tropospheric ozone under Representative Concentration Pathways (RCPs), *Geophys. Res. Lett.*, 38, L05801, doi:10.1029/2010GL046402, 2011.
- Kazil, J., S. McKeen, S.W. Kim, R. Ahmadov, G.A. Grell, R.K. Talukdar, and A.R. Ravishankara, Deposition and rainwater concentrations of trifluoroacetic acid in the United States from the use of HFO-1234yf, *J. Geophys. Res. Atmos.*, 119 (24), 14059–14079, doi:10.1002/2014JD022058, 2014.
- Keith, D.W., D.K. Weisenstein, J.A. Dykema, and F.N. Keutsch, Stratospheric solar geoengineering without ozone loss?, *Proc. Nat. Acad. Sci.*, 113 (52), 14,910–14,914, doi:10.1073/pnas.161557211, 2016.
- Klinkrad, Large satellite constellations and related challenges for space debris mitigation, *J. Space Safety Eng.*, 4 (2), 59–60, doi:10.1016/j.jsse.2017.06.002, 2017.
- Kravitz, B., A. Robock, L. Oman, G. Stenchikov, and A.B. Marquardt, Sulfuric acid deposition from stratospheric geoengineering with sulfate aerosols, *J. Geophys. Res.*, 115 (D16), doi:10.1029/2009JD011918, 2009.
- Kravitz, B., A. Robock, D.T. Shindell, and M.A. Miller, Sensitivity of stratospheric geoengineering with black carbon to aerosol size and altitude of injection, *J. Geophys. Res. Atmos.*, 117, doi:10.1029/2011JD017341, 2012.
- Kravitz, B., K. Caldeira, O. Boucher, A. Robock, P.J. Rasch, K. Alterskjaer, D.B. Karam, J.N.S. Cole, C.L. Curry, J.M. Haywood, P.J. Irvine, D. Ji, A. Jones, J.E. Kristjánsson, D.J. Lunt, J.C. Moore, U. Niemeier, H. Schmidt, M. Schulz, B. Singh, S. Tilmes, S. Watanabe, S. Yang, and J.-H. Yoon, Climate model response from the Geoengineering Model Intercomparison Project (GeoMIP), *J. Geophys. Res.*, 118 (15), 8320, doi:10.1002/jgrd.50646, 2013.
- Kravitz, B., D.G. MacMartin, M.J. Mills, J.H. Richter, S. Tilmes, J.-F. Lamarque, J.J. Tribbia, and F. Vitt, First simulations of designing stratospheric sulfate

- aerosol geoengineering to meet multiple simultaneous climate objectives, *J. Geophys. Res. Atmos.*, *122*, 12,616–12,634, doi:10.1002/2017JD026874, 2017.
- Laakso, A., H. Korhonen, S. Romakkaniemi, and H. Kokkola, Radiative and climate effects of stratospheric sulfur geoengineering using seasonally varying injection areas, *Atmos. Chem. Phys.*, *17*, 6957–6974, doi:10.5194/acp-17-6957-2017, 2017.
- Larson, E.J.L., R.W. Portmann, K.H. Rosenlof, D.W. Fahey, J.S. Daniel, and M.N. Ross, Global atmospheric response to emissions from a proposed reusable space launch system *Earth's Future*, *5* (1), 37–48, doi:10.1002/2016EF000399 2017.
- Laube, J.C., A. Keil, H. Bonisch, A. Engel, T. Rockmann, C.M. Volk, and W.T. Sturges, Observation-based assessment of stratospheric fractional release, lifetimes, and ozone depletion potentials of ten important source gases, *Atmos. Chem. Phys.*, *13* (5), 2779–2791, doi:10.5194/acp-13-2779-2013, 2013.
- Laube, J.C., M.J. Newland, C. Hogan, C.A.M. Brenninkmeijer, P.J. Fraser, P. Martinerie, D.E. Oram, C.E. Reeves, T. Röckmann, J. Schwander, E. Witrant, and W.T. Sturges, Newly detected ozone-depleting substances in the atmosphere, *Nat. Geosci.*, *7*, 266–269, doi:10.1038/ngeo2109, 2014.
- Laube, J.C., N.M. Hanif, P. Martinerie, E. Gallacher, P.J. Fraser, R. Langenfelds, C.A.M. Brenninkmeijer, J. Schwander, E. Witrant, J.L. Wang, C.F. Ouyang, L.J. Gooch, C.E. Reeves, W.T. Sturges, and D.E. Oram, Tropospheric observations of CFC-114 and CFC-114a with a focus on long-term trends and emissions, *Atmos. Chem. Phys.*, *16* (23), 15347–15358, doi:10.5194/acp-16-15347-2016, 2016.
- Leedham, E.C., C. Hughes, F.S.L. Keng, S.M. Phang, G. Malin, and W.T. Sturges, Emission of atmospherically significant halocarbons by naturally occurring and farmed tropical macroalgae, *Biogeosciences*, *10* (6), 3615–3633, doi:10.5194/bg-10-3615-2013, 2013.
- Leedham Elvidge, E.C., D.E. Oram, J.C. Laube, A.K. Baker, S.A. Montzka, S. Humphrey, D.A. O'Sullivan, and C.A.M. Brenninkmeijer, Increasing concentrations of dichloromethane, CH₂Cl₂, inferred from CARIBIC air samples collected 1998–2012, *Atmos. Chem. Phys.*, *15* (4), 1939–1958, doi:10.5194/acp-15-1939-2015, 2015.
- Lu, P., H. Zhang, and J. Wu, Inhomogeneous radiative forcing of NF₃, *Atmosphere*, *8* (1), doi:10.3390/atmos8010017, 2017.
- Luecken, D.L., R.L. Waterland, S. Pappasavva, K. Tadonio, W.T. Hutzell, J.P. Rugh, and S.O. Andersen, Ozone and TFA impacts in North America from degradation of 2,3,3,3-tetrafluoropropene (HFO-1234yf), a potential greenhouse gas replacement, *Environ. Sci. Technol.*, *44* (1), 343–348, doi:10.1021/es902481f, 2010.
- McCulloch, A., and P.M. Midgley, The history of methyl chloroform emissions: 1951–2000, *Atmos. Environ.*, *35* (31), 5311–5319, doi:10.1016/S1352-2310(01)00306-5, 2001.
- McCulloch, A., and A. Lindley, From mine to refrigeration: a life cycle inventory analysis of the production of HFC-134a, *International Journal of Refrigeration-Reveu Internationale du Froid*, *26* (8), 865–872, doi:10.1016/S0140-7007(03)00095-1 2003.
- Miller, B.R., M. Rigby, L.J.M. Kuijpers, P.B. Krummel, L.P. Steele, M. Leist, P.J. Fraser, A. McCulloch, C. Harth, P. Salameh, J. Muhle, R.F. Weiss, R.G. Prinn, R.H.J. Wang, S. O'Doherty, B.R. Grealley, and P.G. Simmonds, HFC-23 (CHF₃) emission trend response to HCFC-22 (CHClF₂) production and recent HFC-23 emission abatement measures, *Atmos. Chem. Phys.*, *10* (16), 7875–7890, doi:10.5194/acp-10-7875-2010, 2010.
- Mills, M.J., O.B. Toon, J. Lee-Taylor, and A. Robock, Multidecadal global cooling and unprecedented ozone loss following a regional nuclear conflict *Earth's Future*, *2* (4), 161–176, doi:10.1002/2013EF000205 2014.
- Mills, M.J., J. Richter, S. Tilmes, B. Kravitz, D.G. MacMartin, S.A. Glanville, J.J. Tribbia, J.F. Lamarque, F. Vitt, A. Schmidt, A. Gettelman, R.B. Neale, C. Hannay, J. Bacmeister, and D.E. Kinnison, Radiative and chemical response to interactive stratospheric aerosols in fully coupled CESM1(WACCM), *J. Geophys. Res. Atmos.*, *122*, 13,061–13,078, doi:10.1002/2017JD027006, 2017.
- Montzka, S.A., G.S. Dutton, P. Yu, E. Ray, R.W. Portmann, J.S. Daniel, L. Kuijpers, B.D. Hall, D. Mondeel, C. Siso, J.D. Nance, M. Rigby, A.J. Manning, L. Hu, F. Moore, B.R. Miller, and J.W. Elkins, An unexpected and persistent increase in global emissions of ozone-depleting CFC-11, *Nature*, *557* (7705), 413–417, doi:10.1038/s41586-018-

- 0106-2, 2018.
- Myhre, G., and D. Shindell (Coordinating Lead Authors), F.-M. Breon, W. Collins, J.S. Fuglestedt, J. Huang, D. Koch, J.-F. Lamarque, D. Lee, B. Mendoza, T. Nakajima, A. Robock, G. Stephens, T. Takemura, and H. Zhang, Anthropogenic and natural radiative forcing. In: *Climate Change 2013: The physical science basis, contribution of working group I to the fifth assessment report of the intergovernmental panel on climate change*, 659–740 pp., Cambridge, United Kingdom and New York, New York, USA, 2013.
- Nevison, C. V.K. Gupta, and L. Klinger, Self-sustained temperature oscillations on Daisyworld, *Tellus B*, 51 (4), 806–814, doi:10.1034/j.1600-0889.1999.t01-3-00005.x, 1999.
- Newman, P.A., J.S. Daniel, D.W. Waugh, and E.R. Nash, A new formulation of equivalent effective stratospheric chlorine (EESC), *Atmos. Chem. Phys.*, 7 (17), 4537–4552, doi:10.5194/acp-7-4537-2007, 2007.
- Niemeier, U., and C. Timmreck, What is the limit of climate engineering by stratospheric injection of SO₂, *Atmos. Chem. Phys.*, 15 (16), 9128–9141, doi:10.5194/acp-15-9129-2015, 2015.
- Niemeier, U., and H. Schmidt, Changing transport processes in the stratosphere by radiative heating of sulfate aerosols, *Atmos. Chem. Phys.*, 17, 14,871–14,886, doi:10.5194/acp-2017-470, 2017.
- Nowack, P.J., N.L. Abraham, P. Braesicke, and J.A. Pyle, Stratospheric ozone changes under solar geo-engineering: implications for UV exposure and air quality, *Atmos. Chem. Phys.*, 16, 4191–4203, doi:10.5194/acp-16-4191-2016, 2016.
- O'Neill, B.C., E. Kriegler, K.L. Ebi, E. Kemp-Benedict, K. Riahi, D.S. Rothman, B.J. van Ruijven, D.P. van Vuuren, J. Birkmann, K. Kok, M. Levy, and W. Solecki, The roads ahead: Narratives for shared socioeconomic pathways describing world futures in the 21st century, *Global Environ. Change*, 42, 169–180, doi:10.1016/j.gloenvcha.2015.01.004, 2017.
- Oman, L.D., A.R. Douglass, R.J. Salawitch, T.P. Canty, J.R. Ziemke, and M. Manyin, The effect of representing bromine from VSLS on the simulation and evolution of Antarctic ozone, *Geophys. Res. Lett.*, 43, 9869–9876, doi:10.1002/2016GL070471, 2016.
- Oram, D.E., M.J. Ashfold, J.C. Laube, L.J. Gooch, S. Humphrey, W.T. Sturges, E. Leedham-Elvidge, G.L. Forster, N.R.P. Harris, M.I. Mead, A. Abu Samah, S.M. Phang, C.F. Ou-Yang, N.H. Lin, J.L. Wang, A.K. Baker, C.A.M. Brenninkmeijer, and D. Sherry, A growing threat to the ozone layer from short-lived anthropogenic chlorocarbons, *Atmos. Chem. Phys.*, 17 (19), 11,929–11,941, doi:10.5194/acp-17-11929-2017, 2017.
- Orkin, V.L., L.E. Martynova, and M.J. Kurylo, Photochemical properties of trans-1-chloro-3,3,3-trifluoropropene (trans-CHCl=CHCF₃): OH reaction rate constant, UV and IR absorption spectra, global warming potential, and ozone depletion potential, *J. Phys. Chem. A*, 118 (28), 5263–5271, doi:10.1021/jp5018949, 2014.
- Ostermoller, J., H. Bonisch, P. Jockel, and A. Engel, A new time-independent formulation of fractional release, *Atmos. Chem. Phys.*, 17, 3785–3797, doi:10.5194/acp-17-3785-2017, 2017.
- Papanastasiou, D.K., A. Beltrone, P. Marshall, and J.B. Burkholder, Global warming potentials for the C₁-C₃ hydrochlorofluorocarbons (HCFCs) included in the Kigali Amendment to the Montreal Protocol, *Atmos. Chem. Phys.*, doi:10.5194/acp-2018-27, 2018.
- Patten, K.O., and D.J. Wuebbles, Atmospheric lifetimes and Ozone Depletion Potentials of trans-1-chloro-3,3,3-trifluoropropylene and trans-1,2-dichloroethylene in a three-dimensional model, *Atmos. Chem. Phys.*, 10 (22), 10867–10874, doi:10.5194/acp-10-10867-2010, 2010.
- Pelton, J., and B. Jacque, Distributed internet-optimized services via satellite constellations, in *Handbook of Satellite Applications*, Springer, New York, New York, doi:10.1007/978-1-614-6423-5_96-1, 2016.
- Pitari, G., V. Aquila, B. Kravitz, A. Robock, S. Watanabe, N.D. Luca, G.D. Genova, E. Mancini, S. Tilmes, and I. Cionni, Stratospheric ozone response to sulfate geoengineering: Results from the Geoengineering Model Intercomparison Project (GeoMIP), *J. Geophys. Res.*, 119 (5), 2629–2653, doi:10.1002/2013JD020566, 2014.
- Pongratz, J., D.B. Lobell, L. Cao, and K. Caldeira, Crop yields in a geoengineered climate, *Nat. Clim. Change*, 2, 101–105, doi:10.1038/nclimate1373, 2012. Haigh, J.D., and J.A. Pyle, Ozone perturbation experiments in a two-dimensional

- circulation model, *Q. J. Roy. Meteorol. Soc.*, 108, 551–574, doi:10.1002/qj.49710845705, 1982.
- Jackman, C.H., D.R. Marsh, D.E. Kinnison, C.J. Mertens, and E.L. Fleming, Atmospheric changes caused by galactic cosmic rays over the period 1960–2010, *Atmos. Chem. Phys.*, 16, 5853–5866, doi:10.5194/acp-16-5853-2016, 2016.
- Portmann, R.W., and S. Solomon, Indirect radiative forcing of the ozone layer during the 21st century, *Geophys. Res. Lett.*, 34, L02813, doi:10.1029/2006GL028252, 2007.
- Radulovich, R., A. Neori, D. Valderrama, C.R.K. Reddy, H. Cronin, and J. Forster, Farming of seaweeds, Chapter 3 in *Seaweed Sustainability: Food and Non-Food Applications*, edited by B.K. Tiwari and D.J. Troy, pp. 27–59, Elsevier, Amsterdam, 2015.
- Randeniya, L., P.F. Vohrolik, and I.C. Plumb, Stratospheric ozone depletion at northern mid latitudes in the 21st century: The importance of future concentrations of greenhouse gases nitrous oxide and methane, *Geophys. Res. Lett.*, 29 (4), doi:10.1029/2001GL014295, 2002.
- Ravishankara, A.R., A.A. Turnipseed, N.R. Jensen, S. Barone, M. Mills, C.J. Howard, and S. Solomon, Do hydrofluorocarbons destroy stratospheric ozone, *Science*, 263 (5143), 71–75, doi:10.1126/science.263.5143.71, 1994.
- Revell, L.E., G.E. Bodeker, P.E. Huck, B.E. Williamson, and E. Rozanov, The sensitivity of stratospheric ozone changes through the 21st century to N₂O and CH₄, *Atmos. Chem. Phys.*, 12, 11,309–11,317, doi:10.5194/acp-12-11309-2012, 2007.
- Revell, L.E., F. Tummon, R.J. Salawitch, A. Stenke, and T. Peter, The changing ozone depletion potential of N₂O in a future climate, *Geophys. Res. Lett.*, 42 (22), 10,047–10,055, doi:10.1002/2015GL065702, 2015.
- Riahi, K., D.P. van Vuuren, E. Kriegler, J. Edmonds, B.C. O'Neill, S. Fugimori, N. Bauer, K. Calvin, R. Delink, O. Fricko, W. Lutz, A. Popp, J.C. Cuaresma, S. KC, Leimbach, M., L. Jiang, T. Kram, S. Rao, J. Emmerling, K. Ebi, T. Hasegawa, P. Havlik, F. Humpenoder, L.A. Da Silva, S. Smith, E. Stehfest, V. Bosetti, J. Eom, D. Gernaat, T. Masui, J. Rogelj, J. Strefler, L. Drouet, V. Krey, G. Luderer, M. Harmsen, K. Takahashi, L. Baumstark, J.C. Doelman, M. Kainuma, Z. Klimont, G. Marangoni, H. Lotze-Campen, M. Obersteiner, A. Tabeau, and M. Tavoni, The shared socioeconomic pathways and their energy, land use, and greenhouse gas emissions implications: An overview, *Global Environ. Change*, 42, 153–168, doi:10.1016/j.gloenvcha.2016.05.009, 2017.
- Richter, J.H., S. Tilmes, M.J. Mills, J.J. Tribbia, B. Kravitz, D.G. MacMartin, F. Vitt, and J.F. Lamarque, Stratospheric Dynamical Response and Ozone Feedbacks in the Presence of SO₂ Injections, *J. Geophys. Res. Atmos.*, 122 (23), 12,557–12,573, doi:10.1002/2017jd026912, 2017.
- Richter, J.H., S. Tilmes, A.S. Glanville, M.J. Mills, J.J. Tribbia, B. Kravitz, F. Vitt, and J.-F. Lamarque, Stratospheric response in geoengineering simulation meeting multiple surface climate objectives, *J. Geophys. Res. Atmos.*, 123, 5762–5782, doi:10.1029/2018JD028285, 2018.
- Rigby, M., R.G. Prinn, S. O'Doherty, B.R. Miller, D. Ivy, J. Muhle, C.M. Harth, P.K. Salameh, T. Arnold, R.F. Weiss, P.B. Krummel, L.P. Steele, P.J. Fraser, D. Young, and P.G. Simmonds, Recent and future trends in synthetic greenhouse gas radiative forcing, *Geophys. Res. Lett.*, 41 (7), 2623–2630, doi:10.1002/2013gl059099, 2014.
- Robock, A., Albedo enhancement by stratospheric sulfur injections: More research needed, *Earth's Future*, 4 (12), 644–648, doi:10.1002/2016ef000407, 2016.
- Rogelj, J., M. den Elzen, N. Hohne, T. Fransen, H. Fekete, H. Winkler, R. Schaeffer, F. Sha, K. Riahi, and M. Meinshausen, Paris Agreement climate proposals need a boost to keep warming well below 2 degrees C, *Nature*, 534 (7609), 631–639, doi:10.1038/nature18307, 2016.
- Ross, M.N., and P.M. Sheaffer, Radiative forcing caused by rocket engine emissions, *Earth's Future*, 2 (4), 177–196, doi:10.1002/2013EF000160, 2014.
- Ross, M., M.J. Mills, and D. Toohey, Potential climate impact of black carbon emitted by rockets, *Geophys. Res. Lett.*, 37, doi:10.1029/2010GL044548, 2010.
- Russell, M.H., G. Hoogeweg, E.M. Webster, D.A. Ellis, R.L. Waterland, and R.A. Hoke, TFA from HFO-1234yf: Accumulation and aquatic risk in terminal water bodies, *Environ. Toxicol. Chem.*, 31 (9), 1957–1965, doi:10.1002/etc.1925, 2012.
- Saiz-Lopez, A., S. Baidar, C.A. Cuevas, T.K. Koenig, R.P. Fernandez, B. Dix, D.E. Kinnison, J.-F. Lamarque, X. Rodriguez-Lloveras, T.L. Campos,

- and R. Volkamer, Injection of iodine to the stratosphere, *Geophys. Res. Lett.*, 42 (16), 6852–6859, doi:10.1002/2015GL064796, 2015.
- Scheurer, M., K. Nödlér, F. Freeling, J. Janda, O. Hapfel, M. Riegel, U. Müller, F.R. Störck, M. Fleig, F.T. Lange, A. Brunsch, and H.-J. Brauch, Small, mobile, persistent: Trifluoroacetate in the water cycle - overlooked sources, pathways, and consequences for drinking water supply, *Water Res.*, 126, 460–471, doi:10.1016/j.watres.2017.09.045, 2017.
- Seifritz, W., Mirrors to halt global warming?, *Nature*, 340, 603, doi:10.1038/340603a0, 1989.
- Shah, N., M. Wei, V.E. Letschert, and A.A. Phadke, Benefits of leapfrogging to superefficiency and low global warming potential refrigerants in room air conditioning, *Report LBNL-1003671*, Lawrence Berkeley National Laboratory, Berkeley, California, 2015.
- Sherwen, T., M.J. Evans, L.J. Carpenter, J.A. Schmidt, and L. Mickley, Halogen chemistry reduces tropospheric O₃ radiative forcing, *Atmos. Chem. Phys.*, 17 (2), 1557–1569, doi:10.5194/acp-17-1557-2017, 2017.
- Simmonds, P.G., A.J. Manning, D.M. Cunnold, A. McCulloch, S. O'Doherty, R.G. Derwent, P.B. Krummel, P.J. Fraser, B. Dunse, L.W. Porter, R.H.J. Wang, B.R. Grealley, B.R. Miller, P. Salameh, R.F. Weiss, and R.G. Prinn, Global trends, seasonal cycles, and European emissions of dichloromethane, trichloroethene, and tetrachloroethene from the AGAGE observations at Mace Head, Ireland, and Cape Grim, Tasmania, *J. Geophys. Res.*, 111, doi:10.1029/2006JD007082, 2006.
- Smalley, K.M., A.E. Dessler, S. Bekki, M. Deushi, M. Marchand, O. Morgenstern, D.A. Plummer, K. Shibata, Y. Yamashita, and G. Zeng, Contribution of different processes to changes in tropical lower-stratospheric water vapor in chemistry-climate models, *Atmos. Chem. Phys.*, 17 (13), 8031–8044, doi:10.5194/acp-17-8031-2017, 2017.
- Solomon, K.R., G.J.M. Velders, S.R. Wilson, S. Madronich, J. Longstreth, P.J. Aucamp, and J.F. Bornman, Sources, fates, toxicity, and risks of trifluoroacetic acid and its salts: Relevance to substances regulated under the Montreal and Kyoto Protocols, *J. Toxicol. Environ. Health Part B*, 19 (7), 289–304, doi:10.1080/10937404.2016.1175981, 2016.
- SPARC CCMVal (Stratospheric Processes and their Role in Climate), *SPARC CCMVal Report on the Evaluation of Chemistry-Climate Models*, edited by V. Eyring, T.G. Shepherd, D.W. Waugh, *SPARC Report No. 5*, WCRP-132, WMO/TD-No. 1526, 2010.
- SPARC, (Stratosphere-troposphere Processes And their Role in Climate), *SPARC Report on Lifetimes of stratospheric ozone-depleting substances, their replacements, and related species*, edited by M.K.W. Ko, P.A. Newman, S. Reimann, and S.E. Strahan, *SPARC Report No. 6*, WCRP-15/2013, <https://www.sparc-climate.org/publications/sparc-reports/>, 2013.
- SPARC, (Stratosphere-troposphere Processes And their Role in Climate), *SPARC Report on the Mystery of Carbon Tetrachloride*, edited by Q. Liang, P.A. Newman, and S. Reimann, *SPARC Report No. 7*, WCRP-13/2016, <https://www.sparc-climate.org/publications/sparc-reports/>, 2016.
- Sterner, E.O., and D.J.A. Johansson, The effect of climate-carbon cycle feedbacks on emission metrics, *Environ. Res. Lett.*, 12 (3), doi:10.1088/1748-9326/aa61dc, 2017.
- Strahan, S.E., A.R. Douglass, R.S. Stolarski, H. Akiyoshi, S. Bekki, P. Braesicke, N. Butchart, M.P. Chipperfield, D. Cugnet, S. Dhomse, S.M. Frith, A. Gettelman, S.C. Hardiman, D.E. Kinnison, J.-F. Lamarque, E. Mancini, M. Marchand, M. Michou, O. Morgenstern, T. Nakamura, D. Olivie, S. Pawson, G. Pitari, D.A. Plummer, J.A. Pyle, J.F. Scinocca, T.G. Shepherd, K. Shibata, D. Smale, H. Teyssède, W. Tian, and Y. Yamashita, Using transport diagnostics to understand chemistry climate model ozone simulations, *J. Geophys. Res.*, 116 (D17), doi:10.1029/2010jd015360, 2011.
- Sulback Andersen, M.P., J.A. Schmidt, A. Volkova, and D.J. Wuebbles, A three-dimensional model of the atmospheric chemistry of *E* and *Z*-CF₃CH=CHCl (HCFO-1233(zd) (E/Z)), *Atmos. Environ.*, 179, 250–259, doi:10.1016/j.atmosenv.2018.02.018, 2018.
- Tegtmeier, S., F. Ziska, I. Pisso, B. Quack, and G.J.M. Velders, Oceanic bromoform emissions weighted by their ozone depletion potential, *Atmos. Chem. Phys.*, 15, 13,647–13,663, doi:10.5194/acp-15-13647-2015, 2015.
- Tilmes, S., R.R. Garcia, D.E. Kinnison, A. Gettelman, and P.J. Rasch, Impact of geoengineered aerosols on the troposphere and stratosphere, *J. Geophys.*

- Res., 114 (D12), doi:10.1029/2008JD011420, 2009.
- Tilmes, S., D.E. Kinnison, R.R. Garcia, R. Salawitch, T. Canty, J. Lee-Taylor, S. Madronich, and K. Chance, Impact of very short-lived halogens on stratospheric ozone abundance and UV radiation in a geo-engineered atmosphere, *Atmos. Chem. Phys.*, 12 (22), 10,945–10, 955, doi:10.5194/acp-12-10945-2012, 2012.
- Tilmes, S., J. Fasullo, J.-F. Lamarque, D.R. Marsh, M. Mills, K. Alterskjær, H. Muri, J.E. Kristjánsson, O. Boucher, M. Schulz, J.N.S. Cole, C.L. Curry, A. Jones, J. Haywood, P.J. Irvine, D. Ji, J.C. Moore, D.B. Karam, B. Kravitz, P.J. Rasch, B. Singh, J.-H. Yoon, U. Niemeier, H. Schmidt, A. Robock, S. Yang, and S. Watanabe, The hydrological impact of geoengineering in the Geoengineering Model Intercomparison Project (GeoMIP), *J. Geophys. Res.*, 118 (19), 11,036–011,058, doi:10.1002/jgrd.50868, 2013.
- Tilmes, S., B.M. Sanderson, and B.C. O'Neill, Climate impacts of geoengineering in a delayed mitigation scenario, *Geophys. Res. Lett.*, 43, 8222–8229, doi:10.1002/2016GL070122, 2016.
- Tilmes, S., J.H. Richter, M.J. Mills, B. Kravitz, D.G. MacMartin, F. Vitt, J.J. Tribbia, and J.F. Lamarque, Sensitivity of aerosol distribution and climate response to stratospheric SO₂ injection locations, *J. Geophys. Res.*, 122, 12,591–12,615, doi:10.1002/2017JD026888, 2017.
- Tilmes, S., J.H. Richter, M.J. Mills, B. Kravitz, D.G. MacMartin, R.R. Garcia, D.E. Kinnison, J.F. Lamarque, J. Tribbia, and F. Vitt, Effects of Different Stratospheric SO₂ Injection Altitudes on Stratospheric Chemistry and Dynamics, *J. Geophys. Res. Atmos.*, 123 (9), 4654–4673, doi:10.1002/2017jd028146, 2018.
- Totterdill, A., T. Kovacs, W. Feng, S. Dhomse, C.J. Smith, J.C. Gomez-Martin, M.P. Chipperfield, P.M. Forster, and J.M.C. Plane, Atmospheric lifetimes, infrared absorption spectra radiative forcings and global warming potentials of NF₃ and CF₃CF₂Cl (CFC-115), *Atmos. Chem. Phys.*, 16, 11,451–1,1463, doi:10.5194/acp-16-11451-2016, 2016.
- Trenberth, K.E., and L. Smith, The mass of the atmosphere: A constraint on global analyses, *J. Climate*, doi:10.1175/JCLI-3299.1, 2005.
- UNEP (United Nations Environment Programme), *Assessment of Alternatives to HCFCs and HFCs and Update of the TEAP 2005 Supplement Report Data*, Report of the UNEP Technology and Economic Assessment Panel, Task Force Decision XX/8 Report, 129 pp, Nairobi, Kenya, https://unep.ch/ozone/Assessment_Panels/TEAP/Reports/TEAP_Reports/teap-may-2009-decisionXX-8-task-force-report.pdf, 2009.
- UNEP (United Nations Environment Programme), *HFCs: A Critical Link in Protecting Climate and the Ozone Layer*, 40 pp., Nairobi, Kenya, 2011.
- UNEP (United Nations Environment Programme), *Drawing down N₂O to protect climate and the ozone layer*, A UNEP Synthesis Report, Nairobi, Kenya, 2013.
- UNEP (United Nations Environment Programme), Data Access Centre, Ozone Secretariat, Nairobi, Kenya, 2017.
- UNEP/TEAP (United Nations Environment Programme, Technology and Economic Assessment Panel) *September Decision XXVII/4 Task Force Update Report Further information on Alternatives to Ozone-Depleting Substances, Volume 1*, 179 pp., Nairobi, Kenya, 2016.
- Velders, G.J.M., and J.S. Daniel, Uncertainty analysis of projections of ozone-depleting substances: Mixing ratios, EESC, ODPs, and GWPs, *Atmos. Chem. Phys.*, 14 (6), 2757–2776, doi:10.5194/acp-14-2757-2014, 2014.
- Velders, G.J.M., S.O. Andersen, J.S. Daniel, D.W. Fahey, and M. McFarland, The importance of the Montreal Protocol in protecting climate, *Proc. Natl. Acad. Sci.*, 104 (12), 4814–4819, doi:10.1073/pnas.0610328104, 2007.
- Velders, G.J.M., D.W. Fahey, J.S. Daniel, M. McFarland, and S.O. Andersen, The large contribution of projected HFC emissions to future climate forcing, *Proc. Natl. Acad. Sci.*, 106 (27), 10,949–10,954, doi:10.1073/pnas.0902817106, 2009.
- Velders, G.J.M., A.R. Ravishankara, M.K. Miller, M.J. Molina, J. Alcamo, J.S. Daniel, D.W. Fahey, S.A. Montzka, and S. Reimann, Preserving Montreal Protocol climate benefits by limiting HFCs, *Science*, 335 (6071), 922–923, doi:10.1126/science.1216414, 2012.
- Velders, G.J.M., S. Solomon, and J.S. Daniel, Growth of climate change commitments from HFC banks and emissions, *Atmos. Chem. Phys.*, 14 (9), 4563–4572, doi:10.5194/acp-14-4563-2014, 2014.

- Velders, G.J.M., D.W. Fahey, J.S. Daniel, S.O. Anderson, and M. McFarland, Future atmospheric abundances and climate forcings from scenarios of global and regional hydrofluorocarbon (HFC) emissions, *Atmos. Environ.*, 123 (A), 200–209, doi:10.1016/j.atmosenv.2015.10.071, 2015.
- Visioni, D., G. Pitari, and V. Aquila, Sulfate geoengineering: a review of the factors controlling the needed injection of sulfur dioxide, *Atmos. Chem. Phys.*, 17 (6), 3878–3889, doi:10.5194/acp-17-3879-2017, 2017.
- Visioni, D., G. Pitari, V. Aquila, S. Tilmes, I. Cionni, G. Di Genova, and E. Mancini, Sulfate geoengineering impact on methane transport and lifetime: Results from the Geoengineering Model Intercomparison Project (GeoMIP), *Atmos. Chem. Phys.*, 17, 11,209–11,226, doi:10.5194/acp-17-11209-2017, 2017.
- Voigt, C., U. Schumann, K. Graf, and K.-D. Gottschaldt, Impact of rocket exhaust plumes on atmospheric composition and climate, *Prog. Propulsion Phys.*, 4, 657–670, doi:10.1051/eucass/201304657, 2013.
- Wallington, T.J., W.F. Schneider, D.R. Worsnop, O.J. Nielsen, J. Sehested, W. DeBruyn, and J.A. Shorter, Atmospheric chemistry and environmental impact of CFC replacements: HFCs and HCFCs, *Environ. Sci. Technol.*, 28 (7), 320A–326A, doi:10.1021/es00056a002, 1994.
- Wallington, T.J., M.D. Hurley, J.M. Fracheboud, J.J. Orlando, G.S. Tyndall, J. Sehested, T.E. Møgelberg, and O.J. Nielsen, Role of excited CF_3CFHO radicals in the atmospheric chemistry of HFC-134a, *J. Phys. Chem.*, 100 (46), 8116–1812, doi:10.1021/jp9624764, 1996.
- Wallington, T.J., M.P. Sulbaek Andersen, and O.J. Nielsen, Estimated Photochemical Ozone Creation Potentials (POCPs) of $\text{CF}_3\text{CF}=\text{CH}_2$ (HFO-1234yf) and Related Hydrofluoroolefins (HFOs), *Atmos. Environ.*, 44 (11), 1478, doi:10.1016/j.atmosenv.2010.01.040, 2010.
- Wallington, T.J., M.P. Sulbaek Andersen, and O.J. Nielsen, Atmospheric chemistry of short-chain haloolefins: Photochemical ozone creation potentials (POCPs), global warming potentials (GWPs), and ozone depletion potentials (ODPs), *Chemosphere*, 129, 135–141, doi:10.1016/j.chemosphere.2014.06.092, 2015.
- Wallington, T.J., M.P. Sulbaek Andersen, and O.J. Nielsen, Advances in Atmospheric Chemistry, World Scientific Publishing Company, 2017.
- Wang, Z.Y., Y.H. Wang, J.F. Li, S. Henne, B.Y. Zhang, J.X. Hu, and J.B. Zhang, Impacts of the Degradation of 2,3,3,3-Tetrafluoropropene into Trifluoroacetic Acid from Its Application in Automobile Air Conditioners in China, the United States, and Europe, *Environ. Sci. Technol.*, 52 (5), 2819–2826, doi:10.1021/acs.est.7b05960, 2018.
- Warneck, P., and J. Williams, The atmospheric chemist's companion: Numerical data for use in the atmospheric sciences, Springer, New York, NY, 2012.
- Wigley, T.M.L., A combined mitigation/geoengineering approach to climate stabilization, *Science*, 314 (5798), 452–454, doi:10.1126/science.1131728, 2006.
- WMO (World Meteorological Organization), *Scientific Assessment of Ozone Depletion: 2006*, Global Ozone Research and Monitoring Project–Report No. 50, 572 pp, Geneva, Switzerland, 2007.
- WMO (World Meteorological Organization), *Scientific Assessment of Ozone Depletion: 2010*, Global Ozone Research and Monitoring Project–Report No. 52, 516 pp., Geneva, Switzerland, 2011.
- WMO (World Meteorological Organization), *Scientific Assessment of Ozone Depletion: 2014*, Global Ozone Research and Monitoring Project–Report No. 55, 416 pp., Geneva, Switzerland, 2014.
- Wu, J., J.W. Martin, Z. Zhai, K. Lu, X. Fang, and H. Jin, Airborne trifluoroacetic acid and its fraction from the degradation of HFC-134a in Beijing, China, *Environ. Sci. Technol.*, 48 (7), 3675–3681, doi:10.1021/es4050264, 2014a.
- Wu, J., J.W. Martin, Z. Zhai, K. Lu, X. Fang, and H. Jin, Response to comment on “Airborne trifluoroacetic acid and its fraction from the degradation of HFC-134a in Beijing, China,” *Environ. Sci. Technol.*, 48 (7), 9949, doi:10.1021/es5032568, 2014b.
- Wuebbles, D.J., D. Wang, K.O. Patten, and S.C. Olsen, Analyses of short-lived replacements for HFCs with large GWPs, *Geophys. Res. Lett.*, 40 (17), 4767–4771, doi:10.1002/grl.50908, 2013.
- Xia, L., A. Robock, S. Tilmes, and R.R. Neely III, Stratospheric sulfate geoengineering could enhance the terrestrial photosynthesis rate, *Atmos. Chem. Phys.*, 16, 1479–1489, doi:10.5194/acp-16-1479-2016, 2016.
- Xia, L., P.J. Nowack, S. Tilmes, and A. Robock, Impacts of stratospheric sulfate geoengineering

- on tropospheric ozone, *Atmos. Chem. Phys.*, 17, 11,913-11,928, doi:10.5194/acp-17-11913-2017, 2017.
- Xu, Y., D. Zaelke, G.J.M. Velders, and V. Ramanathan, The role of HFCs in mitigating 21st century climate change, *Atmos. Chem. Phys.*, 13, 6083–6089, doi:10.5194/acp-13-6083-2013, 2013.
- Yang, X., N.L. Abraham, A.T. Archibald, P. Braesicke, J. Keeble, P.J. Telford, N.J. Warwick, and J.A. Pyle, How sensitive is the recovery of stratospheric ozone to changes in concentrations of very short-lived bromocarbons?, *Atmos. Chem. Phys.*, 14 (19), 10,431–10,438, doi:10.5194/acp-14-10431-2014, 2014.
- Ziemke, J.R., and O.R. Cooper, Tropospheric ozone, in State of the Climate in 2016, *Bull. Am. Meteorol. Soc.*, 98, S52–S54, doi:10.1175/2017BAMS-StateofClimate.1, 2017.
- Ziemke, J.R., and O.R. Cooper, Tropospheric ozone, in State of the Climate in 2017, *Bull. Am. Meteorol. Soc.*, 99 (8), doi:10.1175/2018BAMSStateofClimate.1, 2018.

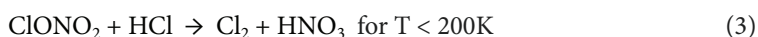
Appendix 6A

Current State of Knowledge on Stratospheric Sulfate Geoengineering

Since geoengineering may be considered in the future, chemical and dynamical changes and their impacts on future column ozone have to be understood. Models incorporate stratospheric chemistry and dynamics with varying degrees of sophistication, and very few single-model studies have investigated changes in ozone due to geoengineering with consideration of interactions between dynamics, chemistry, aerosols, and climate. In this appendix, the current state of knowledge on stratospheric sulfate geoengineering is summarized in more detail than covered in the main chapter.

6A.1 Impact of Stratospheric Sulfate Geoengineering on Net Chemical Ozone Production

An increasing sulfate aerosol burden from possible continuous injection of SO₂ into the tropical stratosphere would result in an enhanced aerosol surface area density in the mid- and lower stratosphere (i.e., up to about 10 hPa in the tropics). This would increase the surface area available for heterogeneous reactions, similar to that observed after large volcanic eruptions (Heckendorn et al., 2009; Pitari et al., 2014; Tilmes et al., 2009; Tilmes et al., 2012; Vioni et al., 2017a). The magnitude and spatial pattern of the increased aerosol surface area density and the associated mass and size distributions, which are strongly model dependent, vary with the amount and location of injections (e.g., Dai et al., 2018; English et al., 2012; Laakso et al., 2017; Niemeier and Timmreck, 2015; Pitari et al., 2014; Tilmes et al., 2017) and on the injection substance. The impact of increased aerosol surface area is particularly significant for three heterogeneous reactions:



Reaction (1), the reduction of nitrogen oxides (NO_y) via hydrolysis of N₂O₅ (e.g., Fahey et al., 1993) would increase ozone abundance, which is in part counteracted by the increase in ozone loss cycles involving reactive chlorine (ClO_x), bromine (BrO_x), and hydrogen (HO_x) families. This reaction is dominant in the tropical mid-stratosphere (**Figure 6A-1**, top left).

Increasing/decreasing the surface area density and NO_y would result in an increase/decrease of the importance of reaction (1), although this effect would saturate at very high aerosol loadings (e.g., Berthet et al., 2017). Reaction (2), the hydrolysis of ClONO₂, results in production of HOCl, increased HO_x and ClO concentrations, and increased ozone loss via the catalytic ClO_x and HO_x cycles. Heterogeneous reactions of ClONO₂ with hydrogen chloride HCl result in additional reactive chlorine. Reactions (2) and (3) are most important in cold regions, especially in the lower stratosphere in polar regions in winter and spring (**Figure 6A-1**, top left). Additional reactions, including the hydrolysis of BrONO₂, play an important role for warmer conditions (Tilmes et al., 2012), as recent observations after small volcanic eruptions have demonstrated (Berthet et al., 2017). The importance of these reactions will decline with the projected decreasing stratospheric halogen burden. A potential increase in the cold point temperature, as the result of aerosol geoengineering and a resulting increase in stratospheric water vapor content (see **Section 6.2.5**), leads to an additional increase in the HO_x ozone loss cycle throughout the stratosphere. Resulting changes in net chemical ozone production are most important in the lower and upper tropical stratosphere, especially in the summer Northern Hemisphere (Tilmes et al., 2018). An increase in the odd oxygen cycle involving reactive oxygen (O_x), resulting from a temperature increase in

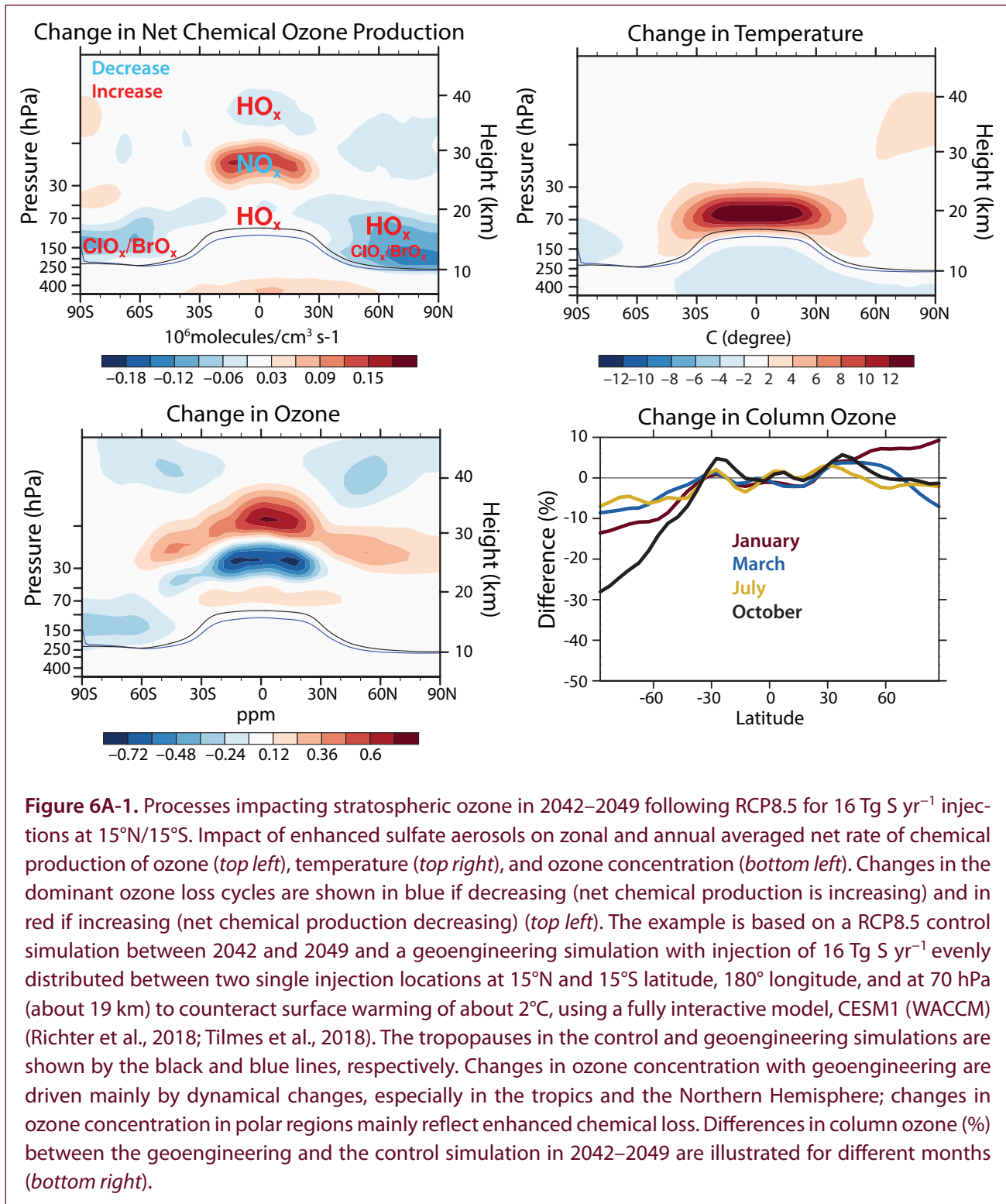


Figure 6A-1. Processes impacting stratospheric ozone in 2042–2049 following RCP8.5 for 16 Tg S yr⁻¹ injections at 15°N/15°S. Impact of enhanced sulfate aerosols on zonal and annual averaged net rate of chemical production of ozone (*top left*), temperature (*top right*), and ozone concentration (*bottom left*). Changes in the dominant ozone loss cycles are shown in blue if decreasing (net chemical production is increasing) and in red if increasing (net chemical production decreasing) (*top left*). The example is based on a RCP8.5 control simulation between 2042 and 2049 and a geoengineering simulation with injection of 16 Tg S yr⁻¹ evenly distributed between two single injection locations at 15°N and 15°S latitude, 180° longitude, and at 70 hPa (about 19 km) to counteract surface warming of about 2°C, using a fully interactive model, CESM1 (WACCM) (Richter et al., 2018; Tilmes et al., 2018). The tropopauses in the control and geoengineering simulations are shown by the black and blue lines, respectively. Changes in ozone concentration with geoengineering are driven mainly by dynamical changes, especially in the tropics and the Northern Hemisphere; changes in ozone concentration in polar regions mainly reflect enhanced chemical loss. Differences in column ozone (%) between the geoengineering and the control simulation in 2042–2049 are illustrated for different months (*bottom right*).

the tropical stratosphere, would also contribute to the change in net chemical ozone. Finally, the decrease in photolysis rates due to scatter by aerosols has been estimated to decrease ozone in the tropical lower stratosphere (Pitari et al., 2014).

6A.2 Impact of Stratospheric Sulfate Geoengineering on Dynamics

According to modeling studies, geoengineering via stratospheric aerosol injection would affect dynamics through two main processes: (1) cooling of the troposphere as the result of reduced incoming shortwave radiation and (2) substantial warming of the tropical stratosphere as the result of diabatic heating caused by the increased sulfate aerosol layer (**Figure 6A-1**, top right) (e.g., Pitari et al., 2014; Tilmes et al., 2018; Richter et al., 2018). These processes result in a drop in tropopause altitude, a weakening of the subtropical jets, and an increase in the tropical cold point temperature, which may increase stratospheric water vapor by up to 90% for very large injections of 40 Tg SO₂ yr⁻¹ (Richter et al., 2018; Tilmes et al., 2018). The vertical component of the residual circulation in the tropics is reduced below the injection location as the result of a decrease in the temperature gradient between the tropics and mid-latitudes above the subtropical jets. On the other hand, the increased tropical upwelling above the injection locations and increased downwelling in high latitudes is consistent with a strengthening of the gravity wave drag and Eliassen–Palm flux (EPF) divergence in mid- and high latitudes and is aligned with a strengthening of the polar night jet (Tilmes et al., 2018; Richter et al., 2018). The strengthening of the polar night jet in high latitudes results in additional ozone depletion (Tilmes et al., 2009), while increases in horizontal advection, especially in winter mid-latitudes in the Northern Hemisphere stratosphere, can result in an increase of ozone above values of non-geoengineered conditions, for example, as shown for large injections of 16 Tg S yr⁻¹ at about 1 km above the tropical tropopause (**Figure A6-1**, bottom left). Changes in advection of ozone, other gases, and sulfate aerosols interact with chemical changes as well as stratosphere-to-troposphere exchange. Resulting changes in tropospheric chemistry, temperature, and UV are estimated to increase methane lifetime by 16% for continuous 4 Tg S yr⁻¹ injections (Visoni et al., 2017b).

Simulations with injections of sulfur at the equator identified a significant prolonging of the westerly phase of the Quasi-Biennial Oscillation (QBO) with increasing injection amounts (Aquila et al., 2014). This would lead to a stronger confinement of particles in the tropics (Niemeier and Schmidt, 2017). However, Richter et al. (2017) have shown that geoengineering in a model with interactive stratospheric chemistry and coupled ocean has a reduced impact on the QBO due to reductions in heating as the result of reductions in ozone around 30 hPa. Furthermore, different injection scenarios at 15°N and 15°S or in addition at 30°N and 30°S with injections up to 25 Tg S yr⁻¹ by the end of the 21st century (Richter et al., 2018) would instead lead to a QBO that is closer to present-day conditions. Large differences and shortcomings in the representation of the QBO in different models exist, and differences in the response to geoengineering have to be investigated in more detail.

6A.3 Impact of Sulfate Aerosol Geoengineering on Column Ozone

In addition to potential changes in column ozone as the result of increasing greenhouse gases (GHGs) (Butler et al., 2016), chemical and dynamical changes due to geoengineering, as discussed above, would affect future column ozone and in part counteract the projected increase of column ozone (“super-recovery”) over most latitudes (**Chapter 3**). In one modeling study, a fixed injection of 4 Tg S yr⁻¹ between 2020 and 2070, which results in 0.5°C of surface cooling, leads to approximately a 4% reduction in the global stratospheric column ozone for 2020 and only a 1% reduction by 2070 (Xia et al., 2017). These results are similar to calculations based on four models using fixed injections of 2.5 Tg S yr⁻¹, which show an average decrease in global column ozone of 2.8% over the same period (Visoni et al., 2017a). The impact of aerosols geoengineering on ozone is therefore small if applied later in the century, when global column ozone absent geoengineering is projected to increase by about ~4% (from 2020 to 2070) due to changes in ODS and GHG concentrations (Cionni et al., 2017).

Simulations using a fully interactive earth system model that includes an interactive aerosol microphysical

scheme coupled to interactive chemistry and radiation, and with an internally generated QBO (Mills et al., 2017), point to the importance of chemistry and dynamical changes on column ozone. Very large injections of 16 Tg S yr^{-1} , to cool the surface by about 2°C in 2042–2049, reduce column ozone values towards present-day conditions in winter and spring high altitudes for both hemispheres (**Figure 6A-1**, bottom right). Maximum reductions of 8% in March over the Arctic, and 28% in October over Antarctica are reached in comparison to the RCP8.5 control simulation (**Figure 6A-1**, bottom right). On the other hand, an increase of column ozone above non-geoengineered levels up to 8% is simulated for the Northern Hemisphere mid-latitudes in winter. A different experiment that reached the same surface cooling but applied injections at higher altitudes ($\sim 5 \text{ km}$ about the tropopause) indicated that advection is less important and resulted in a larger decrease in column ozone at high latitudes, with up to 18% loss over the Arctic and up to 40% over Antarctica in spring. The impact on column ozone is therefore dependent on the injection strategy (Richter et al., 2018; Tilmes et al., 2018).

A transient simulation based on RCP8.5 GHG forcings with continuously increasing SO_2 injections at 15°N , 15°S , 30°N , and 30°S at $\sim 5 \text{ km}$ about the tropopause required injections up to 25 Tg S yr^{-1} by the end of the century to maintain temperatures at 2020 levels (Kravitz et al., 2017). In this simulation, ozone recovery in the Southern Hemisphere polar vortex was delayed until the end of the 21st century. Besides, column ozone reached values close to pre-ozone hole conditions for the Southern Hemisphere and tropics and well above pre-ozone hole conditions for northern mid-latitudes in winter and spring (Richter et al., 2018). By the end of the 21st century, geoengineering resulted in higher column ozone values compared to non-geoengineering conditions for tropics and winter northern mid-latitudes.

Comparison of Past and Future Ozone Projections of the GSFC 2-D Model with GEOSCCM 3-D Simulations

In this appendix, predictions of past and future ozone with the GSFC 2-D model (GSFC 2D), used in this chapter, are shown to be in very good agreement with the GEOSCCM 3-D simulations used in **Chapters 3, 4, and 5**. The GEOSCCM has a comprehensive tropospheric and stratospheric chemical mechanism (e.g., Oman et al., 2016) and performed well in both chemical- and transport-related process evaluations (SPARC CCMVal, 2010; Strahan et al., 2011; Douglass et al., 2012). The GSFC 2-D model has complete stratospheric chemistry but contains a limited subset of tropospheric species (Fleming et al., 2011; Jackman et al., 2016). The GSFC 2-D model compares well with observations and the GEOSCCM in simulating various transport-sensitive features in the meridional plane (e.g., long-lived tracers), as well as long-term changes in temperature and age of air over the 1950–2100 period (Fleming et al., 2011; SPARC, 2013). In this appendix, we also show comparisons of the baseline simulation with the CCMI multi-model mean (MMM, $\pm 1\sigma$) for the total and stratospheric column, and with selected observations where available.

Figure 6B-1 shows comparisons of the GSFC 2-D model and GEOSCCM global/annually averaged ozone from the CCMI baseline REF-C2 simulations for 1960–2100. These simulations include past stratospheric aerosol variations and solar ultraviolet flux variability associated with the 11-year solar cycle, with a repeating 11-year cycle projected out to 2100. The 2-D model stratospheric column ozone agrees quite well with the GEOSCCM, both in absolute amount and the pre-2000 decline and future ozone recovery out to 2100 (**Figure 6B-1b**). While tropospheric column ozone is similar in the two models during the 1960s, GSFC 2-D underestimates the time-dependent increases in tropospheric ozone in the GEOSCCM from ~1970 through the mid-21st century (**Figure 6B-1c**). This is likely due to the limited tropospheric chemical scheme used in the 2-D model, as mentioned above. This results in a low bias in tropospheric ozone throughout the 21st century, which is as large as 15% (5 DU) in 2050–2060. This low bias is also reflected in the future total column ozone comparison through the 21st century (**Figure 6B-1a**). For the total and stratospheric column, GSFC 2D and GEOSCCM show overall agreement with the observations but show a stronger decline and stronger recovery compared with the CCMI MMM (gray shading indicates $\pm 1\sigma$). For the tropospheric column, the limited available data fall between the two models (see the figure caption for details of the observations and MMM).

Figure 6B-2 shows stratospheric column ozone from the REF-C2 simulations at selected latitude zones. The GSFC 2D low bias in tropospheric ozone, and therefore in the total column, is similar to that of the global average (**Figure 6B-1**); therefore, the focus here is on stratospheric ozone. The 2-D model captures well the decline and recovery of stratospheric ozone simulated by the GEOSCCM and CCMI MMM during the Antarctic spring and the tropical and Northern mid-latitude annual average. The models show general agreement with the observations, which have significant year-to-year variability, although the CCMI MMM shows a somewhat weaker ozone decline during the Antarctic spring. The models also show the GHG-induced “super-recovery” at Northern Hemisphere mid-latitudes, where stratospheric ozone is 15–20 DU higher in 2100 than in 1960 (the CCMI MMM shows a somewhat smaller increase). The GEOSCCM, GSFC 2D, and CCMI MMM all show a similar decrease in tropical stratospheric ozone during the late 21st century, again driven primarily by GHG changes as discussed in **Chapter 3** (see **Sections 3.4.2 and 3.4.3.1** and **Figures 3-26, 3-29, and 3-30**).

GSFC 2D also compares well with the GEOSCCM in simulating the ozone response to the CH₄ perturbations discussed in **Chapters 3 and 4**. **Figure 6B-3** shows the profile ozone mixing ratio difference (ppm) between the RCP8.5 (high) CH₄ simulation and REF-C2 (RCP6.0 CH₄), averaged over 2070–2100. In the stratosphere, increased CH₄ loading leads to increased ozone due to the conversion of active chlorine to reservoir chlorine via the reaction CH₄ + Cl → HCl + CH₃, which reduces the chlorine-catalyzed ozone loss, although this process will

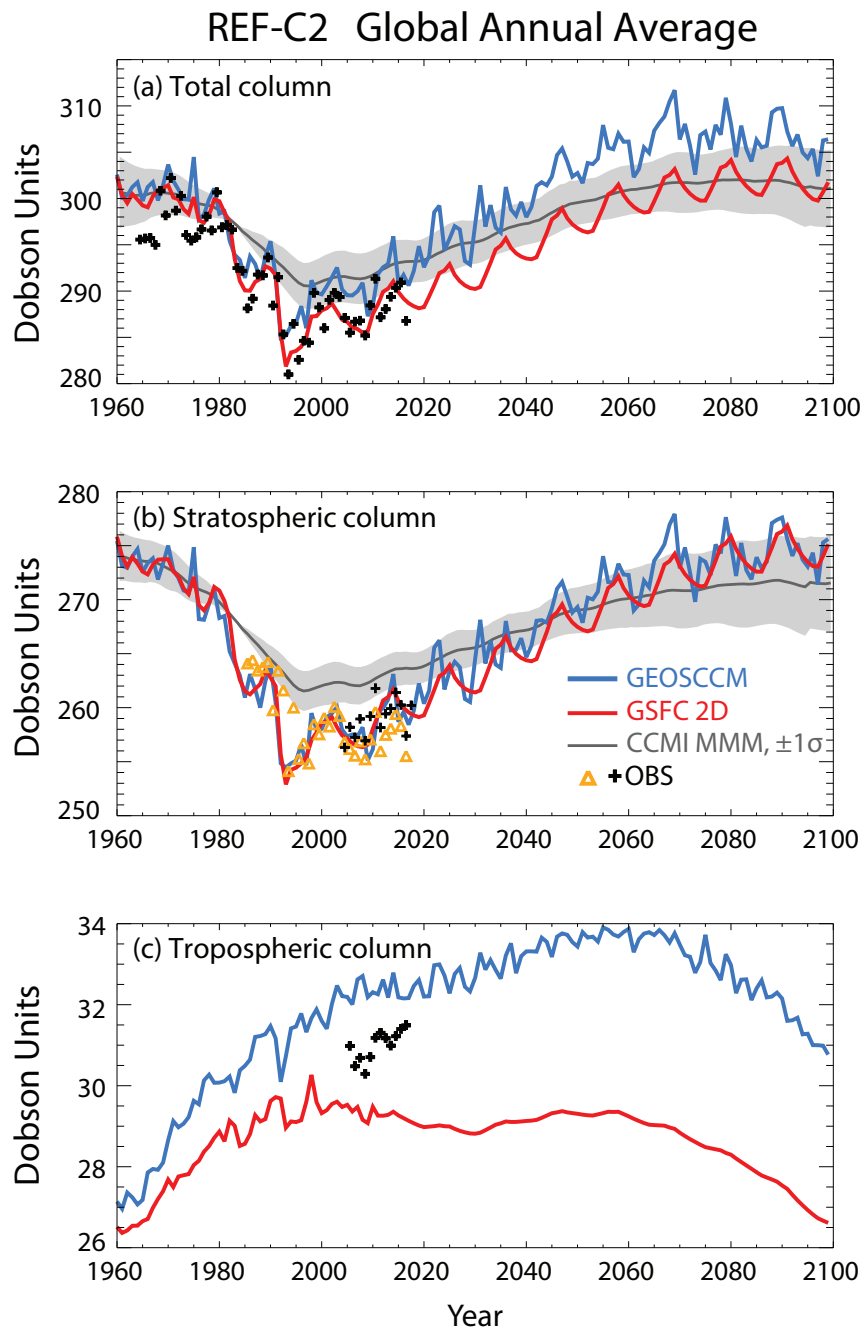


Figure 6B-1. Comparison of past and future globally averaged ozone from the REF-C2 simulations and observations. This shows the ozone columns below (c) and above (b) the latitude- and seasonally-dependent tropopause, and the total column (a), from the GSFC 2-D model (red line) and GEOSCCM 3-D model (blue line) for 1960–2100. Also shown are the CCMI multi-model mean (MMM, dark gray line) with $\pm 1\sigma$ (gray shading) (see Sections 3.4 and 4.5 of this Assessment, and Dhomse et al., 2018 for details). The observations are (a) ground-based total ozone for 1964–2016 updated from Fioletov et al. (2002); (b) stratospheric column ozone from: Aura/MLS version 4.2 for 2005–2017 (black +), and Global Ozone Chemistry And Related trace gas Data records for the Stratosphere (GOZCARDS) version 2.20 for 1985–2016, updated from Froidevaux et al. (2015) and time-interpolated to fill in missing data (orange Δ); and (c) tropospheric column ozone derived from OMI/MLS averaged over 60°S to 60°N for 2005–2016 (Ziemke and Cooper, 2017; 2018). To facilitate visual comparison and minimize the model biases in the 1960s, the following offsets were applied: (a) MMM: +6.5 DU; (b) MMM: -3 DU, GOZCARDS: +3 DU.

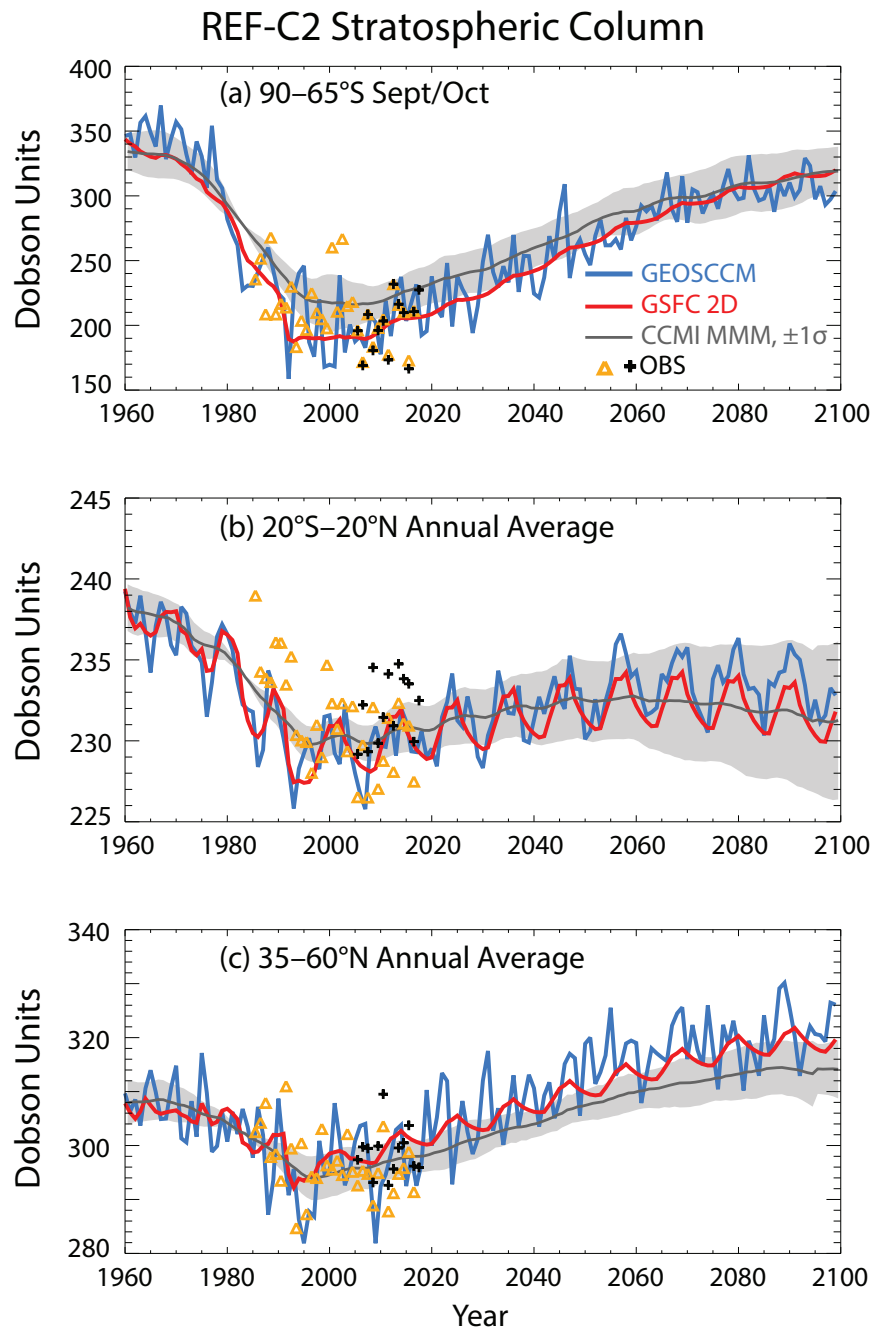
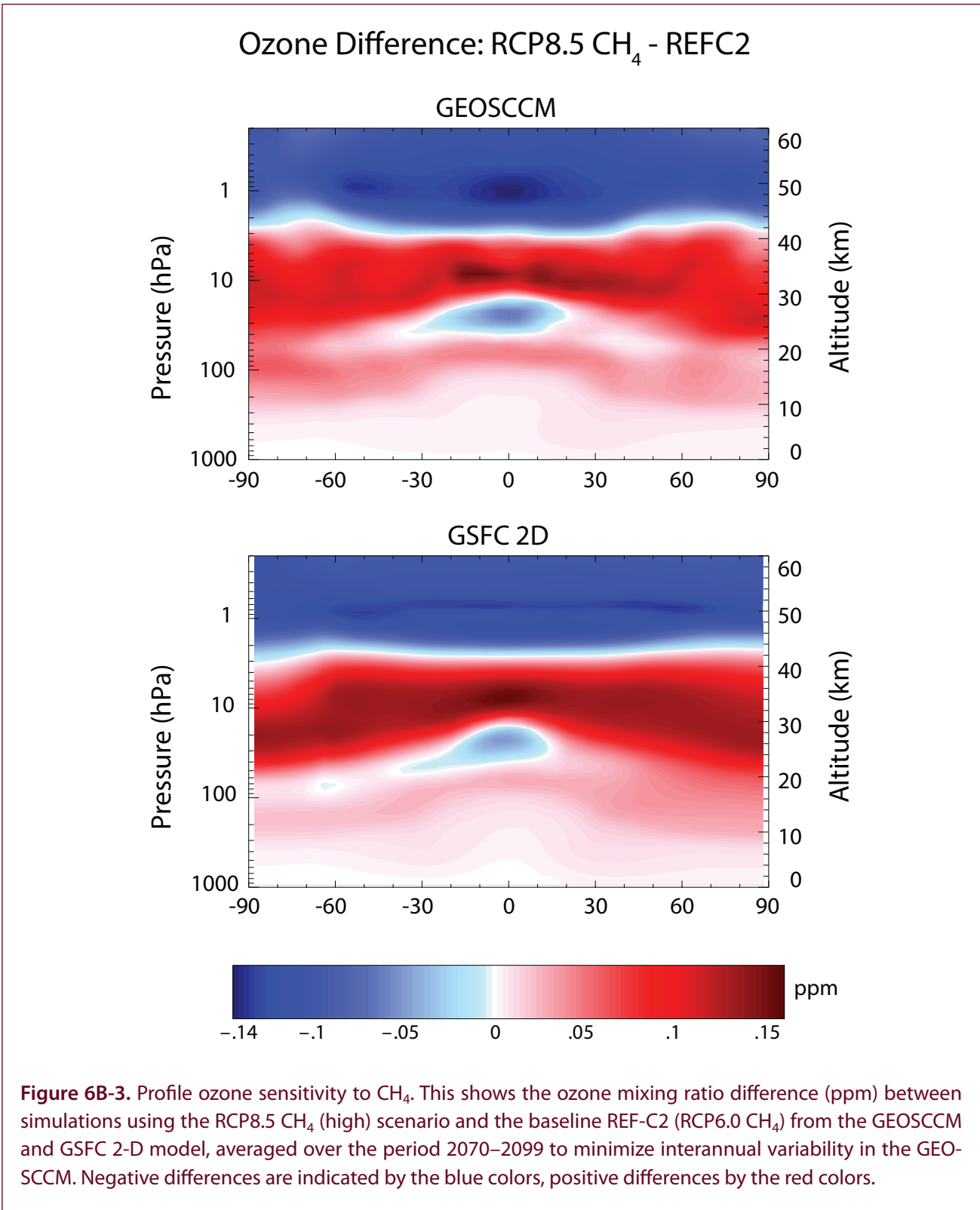


Figure 6B-2. Comparison of past and future stratospheric column ozone in select latitude bands from the baseline REF-C2 simulations and observations. This shows the ozone column above the tropopause (seasonally- and latitude-dependent) from the GSFC 2-D model (red line) and GEOSCCM 3-D model (blue line) for 1960–2100. Also shown are the CCMI multi-model mean (MMM, dark gray line) with $\pm 1\sigma$ (gray shading) (see Sections 3.4 and 4.5 of this Assessment, and Dhomse et al., 2018 for details). The observations are stratospheric column ozone from: Aura/MLS version 4.2 for 2005–2017 (black +), and Global Ozone Chemistry And Related trace gas Data records for the Stratosphere (GOZCARDS) version 2.20 for 1985–2016, updated from Froidevaux et al., 2015 and time-interpolated to fill in missing data (orange Δ). To facilitate visual comparison and minimize the model biases in the 1960s, the following offsets were applied: (a) MMM: +15 DU; (b) MMM: –16 DU, GOZCARDS: +2 DU; (c) GEOSCCM: –5 DU, GOZCARDS: +2 DU.



become less important as chlorine diminishes through the late 21st century. Methane oxidation also increases stratospheric HO_x, which (1) increases the HO_x-ozone loss and (2) sequesters NO_x in the reservoir HNO₃ via the reaction OH + NO₂, thereby reducing ozone loss in the mid-stratosphere (Nevison et al., 1999; Randeniya et al., 2002). There is also a contribution due to the increased water vapor from methane oxidation, which enhances stratospheric cooling and reduces the ozone chemical loss rates (e.g., WMO, 2014). In the troposphere and lowermost stratosphere, CH₄ oxidation leads to enhanced NO_x-induced ozone production, which is strongly dependent on the amount of ambient NO_x (e.g., see Jacob, 1999; Portmann and Solomon, 2007; Fiore et al., 2008; Kawase et al., 2011; WMO, 2014). The net impact of these processes yields ozone increases throughout most of the stratosphere below ~42 km and ozone decreases above ~42 km. The small area of negative ozone change in the tropical mid-stratosphere is likely due to “reverse self-healing,” in which increased ozone concentrations at higher altitudes allow less UV radiation to penetrate to lower altitudes, thereby reducing ozone production (e.g., Haigh and Pyle, 1982; Portmann and Solomon, 2007).

Figure 6B-4 shows time series of the global ozone difference from the REF-C2 simulation using (1) fixed (low) 1960 CH₄ throughout 1960–2100 and (2) RCP8.5 (high) CH₄ for 2000–2100. Globally, tropospheric and stratospheric column ozone both increase with larger methane concentrations and decrease with smaller methane concentrations. GEOSCCM and GSFC 2D give very similar global tropospheric and stratospheric ozone responses to both low and high methane concentrations throughout 1960–2100 (**Figure 6B-4b** and **c**). Although GSFC 2D has limited tropospheric chemistry and underestimates the GEOSCCM baseline tropospheric ozone, the large-scale NO_x distribution is similar to the GEOSCCM. As a result, GSFC 2D simulates quite well the methane-induced global tropospheric ozone perturbations (difference from REF-C2) simulated by GEOSCCM (**Figure 6B-4c**). The total column ozone responses are therefore also quite similar between the two models (**Figure 6B-4a**), which gives confidence in the fidelity of the 2-D model total ozone responses to the CH₄ sensitivity simulations discussed in **Section 6.4.3.1** (**Figure 6-4c**). **Figure 6B-4** also indicates that changes in stratospheric and tropospheric ozone each account for roughly 50% of the total ozone response to the CH₄ sensitivity simulations shown in **Figure 6-4c**.

Figure 6B-5 shows the model ozone mixing ratio sensitivity to N₂O as discussed in **Chapters 3** and **4**. The difference between simulations using fixed (low) 1960 N₂O versus the baseline REF-C2 (RCP6.0 N₂O) results in positive ozone changes in the mid-upper stratosphere, owing to the reduced NO_x-ozone loss. Negative ozone changes occur in the lower stratosphere and upper troposphere as the reduced NO_x decreases the NO_x-induced ozone production cycle. Some of the negative changes are also likely caused by “reverse self-healing” as discussed above. The zero ozone difference line occurs at ~28 km in the tropics and descends with latitude to ~18 km at the poles (see also Revell et al., 2012; Figure 2-25 of Parwon, Steinbrecht, et al., 2014; and **Chapter 3** of this Assessment). To emphasize these positive and negative ozone differences, time series of the global column ozone below and above this zero difference line are shown in **Figure 6B-6c** and **d**. GSFC 2D is similar to the GEOSCCM in simulating the positive ozone changes above the zero difference line through the 21st century (**Figure 6B-6c**). However, GSFC 2D underestimates the negative ozone differences below the zero difference line at Northern Hemisphere mid-high latitudes at 10–18 km (**Figure 6B-5**) and in the global average (**Figure 6B-6d**). As a result, the 2-D model has larger positive changes in the global total column in the later part of the 21st century (**Figure 6B-6a**). However, GSFC 2D is very similar to the GEOSCCM in simulating the positive column ozone differences above 28 km, the primary region of stratospheric NO_x-ozone loss (**Figure 6B-6b**).

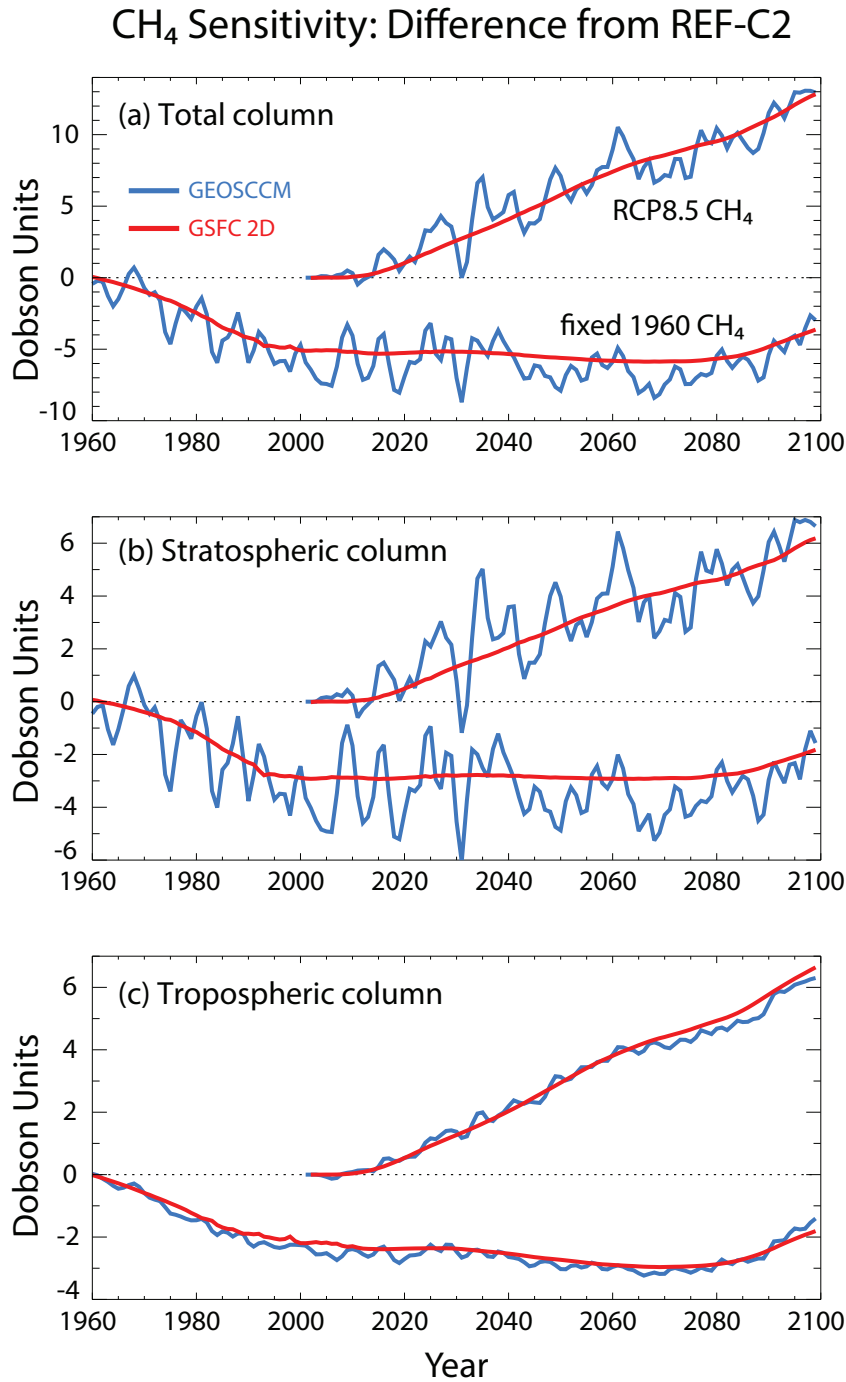


Figure 6B-4. Comparison of the past and future global ozone sensitivity to CH₄ variations. This shows the 1960–2100 global ozone difference from the baseline REF-C2 (RCP6.0 CH₄) of simulations using fixed (low) 1960 CH₄ (negative ozone anomalies) and the RCP8.5 CH₄ (high) scenario (positive ozone anomalies). Shown are the global tropospheric (c) and stratospheric (b) columns (separated by the latitude- and seasonally-dependent tropopause), and the total column (a) from the GSFC 2-D model (red line) and GEOSCCM 3-D model (blue line). Note that interannual variability in the 2-D model, due to tropospheric NO_x and CO emissions and the 11-year solar cycle, is the same for all simulations, so that the 2-D model difference curves (red) show minimal variability.

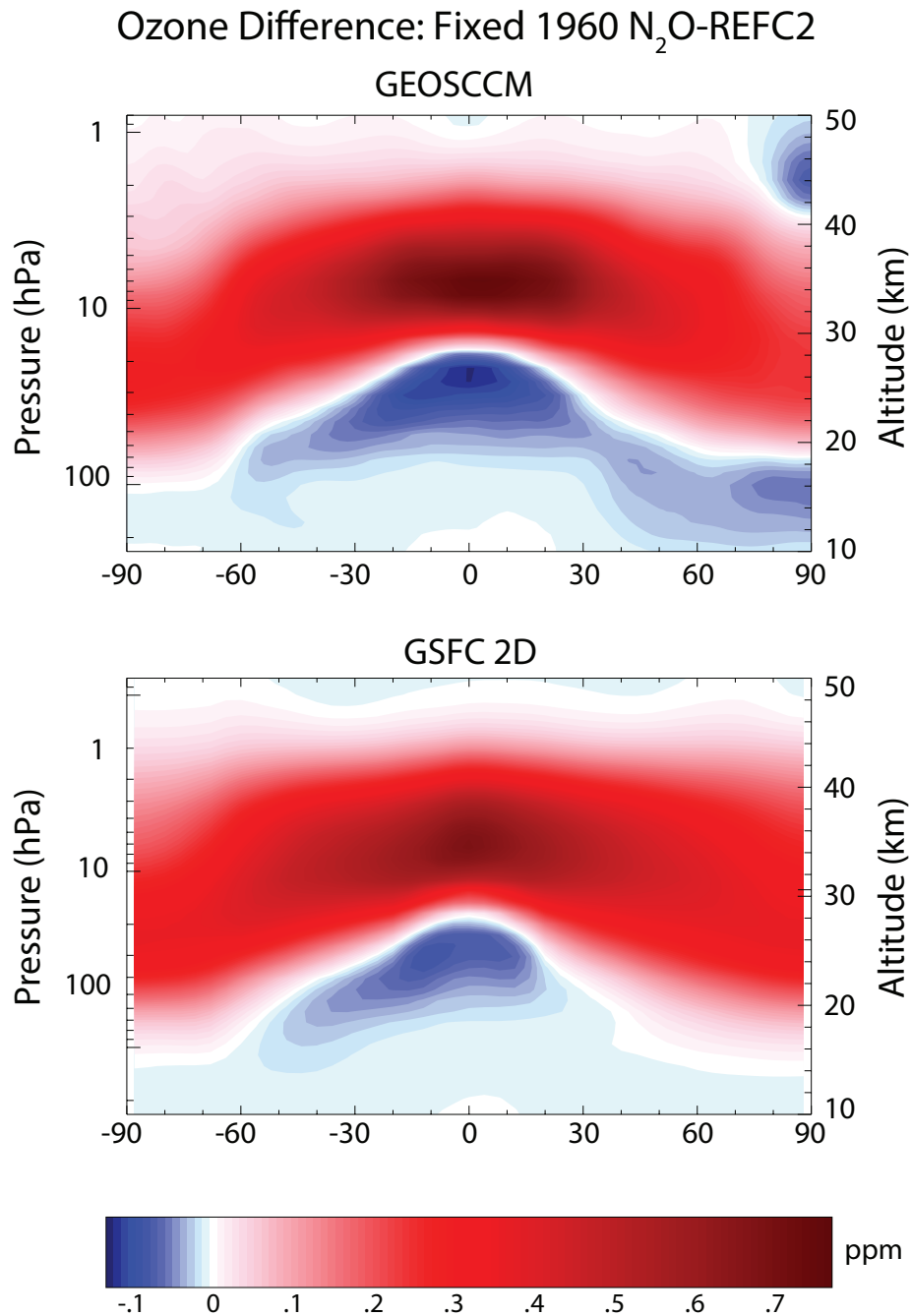


Figure 6B-5. Profile ozone sensitivity to N₂O. This shows the ozone mixing ratio difference (ppm) between simulations using fixed (low) 1960 N₂O and the baseline REF-C2 (RCP6.0 N₂O) from the GEOSCCM and GSFC 2-D model, both averaged over the period 2070–2099 to minimize interannual variability in the GEOSCCM. Negative differences are indicated by the blue colors, positive differences by the red colors.

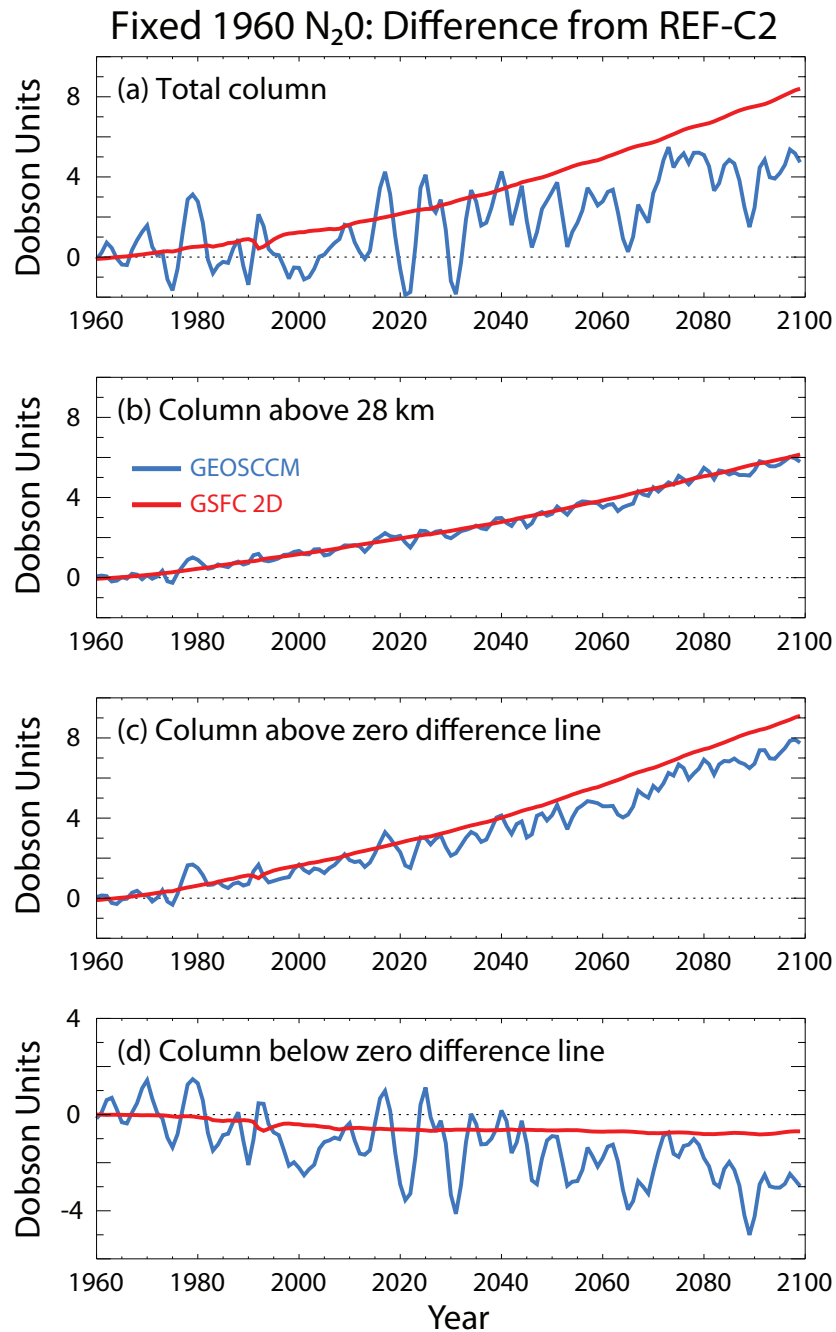


Figure 6B-6. Comparison of the past and future global ozone sensitivity to N₂O. This shows the 1960–2100 global ozone difference between simulations using fixed (low) 1960 N₂O and the baseline REF-C2 (RCP6.0 N₂O). As seen in **Figure 6A-5**, positive ozone differences occur in the mid-upper stratosphere, and negative differences in the lower stratosphere: the zero difference line occurs at ~28 km in the tropics and descends with latitude to ~18 km at the poles (see also Figure 2-25 of Pawson, Steinbrecht, et al., 2014, and **Chapter 3** of this Assessment). To emphasize these positive and negative differences, the column ozone below (d) and above (c) the zero difference line is shown in the bottom two panels. Also shown is column ozone above 28 km (b), the primary region of NO_x ozone loss, and the total column (a), from the GSFC 2-D model (red line) and GEOSCCM 3-D model (blue line). Note that interannual variability in the 2-D model, due to tropospheric NO_x and CO emissions and the 11-year solar cycle, is the same for all simulations, so that the 2-D model difference curves (red) show minimal variability.

Evaluation of Alternative Scenarios Using New EESC Formalism

Table 6C-1. Same as Table 6-5, for the part shown, but using the approach to calculating EESC and the fractional release values from Engel et al. (2017). Table 6-5 and its footnotes provide additional information about the scenarios and the calculations used to populate the table.

| Scenario and Cases | Percent Difference in Integrated EESC Relative to Baseline Scenario for the Mid-latitude Case | | Year When EESC is Expected to Drop Below 1980 Value | |
|---|---|---------------------------------|---|--------|
| | Mid-latitude | | Antarctic Vortex | |
| | $\int_{1980}^{\lambda} EESC dt$ | $\int_{2020}^{\lambda} EESC dt$ | | |
| Scenarios | | | | |
| A1: Baseline scenario | 0.0 | 0.0 | 2060.4 | 2077.3 |
| P0: All ODS | -5.0 | -16.4 | 2054.7 | 2071.9 |
| CFCs | 0.0 | 0.0 | 2060.4 | 2077.3 |
| Halons | 0.0 | 0.0 | 2060.4 | 2077.3 |
| HCFCs | -0.9 | -3.0 | 2059.8 | 2076.9 |
| CH ₃ Br for QPS and CUE | -1.6 | -5.4 | 2058.9 | 2075.8 |
| CCl ₄ | -2.7 | -8.9 | 2056.9 | 2073.9 |
| E0: All ODS (does not include N ₂ O) | -9.9 | -32.3 | 2048.9 | 2065.6 |
| CFCs | -2.1 | -6.7 | 2058.0 | 2074.9 |
| Halons | -2.6 | -8.6 | 2057.8 | 2074.6 |
| HCFCs | -2.5 | -8.3 | 2058.8 | 2076.2 |
| CCl ₄ | -2.7 | -8.9 | 2056.9 | 2073.9 |
| CH ₃ CCl ₃ | 0.0 | 0.0 | 2060.4 | 2077.3 |
| CH ₃ Br for QPS and CUE | -1.6 | -5.4 | 2058.9 | 2075.8 |
| B0: All ODS | -6.0 | -19.5 | 2054.4 | 2071.3 |
| CFCs | -2.1 | -6.7 | 2058.0 | 2074.9 |
| Halons | -2.6 | -8.6 | 2057.8 | 2074.6 |
| HCFCs | -1.6 | -5.3 | 2059.5 | 2076.7 |
| B1: All | -4.0 | -13.1 | 2055.4 | 2072.4 |
| CFCs | -1.3 | -4.1 | 2058.6 | 2075.4 |
| Halons | -1.6 | -5.3 | 2058.4 | 2075.1 |
| HCFCs | -1.4 | -4.5 | 2059.3 | 2076.5 |
| Continued emission of CFC-11: | | | | |
| Constant at 67 Gg yr ⁻¹ | +6.0 | +19.7 | 2072.7 | 2098.4 |
| Continued emission of CCl₄ at current levels: | | | | |
| | +1.5 | +4.9 | 2063.7 | 2080.8 |